West Nile Virus NS1 Interaction with *Aedes* Species IMUC1 Facilitates Viral Replication in Mosquito Cells

By

Scott Read

A Thesis submitted to the faculty of Graduate Studies of
The University of Manitoba
In partial fulfillment of the requirements of the degree of

MASTER OF SCIENCE

Department of Biological Science
University of Manitoba
Winnipeg

Copyright© 2008 by Scott Read

THE UNIVERSITY OF MANITOBA

FACULTY OF GRADUATE STUDIES

*****

COPYRIGHT PERMISSION

West Nile Virus NS1 Interaction with *Aedes* Species IMUC1 Facilitates Viral Replication in Mosquito Cells

BY

Scott Read

A Thesis/Practicum submitted to the Faculty of Graduate Studies of The University of Manitoba in partial fulfillment of the requirement of the degree

Of

Master of Science

Scott Read © 2008

Permission has been granted to the University of Manitoba Libraries to lend a copy of this thesis/practicum, to Library and Archives Canada (LAC) to lend a copy of this thesis/practicum, and to LAC's agent (UMI/ProQuest) to microfilm, sell copies and to publish an abstract of this thesis/practicum.

This reproduction or copy of this thesis has been made available by authority of the copyright owner solely for the purpose of private study and research, and may only be reproduced and copied as permitted by copyright laws or with express written authorization from the copyright owner.

Acknowledgements

A great number of people need to be acknowledged for their parts taken in the completion of my Masters thesis. First and foremost, I would like to thank my supervisor, Dr. Steve Whyard, for his support, guidance and endless humor during my stay in the Department of Biological Sciences. I greatly appreciate the extra hours you've put into helping me finish my thesis on time. While I never had the opportunity to be taught by you Steve, I know you're easily as good a teacher as you are a supervisor.

I would also like to recognize the huge amount of support I've been given by my friends and lab mates in the Whyard/Valdimarsson lab as well as the rest of the department. My lab partner for my entire stay, Aditi Singh, has been incredibly patient and will be greatly missed when I leave. I would also like to thank the large number of undergraduate students and technicians who helped me finish my work when the deadlines were pressing.

To my thesis committee, Dr. Gunnar Valdimarsson and Dr. Kevin Coombs, thank you for providing me with the invaluable advice and support needed to complete my thesis in a thorough and timely manner. I would also like to thank Dr. Robbin Lindsay for allowing me to use the facilities at the National Microbiology Laboratory and Dr. Bill Diehl-Jones for helping me with my cell culture work and allowing me to use his lab. Many thanks to Antonia Dibernardo as well for taking the time to teach me the required techniques and take me into containment level 3, an often time consuming process. I would also like to thank Veterinary Services and Animal Holding at the University of Manitoba for providing me with bovine and rat blood required to maintain the mosquito colony.

I would lastly like to thank my friends and family for their huge amount of support and time away from "the lab". While often confused by my incoherent ramblings, they have consistently been available to lend an ear, and take my mind away from it all.

Abstract

The flavivirus nonstructural protein 1 (NS1) is a highly conserved protein with a diversity of forms and functions. West Nile virus (WNV) NS1 is required for viral replication; however, its specific role in viral pathogenesis is unknown, especially in the mosquito host. In this study, yeast two hybrid analysis demonstrated that WNV NS1 interacts with a suite of proteins within the midgut of the mosquito *Aedes aegypti*, including AeIMUC1, which is a key protein in the formation of the midgut's peritrophic matrix. RNA interference was used to reduce the expression of the *AeImuc1* homologue, *AaImuc1* in *Aedes albopictus* cells, to determine its involvement in viral propagation. Interestingly, *AaImuc1* knockdown slowed viral replication, possibly as a result of the hindrance of viral entry or exit from infected cells. These results suggest that WNV NS1 may facilitate the infection and/or release of virus from mosquito cells via interaction with IMUC1.

Table of Contents

ACKNOWLEDGEMENTS ..... **ii**

ABSTRACT ..... **iii**

TABLE OF CONTENTS ..... **iv**

LIST OF FIGURES ..... **vii**

LIST OF TABLES ..... **ix**

ABREVIATIONS ..... **x**

CHAPTER 1. GENERAL INTRODUCTION **1**

1.1 West Nile Virus **1**

1.2. Viral Particle, Genome and Proteome **2**

1.3. Virus Replication **7**

1.4. Viral Replicative Cycle and Transmission Dynamics **11**

1.5. Mosquito Vector Competence **14**

1.6. Yeast Two Hybrid Assay **17**

1.7. Thesis Objectives **18**

CHAPTER 2. MATERIALS AND METHODS **21**

2.1. Mosquito Rearing **21**

2.2. cDNA Library Synthesis, PCR Amplification, Cloning and DNA Sequencing **21**

2.2.a. Isolation of Mosquito RNA 21
2.2.b. cDNA Library Synthesis 22
2.2.c. WNV Gene Amplification 24
2.2.d. WNV Gene Ligation and Cloning 26

2.3. Yeast Culturing **31**

2.4. Yeast Two Hybrid Assay **31**

2.4.a. Preparation of Competent Yeast 31

2.4.b. Transcriptional Activation/Toxicity Test of the DNA-BD WNV Fusion Protein 31
2.4.c. Yeast Two Hybrid Screening by Cotransformation....32
2.4.d. pGADT7 Insert Sequencing....34

2.5. Co-Immunoprecipitation....35

2.6. Cloning of *Aedes albopictus* Homologues....38
2.6.a. Gene Fragment Amplification and Cloning....38
2.6.b.Cloning of an *Aedes albopictus* Mucin Fragment for Real Time PCR....44

2.7. Double Stranded RNA Synthesis....45

2.8. Cell Culture Infectivity Assays....46
2.8.a. Cell Line Maintenance and Virus Propagation....46
2.8.b. Determination of WNV Infection Titer and Cell Plating Density....47
2.8.c. Cell Culture Infection and dsRNA Treatment....51
2.8.d. Plaque Titration....53

CHAPTER 3. RESULTS....55

3.1. Viral and Mosquito DNA Amplification and Cloning....55

3.2. Yeast Two Hybrid Assay....58

3.3. Co-Immunoprecipitation....65

3.4. Y2H Homologue Identification....69

3.5. WNV Infectivity Trials....79
3.5.a. Establishment of an Optimal Cell:Virus Ratio....79
3.5.b. WNV Infection Following dsRNA Mediated Mucin Knockdown....82

CHAPTER 4. DISCUSSION....92

4.1. An Overview....92

4.2 The Utility of the Y2H Assay and the Requirement For Controls....93

4.3. Y2H Identified Proteins and Mosquito Innate Immunity....97

4.4. The Identified Y2H Proteins and Their Possible Roles in WNV Interactions....100
4.4.a. Chitinase....100
4.4.b. Early Trypsin....102

4.4.c. Serine Protease 106
4.4.d. Prefoldin – A Chaperone Protein 108
4.4.e. Elongation Factor 2 110

4.5. NS1-IMUC1 Interaction 111

4.6. Conclusions and Future Directions 120

Works Cited 122

List of Figures

Figure 1.1. Genome organization of WNV 2
Figure 1.2. WNV protein coat structure 4
Figure 1.3. WNV structural polyprotein cleavage 10
Figure 1.4. WNV and mosquito distribution in the Americas 13
Figure 1.5. Route of WNV infection in the mosquito 16
Figure 1.6. Yeast two hybrid methodology 18
Figure 2.1. pGBKT7 cloning strategy 30
Figure 2.2. Co-immunoprecipitation methodology 38
Figure 2.3. pl4440 cloning strategy 43
Figure 2.4. Infectivity assay timeline 51
Figure 3.1. Synthesis of cDNA using SMART primers 56
Figure 3.2. *Aedes aegypti* gut cDNA amplification gel 56
Figure 3.3. pDrive-E NdeI+SmaI digest 58
Figure 3.4. pGADT7 cDNA insert amplification gel 62
Figure 3.5. Phosphor image of *in vitro* translation products 67
Figure 3.6. Phosphor image of Co-IP column eluates 68
Figure 3.7. Phosphor image of negative control column eluates 69
Figure 3.8. Cladogram demonstrating *Aedes* species phylogeny 70
Figure 3.9. *Aedes aegypti and Aedes albopictus* mucin nucleotide sequence alignment 72
Figure 3.10. *Aedes aegypti and Aedes albopictus* mucin amino acid sequence alignment 73
Figure 3.11. *Aedes aegypti and Aedes albopictus* trypsin nucleotide sequence alignment 74
Figure 3.12. *Aedes aegypti and Aedes albopictus* trypsin amino acid sequence alignment 75
Figure 3.13. *Aedes aegypti and Aedes albopictus* EF2 nucleotide sequence alignment 76-7

Figure 3.14 *Aedes aegypti and Aedes albopictus* EF2 amino acid sequence alignment 78
Figure 3.15. C6/36 growth curve 80
Figure 3.16. WNV growth curve 81
Figure 3.17. Mucin gene knockdown 83
Figure 3.18. Relative WNV RNA levels following *AaImuc1* knockdown 85
Figure 3.19. Cell death following WNV infection and dsRNA treatment 87
Figure 3.20. WNV titer following *AaImuc1* knockdown 88
Figure 3.21. Relative extracellular WNV RNA levels following *AaImuc1* knockdown 90
Figure 3.22. Relative decrease in total and extracellular WNV RNA levels following *AaImuc1* knockdown 91
Figure 4.1. *Anopheles gambiae* transcript AGAP006414 expression profile 102
Figure 4.2. Early trypsin expression profile 104
Figure 4.3. *Anopheles gambiae* trypsin expression profiles 106
Figure 4.4. *Aedes aegypti* serine protease expression profile 107
Figure 4.5. Protein domain organization of 3 IMUC1 alleles 112
Figure 4.6. *Aedes aegypti* IMUC1 expression profile 113
Figure 4.7. Hypothetical NS1-IMUC1 protein interaction 118

List of Tables

Table 2.1. cDNA library synthesis and amplification primers 22
Table 2.2. WNV restriction enzyme coupled amplification primers 26
Table 2.3. pDrive colony screening and sequencing primers 27
Table 2.4. pGADT7 insert screening and sequencing primers 30
Table 2.5. *Aedes albopictus* gene degenerate primers 39
Table 2.6. pl4440 screening primers 43
Table 2.7. *Aedes albopictus* mucin fragment amplification primers 45
Table 2.8. qRT-PCR primer list 50
Table 3.1. Yeast two hybrid results table 63
Table 3.2. WNV membrane protein Y2H sequence results 63
Table 3.3. WNV NS1 protein Y2H sequence results 64-5

Abbreviations

Å	Ångström
AaIMUC1	*Aedes albopictus* mucin-like protein
Ac	acetate
AD	activating domain
AeMUC1	*Aedes aegypti* mucin-like protein
BD	binding domain
bp	base pairs
BLAST	basic local alignment tool
BSA	bovine serum albumin
BSL	biosafety level
cDNA	complementary DNA
CI	confidence interval
Co-IP	co-immunoprecipitation
CPE	cytopathic effect
Ct	cycle threshold
DNA	deoxyribonucleic acid
(d)ATP	2'-(deoxy)adenosine 5'-triphosphate
(d)CTP	2'-(deoxy)citidine 5'-triphosphate
(d)GTP	2'-(deoxy)guanosine 5'-triphosphate
(d)NTP	2'-(deoxy)nucleotide 5'-triphosphate
ds	double stranded
DTT	dithiothreitol
(d)TTP	2'-(deoxy)thymidine 5'-triphosphate
EDTA	ethylenediaminetetraacetic acid
FBS	fetal bovine serum
g	gram(s)
GPI	glycosylphophatidylinositol
GUS	beta-glucuronidase
h	hour(s)
HA	hemagglutinin
hpi	hours post-infection
JEV	Japanese encephalitis virus
kb	kilobases
kDa	kilodaltons
LD-PCR	long distance PCR
M	molar
MEB	midgut escape barrier
MEM	minimal essential medium
MIB	midgut infection barrier
MOI	multiplicity of infection
mRNA	messenger RNA
NCBI	National Center for Biotechnology Information
nH_2O	nanopure water
OD	optical density

PM	peritrophic matrix
PBS	phosphate buffered saline
PCR	polymerase chain reaction
PEG	polyethylene glycol
pfu	plaque forming units
QDO	quadruple dropout
RER	rough endoplasmic reticulum
RNA	ribonucleic acid
RNAi	RNA interference
RT	reverse transcriptase
qRT-PCR	real time PCR
siRNA	short interfering RNA
ss	single stranded
TDO	triple dropout
UAS	upstream activating sequence
V	volts
WNV	West Nile virus
Y2H	yeast two hybrid
°C	degrees Celsius

Chapter 1. General Introduction

1.1. West Nile Virus

West Nile virus (WNV) is an arbovirus belonging to the family *Flaviviridae* and genus *Flavivirus* and was first isolated in 1937 from the blood of a febrile woman in Uganda (52). WNV is considered endemic in many tropical and temperate regions including Africa, the Middle East and western Asia, although more recent outbreaks have occurred in Europe and North America (23, 52). The well publicized 1999 outbreak of meningoencephalitis in New York was attributed to WNV and brought the virus to the forefront of virus research in an effort to contain the spread of the disease. The recent spread of WNV across the western hemisphere has been attributed to bird migration; however, birds only very rarely directly transmit the virus (110). The viral transmission cycle is maintained via bird and mosquito infection, but infection in humans can arise when a person is bitten by an infected mosquito. Because mosquitoes are the principle vectors of WNV, they are largely responsible for shaping the distribution of flavivirus disease throughout the globe and perhaps play the most important role in disease transmission (52). This review will focus on the molecular biology of WNV as well as its interactions and effects on its vector species. Given the importance of mosquitoes in transmitting this arboviral disease, the relationship of WNV to mosquitoes will be emphasized.

1.2. Viral Particle, Genome and Proteome

WNV is a member of the Japanese encephalitis virus (JEV) serogroup, which is one of twelve serogroups within the *Flavivirus* genus (23). Although most similar to viruses of its own serogroup such as St. Louis encephalitis, WNV shares conserved protein motifs and gene organization with all members of the family *Flaviviridae* (23). The 11 kb positive strand RNA genome of WNV contains ten genes, three of which are structural and seven are non-structural (Fig. 1.1.) (75). Flanking the virally encoded genes are 5' and 3' untranslated regions that form thermodynamically stable stem loop structures and are required for viral minus strand RNA synthesis and replication (132). Like other flaviviruses, WNV encodes a single ~10 kb ORF that is translated as a single polyprotein and is cleaved using viral and host derived proteases to produce functional proteins (87).

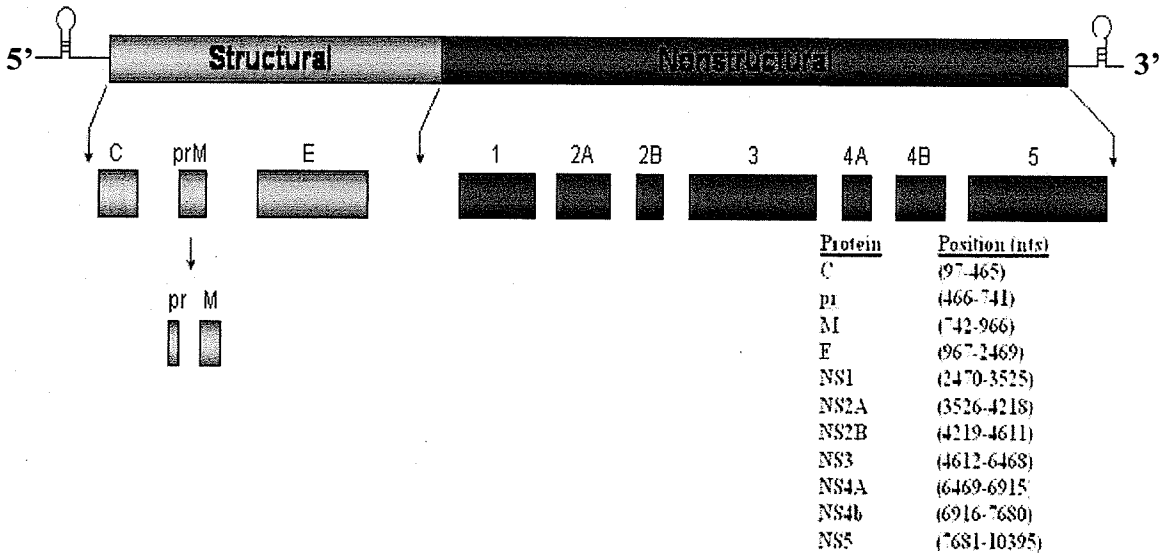

Figure 1.1. Genome organization of WNV. The 3 structural genes are located at the 5' end followed by the 7 non-structural genes (reproduced from (23)).

The mature WNV particle is approximately 500 Å in diameter and consists of three viral proteins: the capsid protein (C), membrane protein (M) and envelope glycoprotein (E), as well as a host-derived membrane envelope (95). The internal structure of the West Nile virion consists of multiple copies of the ~120 amino acid capsid protein that surrounds the genome producing an icosahedral nucleocapsid core (96). To ensure efficient assembly of the nucleocapsid core, the capsid protein contains a conserved C-terminal domain that interacts with host intracellular membranes (where self assembly occurs), as well as basic sequences at the carboxyl and amino-termini that interact with the viral genetic material (70, 80). Surrounding the nucleocapsid core is a host cell-derived membrane containing the viral type I integral membrane proteins E and M (95). The E and M proteins protrude from the membrane, enclosing the virus in a pseudo-icosahedral protein shell composed of triplets of E protein homodimers (figure 1.2A) (107). The M protein of the infective virion lies between the membrane and the E protein and is not exposed on the outer surface of the viral particle (Figure 1.2B) (133). Aside from maintaining structural integrity of the virion, the M protein may act as a chaperone for the E glycoprotein. This is due to the close involvement of the two proteins during virion assembly and the requirement of M for efficient transport of E to the viral envelope (82). However, it is possible that the M protein may contribute to receptor binding due to its placement outside the membrane and close proximity to the E glycoprotein. It has been speculated recently that the M protein may partake in cellular attachment due to its similarity in conformation to a specific region of the WNV E glycoprotein and inhibition of infectivity when treated with M-specific antibodies (19).

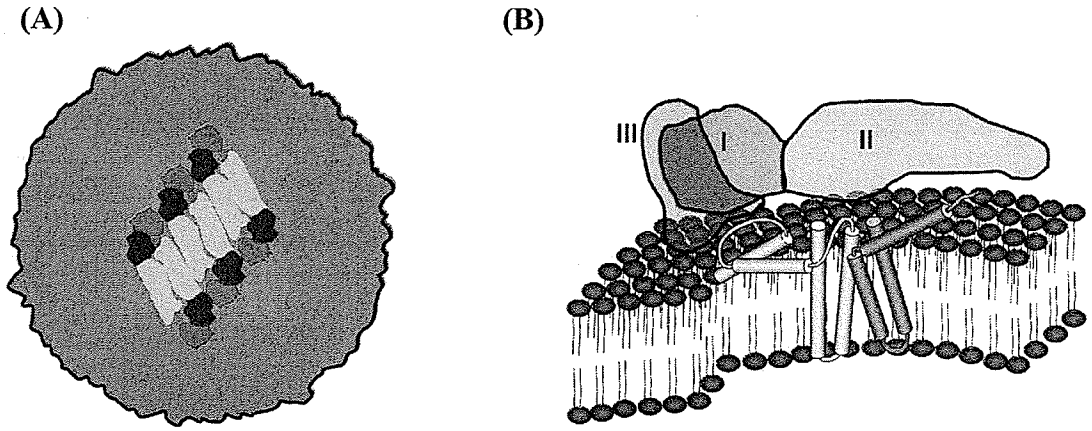

Figure 1.2. (A) One set of E homodimer triplets (bolded) as seen from the outside of a mature virion (reproduced from (96)). (B) A cross section of a flavivirus envelope showing the interaction between E and M proteins. The envelope protein lies primarily on top of the cell-derived membrane (domains I, II and III) and is anchored by two transmembrane helices (blue). The M protein lies beneath the E protein and contains two transmembrane loops (orange) (reproduced from (133)).

The most studied and well understood of the WNV structural proteins is the E glycoprotein. Due to its primary function of host cell attachment via receptor binding, it is not surprising that the E glycoprotein is the most conserved of the structural proteins (10). The E glycoprotein of WNV contains a three domain structure similar to previously characterized surface glycoproteins belonging to such flaviviruses as dengue and tick-borne encephalitis virus (107). The central domain I consists of a nine-stranded beta barrel and is flanked on either side by domains II and III (68). Domain II contains a dimerization domain responsible for producing the E homodimers present on the viral surface. A fusion loop is also present at its tip and is responsible for host-virus membrane fusion following virus attachment (68). Domain III flanks the opposite end of domain I and contains an immunoglobulin-like fold thought to possess the putative receptor

binding site (107). The three domains, although physically attached, are fluid in terms of their orientations to one another and interactions with other proteins. This fluidity is required to allow WNV to accomplish the many tasks required to infect and replicate efficiently within a cell. This includes binding and penetration of the host cell membrane as well as the low pH-induced membrane fusion required to release the viral capsid into the cytoplasm (22).

The non-structural genes of the WNV genome produce proteins translated during replication within the host cell but not encapsulated within the mature virion. The resulting proteins predominantly aid in viral replication and protein processing, although other functions have been speculated including inhibition of multiple factors of the host immune response (78).

NS1 is primarily a membrane-associated protein and was initially characterized as a viral protein required for WNV replication (97, 129). Thought to be present in many forms, intracellular NS1 is most commonly found in soluble monomer and membrane-associated homodimer forms (131). The membrane-associated homodimers are a requirement for efficient genome replication, which occurs mostly within virally-induced membrane vesicles. Although the primary role of NS1 may be in replication, NS1 may possess multiple functions depending on its location, form and glycosylation (23). Possibly most surprisingly, post-translational modifications such as the addition of a glycosylphophatidylinositol (GPI) anchor have been found on dengue virus NS1 (64). The addition of 26 amino acids from NS2A to the carboxyl terminus of NS1 permits the addition of a GPI anchor that incorporates into the outer cell membrane, possibly playing a role in signal transduction (64, 102). This could prove advantageous to the virus as it

may permit WNV to interrupt or alter signal transduction between the infected cell and the resulting immune response.

Interestingly, NS1 has been shown to aggregate as a soluble hexamer within the cell, where it is then secreted during mammalian but not mosquito infection (84, 131). Whether this is a result of differential post-translational modifications or merely differences in host-virus interaction is unknown; however, it is speculated that species specific NS1 glycosylation may play a role in its localization. Secreted NS1 interacts with the plasma membrane of uninfected cells via interactions with heparan sulfate and chondroitin sulfate and can be endocytosed by uninfected hepatocytes (4, 7). A subsequent challenge with WNV resulted in a 7-fold increase in viral infection and replication within the NS1-treated hepatocytes, indicating that the secreted NS1 may "prime" uninfected cells for future infection (4). An immunomodulatory role of secreted NS1 has also been demonstrated by its association with the complement regulatory protein factor H (31). The binding of NS1 to factor H increases the rate at which factor H cleaves complement factor C3b, thus preventing the membrane attack complex from forming and partially inhibiting the function of complement in the immune response (31).

NS3 is a highly conserved multifunctional protein divided into two regions. The N-terminus encodes a serine protease used to cleave the WNV polyprotein (in conjunction with NS2B) to produce functional viral proteins (98). The C-terminus is closely involved with viral replication, as it has strong homology with other DEAD family RNA helicases, which are responsible for RNA unwinding (49, 85). Nucleoside triphosphatase and RNA triphosphatase activity have also been associated with NS3, and

it is speculated that RNA triphosphatase is responsible for 5'cap formation on the viral genome (127, 128).

NS5 is the largest of the non-structural proteins. It encodes a viral RNA dependent RNA polymerase as well as a methyltransferase at its N-terminus (69, 72). The functions of NS2A, NS4A and NS4B are unconfirmed, although their interaction with NS5 suggests an involvement in the replication complex (10). These 3 proteins as well as NS2B and NS3 have additionally been shown to inhibit the signaling cascade produced by interferon binding to cellular receptors on infected cells (78). While interferon is still capable of binding to infected cells, interferon-induced transcription of anti-viral genes is prevented, allowing the virus to replicate more efficiently.

1.3. Virus Replication

Like other flaviviruses, WNV utilizes receptor-mediated endocytosis (96) in order to gain access to the host cell machinery. Interestingly, WNV has been observed to infect many species of mammals, birds, reptiles and mosquitoes (10). The seemingly indiscriminate nature of WNV infection indicates that the virus is either capable of binding to a variety of host factors to gain entry into the cell, or the receptor used is highly conserved among a wide variety of species. The structural protein responsible for flavivirus attachment is the E glycoprotein due to its position surrounding the viral membrane (96). The glycosylation of E is variable depending on the host species and viral strain, and consequently affects rates of infectivity (54). For example, lack of glycosylation on the E glycoprotein increased C6/36 mosquito embryonic cell line infection drastically while other cell types displayed only a modest increase in infection

(54). Glycosylation of E, however, produces an increased release of sub-viral particles indicating it may speed up the process of virion release from the infected cell (54). Because WNV can infect multiple species to maintain its transmission cycle, it is possible that differential glycosylation allows for a more efficient cellular binding, infection and release of the WNV particle within the infected organism in question. For example, viral protein glycosylation produced within the mosquito species may facilitate infection and dissemination within some avian species and perhaps restrict infection in other mammalian species.

Many putative host cell surface receptors have been identified for dengue virus, including glycosaminoglycans, DC-SIGN, laminin receptor, BiP, $\alpha_v\beta_3$ integrin, Hsp70 and Hsp90 (26, 30, 66, 99, 112, 120). In contrast, considerably less is known about possible receptors for WNV. One report observed that the cell attachment protein $\alpha_v\beta_3$ integrin could facilitate WNV infection in mammalian cells (30). More recently, however, Medigeshi *et al.* (88) have questioned the significance of $\alpha_v\beta_3$ as a WNV receptor. They found that WNV infection was limited only when cholesterol-rich microdomains were removed from the membrane whereas $\alpha_v\beta_3$ removal caused no reduction in infection. As of yet, there has been no receptor identified for mosquito cells, although the nature of a putative receptor has been described. Two proteins, approximately 70 and 95 kDa, found on the outer membrane of mosquito cells bound strongly to the WNV particle (29). Unlike several other mosquito-borne flaviviruses, however, the virion did not require heparin sulfate to infect the C6/36 *Aedes albopictus* embryonic cell line (29).

To assist the putative WNV receptor, WNV appears to use an attachment protein termed DC-SIGNR (dendritic-cell-specific ICAM-grabbing non-integrin) to aid in mosquito and human cell line infection (34). Unlike viral receptors, attachment proteins are not required for infection, but can promote viral binding to the host cell and vastly increase the chance of interactions with the viral receptor. DC-SIGNR is a mannose binding lectin that has been proposed to bind N-linked glycosylation sites on the E glycoprotein of WNV (34). It is commonly expressed in microvascular endothelial cells, which are believed to be a site of primary WNV infection (60).

Once bound to a receptor, WNV enters a host cell via clathrin-mediated endocytosis (28). The internalized virion is then shunted into the endosomal pathway whereby the endosome pH is lowered to facilitate digestion. The low pH causes a structural reconfiguration of the viral envelope in which the E glycoprotein dimers dissociate from their native configuration and reassociate as trimers (22, 71). X-ray crystallographic structures have suggested that domains I and II of the WNV E glycoprotein shift from their flat position against the membrane and project outwards as spikes (5). This allows the fusion loop present on domain II to interact with the host vesicular membrane, allowing fusion of viral and host membrane and release of the nucleocapsid. Once inside the cell, the nucleocapsid and viral genome dissociate, and due to the positive strand nature of the WNV genome, a single polyprotein is immediately translated (23). The resulting polyprotein is then cleaved by host proteases as well as the NS3/NS2B complex. The three structural proteins remain uncut and migrate to the rough endoplasmic reticulum (RER) where they anchor via multiple hydrophobic signal sequences (Figure 1.3) (96). They are then cleaved, allowing the capsid proteins to

aggregate in the cytoplasmic side of the RER along with the viral genome. The viral genome and surrounding nucleocapsid then bud into the RER becoming surrounded by an immature envelope composed of a membrane surrounded by an E glycoprotein-prM protein heterodimer coat (96). The prM protein is so named due to an additional N-terminal sequence that is present prior to viral maturation that is thought to act as a chaperone for the E glycoprotein prior to particle assembly (10). During exocytosis from the cell, host cell furin cleaves prM to produce M (116). This produces another conformational change whereby E and M dissociate and E glycoproteins form homodimers once again. Mature virions depart from the trans-Golgi network in cellular vesicles and fuse with the host plasma membrane allowing further infection to occur (96).

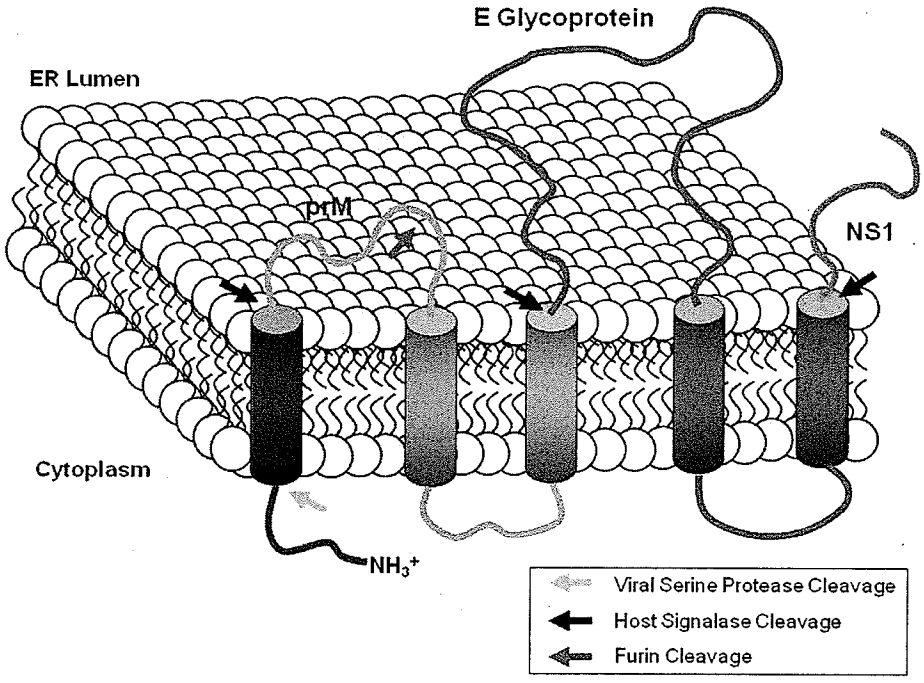

Figure 1.3. The integrated form of the WNV structural proteins and their respective cleavage sites (reproduced from (96)).

WNV, like many other flaviviruses, induces vesicle formation within infected cells, where genome replication occurs in conjunction with many of the non-structural proteins (60, 101). The viral RNA dependant RNA polymerase produces a double stranded replicative form of the RNA that serves as a template for production of genomic positive strand RNA (121). The majority of the transcriptional process appears to occur within cytoplasmic vesicles, which may explain why actively replicating WNV has shown resistance to RNA interference (RNAi) knockdown via short interfering RNA treatment (siRNA) (46). A plausible explanation for these findings is that virally-induced vesicles may have evolved as a protection mechanism against anti-viral responses within infected cells.

1.4. Viral Replicative Cycle and Transmission Dynamics

WNV is maintained predominantly in a mosquito-bird replicative cycle, in which the mosquito acts as the primary vector and the bird serves as the primary amplifying host (59). Birds are an optimal amplifying host as many species are susceptible to infection while remaining viraemic for several days (126). WNV appears to share the similar bird-mosquito replicative cycle of other flaviviruses common to North America such as St. Louis encephalitis and western equine encephalitis virus; however, WNV may pose a much larger threat due to the naivety of the population towards this newly introduced virus (86).

WNV has been isolated from over 40 species of mosquitoes, with the vast majority belonging to the genus *Culex* (52). Other host mosquito genera include *Aedes,*

Anopheles, Coquillettidia and *Ochlerotatus* (52). Because WNV infects such a variety of avian species, its distribution around the globe is largely mediated by the vector mosquito species present. When comparing mosquito distributions to cases of WNV, it becomes evident that mosquito species distributions play a large role in determining WNV distribution (Figure 1.4).

Because some mosquito vector species of WNV do not limit their feeding to one species, infection is common in many vertebrates including but not limited to humans, dogs, squirrels, bats and crocodiles (10). Outbreaks in North America have been attributed to mosquitoes such as *Culex tarsalis* that display this characteristic. *Culex tarsalis* is notorious for feeding indiscriminately on birds as well as humans (52). Most infected vertebrate hosts are considered dead end hosts as viremia does not reach a level in which transmission can occur (59).

Due to the presence of WNV infections in male mosquitoes, transmission between male and female mosquitoes has also been questioned (6). Mosquito ovaries tested positive for viral antigen indicating that transovarial transmission is a distinct possibility in multiple species (90). Transovarial WNV transmission has in fact been documented (91); however, more species data is required to further understand if the proportion of infected offspring differs. The occurrence of transovarial transmission does not, however, rule out the possibility that sexual transmission of WNV between mosquitoes can occur, but there is no evidence yet to support this possibility.

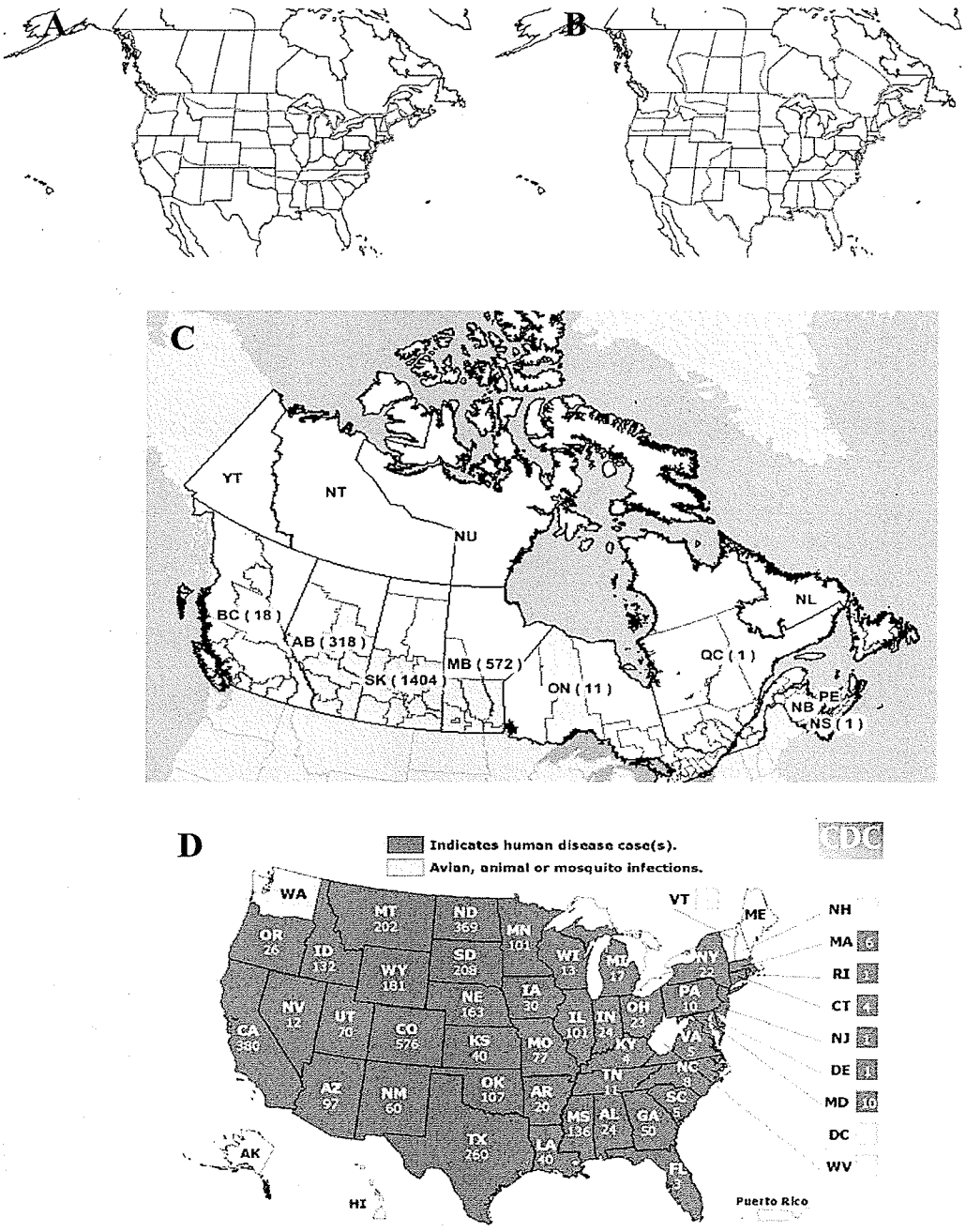

Figure 1.4. Distribution of (A) *Culex pipiens* (B) *Culex restuans* (reproduced from http://svs.gsfc.nasa.gov/vis/a000000/a002500/a002565/index.html). (C) The number of symptomatic WNV cases by province in Canada for the year 2007 (http://www.phac-aspc.gc.ca/wnv-vwn/index-eng.php). (D) The number of WNV cases by state in the USA for the year 2007 (http://www.cdc.gov/ncidod/dvbid/westnile/Mapsactivity/surv&control07Maps.htm). *Culex tarsalis* is distributed throughout the United Stated, northern Mexico and the southern plains of Canada.

Prior to 1999, WNV transmission had been reported in Europe, the Middle East, India, Africa, Asian and Australia (59). During the summer of 1999, the first case of WNV in the Western hemisphere was diagnosed in New York City. Since its introduction, WNV has spread from the east coast to the west coast of North America in less than 3 years and is now present throughout the United States, southern Canada, Mexico and parts of South America (http://www.cdc.gov/ncidod/dvbid/westnile/surv&control.htm). This is largely due to the ability of WNV to infect and replicate within the resident bird and mosquito species of North America.

1.5. Mosquito Vector Competence

Vector competence is defined as the ability of a mosquito to serve as a disease vector (12). In other words, vector competence is governed by the inherent traits possessed by a species or population of mosquitoes that enable WNV to infect and replicate more efficiently. Patterns of flavivirus susceptibility have revealed a great degree of variation of infection rate among species as well as strains (56). Factors affecting mammalian infection are often studied; however, it is equally if not more important to understand what enables replication within the mosquito system due to their integral role in the WNV transmission cycle.

To infect and replicate within mosquitoes, WNV must surpass multiple physiological barriers to produce a titer high enough to allow transmission (Figure 1.5). Once WNV has been ingested in a blood meal, the virion must bind and penetrate the

midgut. Release of digestive and antihemostatic enzymes as well as the production of the peritrophic matrix all affect the degree of viral penetrance into the mosquito midgut (12). While proteolytic digestive enzymes and pH may inhibit WNV entry in a chemically-dependent manner, species' ability to prevent coagulation may actually enable viral entry by maintaining the ingested blood in a liquid state. Reduction in filarial parasite infection due to increased rate of blood coagulation has in fact been demonstrated in the mosquito model (12). The peritrophic matrix (PM), which is secreted following a blood meal, is composed of a number of highly glycosylated proteins embedded within a chitin matrix, and is speculated to protect against pathogens as well as physical damage to the midgut epithelium (118). The pore size of the PM varies among mosquito species, but it seems widely accepted that it is too small to allow viral penetrance (39, 114). The speed and efficacy of peritrophic membrane production is therefore very important in preventing WNV infection of the midgut cells, assuming the virus has no way of inhibiting peritrophic matrix formation or digesting its components.

Once the virus has infected the midgut epithelial cells, it must pass through the basal lamina in order to reach the hemocoel where infection can become systemic and be spread to other organs such as the salivary glands (16). Within the hemocoel, the immune components required to produce the innate immune response are present (12). Although all species of mosquito possess only the innate immune response, the efficacy of non-self recognition, phagocytosis, encapsulation and nodule formation will vary, as it does in humans, between individuals, strains and species (16, 40).

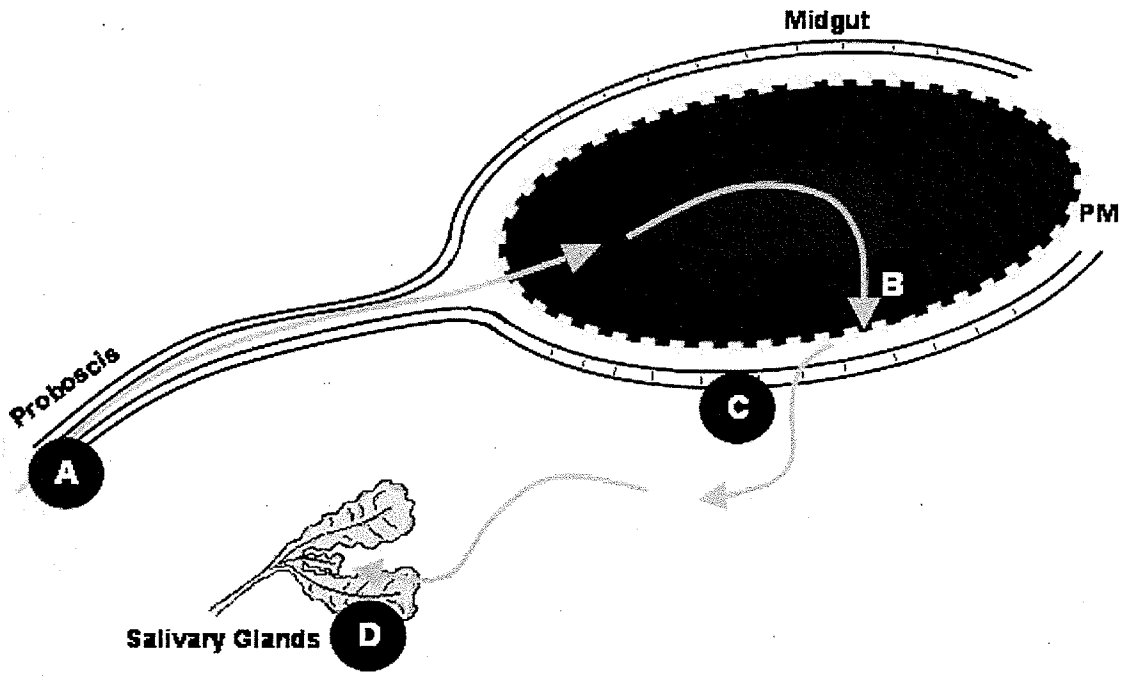

Figure 1.5. In order for WNV to be transmitted by a mosquito species, it must enter the midgut lumen in a blood meal (A), pass the peritrophic matrix and intestinal epithelium (B and C), and infect the salivary glands through the hemolymph (D) where it may be passed on to another host during blood feeding (reproduced from (12)).

Whether WNV enters the salivary glands and midgut using the same receptor is unknown. If, like the mammalian model, an integrin molecule is used for binding in the gut, then it is likely that a similar receptor is used for the salivary glands due to the abundant distribution of integrin molecules. The titer within the salivary glands is perhaps the most important factor when determining a mosquito's ability to infect its host, as it is the final organ in which the virus accumulates before blood feeding.

1.6. Yeast Two Hybrid Assay

While much research has been conducted on human infection with WNV, comparatively little is known concerning infection in the vector species of mosquitoes. Because mosquitoes arguably possess the most important role in the viral life cycle, understanding similarities and differences in virus-mosquito interactions is important and necessary. One of the main objectives of this study is to identify how WNV proteins interact with their mosquito host cells, and more specifically, the protein interactions that facilitate WNV infection and replication. The yeast two hybrid (Y2H) assay, first described by Fields and Song (41), is a method designed to detect protein-protein interactions. Although initially used to screen for individual protein interactions, the assay was further improved to screen entire cDNA libraries for specific interactions with a protein of interest. The yeast two hybrid screen produces two fusion proteins, one of which is a protein of interest (the bait) bound to a DNA binding domain (DBD), while the other is one of many possible cDNA encoded proteins bound to a transcriptional activating domain (AD). If the two proteins specifically bind, they will yield a functional transcriptional activator capable of binding to an upstream activating sequence (UAS) and activating transcription of a reporter gene, or set of reporter genes (Figure 1.6) that are typically required for yeast growth and survival. Metabolic genes such as ADE2 (phosphoribosylaminoimidazole carboxylase required for adenine synthesis) and HIS3 (imidazoleglycerol-phosphate dehydratase required for histidine synthesis) are most commonly used in conjunction with metabolically deficient strains of yeast. When grown on minimal media (media lacking histidine and adenine for example), only the yeast cells containing the functional bipartite transcriptional activator are able to grow. The resulting

yeast colonies can then be screened to determine the identity of the cDNA whose protein product is interacting with a protein of interest.

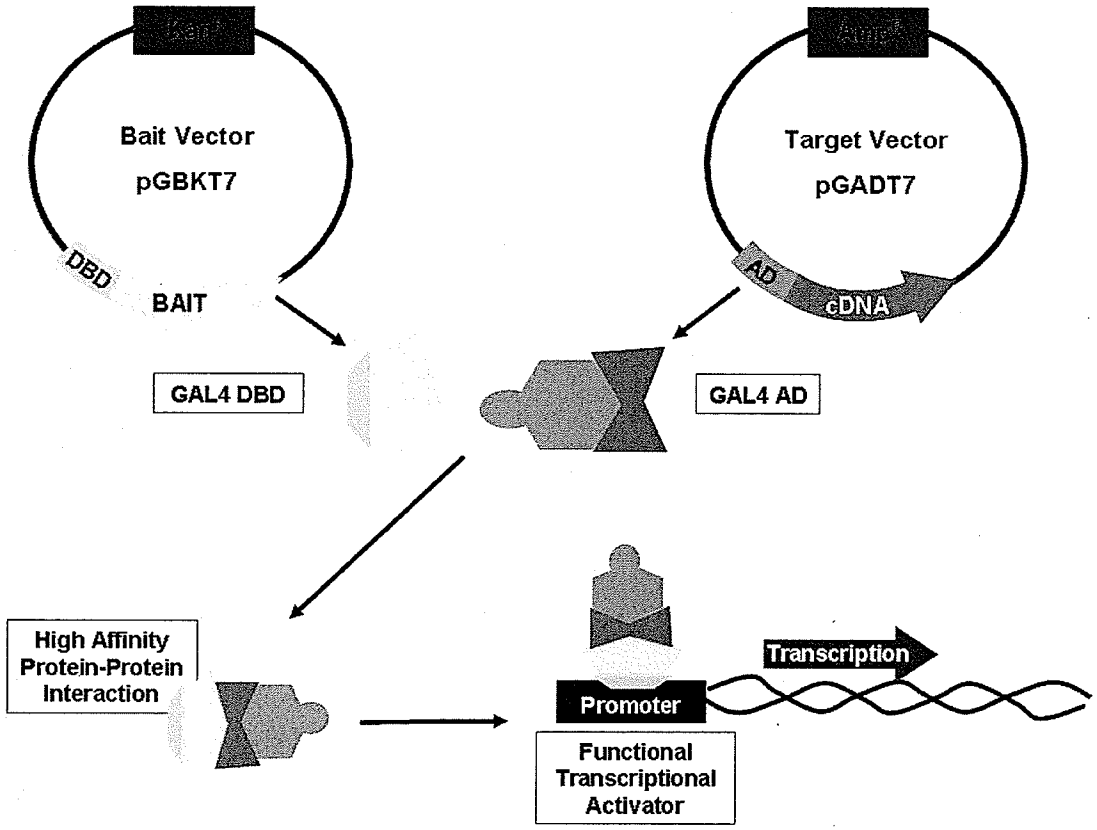

Figure 1.6. Target and bait vectors are co-transfected into yeast cells and produce respective fusion proteins. Upon interaction, transcription of reporter genes is activated and yeast are able to grow on selective media.

1.7. Thesis Objectives

WNV knowledge has greatly increased since the emergence of WNV infection in North America. The sudden eruption of research can most certainly be explained by the nature of the virus itself. WNV is an arbovirus, spread mostly via a mosquito vector, and can infect any member of the population that spends time outdoors during the summer months. The seemingly indiscriminate nature of mosquito feeding means that a sudden

onset of flu-like symptoms, with possibility of very serious encephalitic disease can strike just about anyone. For example, the United States experienced 1217 cases of WNV encephalitis/meningitis cases in 2007, and 124 deaths as a result of WNV infection (http://www.cdc.gov/ncidod/dvbid/westnile). This, in combination with the naivety of the American human and bird population makes the appearance of WNV in North America an incursion to which we have no experience. Considerable effort has been invested to understand and treat human WNV infections, but understanding mosquito infection is perhaps even more important. By understanding how WNV interacts with the mosquito on a molecular level, we may someday be able to stop the spread of the disease all together.

The penetration of the mosquito midgut is a critical step in WNV infection, and still very little is known as to how the virus surpasses the many physiological barriers. Understanding the specific protein interactions that occur within the infected midgut cells may allow us to determine how WNV efficiently replicates within host cells and how it infects and disseminates within the mosquito. The objectives of my research are as follows:

1. Uncover novel protein interactions between *Aedes aegypti* gut proteins and WNV proteins using a yeast two-hybrid approach.

Although a number of protein interactions have been identified, it is not possible to examine all of them within the time frame of an M.Sc. A small number of NS1 interacting proteins have therefore been chosen for study. One of these, IMUC1, will be examined in relation to WNV infection in mosquito cell culture. Analyzing specific

mosquito-WNV interactions may eventually provide interesting insights into the adaptation of the virus to the vector.

2. Uncover virus-interacting gene homologues in the mosquito species *Aedes albopictus*.

To facilitate the study of mosquito-virus interaction, a cell-based assay was used. Due to the limited amount of mosquito lab strains and mosquito cell lines available, it was necessary to use different species for the Y2H and cell culture. The only immortal cell line available is an *Aedes albopictus* embryonic cell line termed C6/36. Because *Aedes albopictus* is not native to Canada, it would likely be difficult to obtain in order to start a lab-bred colony. For this reason, and because Dr. Whyard already possesses a colony of *Aedes aegypti*, the Y2H screen was conducted on *A. aegypti* cDNA, and then homologues of the NS1-interacting genes were isolated from *A. albopictus* cDNA, with the intent to examine the interaction of these genes' products with NS1 within the *A. albopictus* cells.

3. Determine whether RNAi knockout of virus interacting mosquito genes affects viral infection and/or replication.

RNAi produces transient knockdown of gene-specific transcripts using double stranded RNA (dsRNA). Due to the relative ease and low cost of production and delivery of dsRNA, RNAi has become a widely used method to create loss-of-function mutations to discover the roles of many newly described genes and their associated proteins [reviewed in (55)]. In this study, gene-specific RNAi will be used to reduce the expression of protein(s) that have shown confirmed interaction with WNV NS1, to determine whether they play a role in WNV infection, replication and/or dissemination.

Chapter 2. Materials and Methods

2.1. Mosquito Rearing

McAllen strain *Aedes aegypti* mosquitoes were reared at 25°C and 50% relative humidity with a photoperiod of 16:8 hour light:dark cycle. Larvae were raised in filtered tap water and fed ground bovine liver powder and hamster meal. Adults were maintained on a 10% sucrose solution diet, and females were blood-fed weekly. To facilitate blood feeding, a "blood bag" was prepared by stretching Nescofilm (Karlan Research Products) over 2mL of bovine blood that was derived from dairy cows maintained at the Glenlea Experimental Farm, MB. The blood was warmed to 42°C and placed inside the mosquito cage, where it gradually cooled as the mosquitoes fed.

2.2. cDNA Library Synthesis, PCR Amplification, Cloning and DNA Sequencing

2.2.a. Isolation of Mosquito RNA

Female *Aedes aegypti* dissections were performed in order to isolate gut tissue for RNA extraction, followed by cDNA library construction. Female mosquitoes were anesthetized on ice and their guts were gently removed using dissecting forceps. Approximately 200 female mosquito guts were collected and stored in RNAlater (Applied Biosystems) at -80°C to prevent RNA degradation. RNA was extracted from the gut tissue using the RNeasy kit (Qiagen) according to the manufacturer's specifications, with some minor modifications. Briefly, mosquito guts were removed from the RNAlater solution using a sterile syringe, and placed in 600µl of lysis buffer RLT containing 1% β-mercaptoethanol. Guts were homogenized by passing them through a 20 gauge syringe 6

times. The lysate was then centrifuged at 13,000 rpm for 3 minutes and the supernatant was placed in a new tube. One volume of 70% ethanol was added, and the entire solution was pipetted onto an RNeasy spin column and spun at 13,000 rpm for 15 seconds. The eluate was discarded and the column was further washed twice with buffer RPE. Purified RNA was finally eluted into 50µl of Nanopure water (nH_2O), to be used for cDNA synthesis.

2.2.b. cDNA Library Synthesis

cDNA library synthesis was performed using the Matchmaker Library Construction and Screening Kit (Clontech). To generate first strand cDNA, 2µl of purified gut RNA was incubated at 72°C for 2 minutes with 1µl of nH_20 and 1µl (10µM) of poly-T CDS III primer (Table 2.1). The reaction was then placed on ice and 2µl of 5x first strand buffer (250 mM Tris (pH 8.3), 30 mM $MgCl_2$, 375 mM KCl), 1µl of DTT (20mM), 1µl of dNTP mix (10mM) and 1µl of MMLV (Moloney murine leukemia virus) reverse transcriptase was added. Following incubation at 42°C for 10 minutes, 1µl of the SMART III oligonucleotide (10µM; Table 2.1) was added and incubation at 42°C continued for 1 hour. First strand synthesis was then terminated by incubating at 75°C for 10 minutes. 1µl of RNase H was added to the cooled reaction and placed at 37°C for 10 minutes to remove any remaining RNA template. For an explanation of SMART cDNA synthesis, please refer to section 3.1

Duplicate long-distance PCR (LD-PCR) reactions were then performed to amplify sufficient cDNA template produced in the first strand synthesis reaction. Briefly, 2µl of first strand cDNA was combined with 10µl of 10x Advantage 2 PCR buffer (400mM Tricine KOH, 150mM potassium acetate, 35mM magnesium acetate, 37.5µg/ml BSA,

0.05% Tween 20, 0.05% Nonidet-P40), 10µl of 10x GC melt solution, 2µl of 50x dNTPs (10 mM each of dATP, dCTP, dGTP, and dTTP), 2µl each of 10µM 5' and 3' PCR primers (Table 2.1), 2µl of Advantage 2 polymerase mix and 70µl of nH_20 to a total volume of 100µl. An MJ Mini thermocycler (Bio-Rad) was used to amplify the cDNA using the following thermal cycler conditions: denaturation at 95°C for 30 seconds; 23 cycles of 95°C for 10 seconds (DNA denaturation) and 68°C for 6 minutes (primer annealing and extension); a final elongation step at 68°C for 5 minutes. Following PCR amplification, a 7µl aliquot was combined with 1.4µl of 6x loading buffer and resolved on a 1% agarose gel alongside a 1 kb plus ladder (Fermentas) to ensure that adequate amplification occurred. Amplified cDNA was then stored at -20°C until it was required for insertion into the pGADT7 vector.

Table 2.1. cDNA library synthesis and amplification primers.

Primer Name	Primer Sequence
CDS III	5' ATTCTAGAGGCCGAGGCGGCCGACATG-d(T)30 3'
Smart III	5' AAGCAGTGGTATCAACGCAGAGTGGCCATTATGGCCGGG 3'
LD-PCR 5'	5' TTCCACCCAAGCAGTGGTATCAACGCAGAGTGG 3'
LD-PCR 3'	5' GTATCGATGCCCACCCTCTAGAGGCCGAGGCGGCCGACA 3'

cDNA library purification was performed using Chroma Spin TE-400 columns (Clontech). Approximately 95µl of the duplicate PCR reactions were pipetted onto the center of the column and spun at 500 x g for 5 minutes. Flow through from duplicate cDNA syntheses was combined and precipitated for 3 hours at -20°C using 0.1x 3M sodium acetate and 2.5x 95% ethanol. Solution was then spun at 13,000 rpm for 25 minutes to pellet cDNA and all liquid was removed. The pellet was air-dried for 1 hour and resuspended in 20µl of nH_2O.

2.2.c. WNV Gene Amplification

WNV-infected Vero E6 (VE6) cell lysates were kindly donated by Antonia Dibernardo at the National Microbiology Laboratory in Winnipeg, Canada. Cell lysate RNA was purified using the RNeasy kit (Qiagen) as described above (section 2.2.2.). The cell lysate was, however, homogenized using the Qiashredder spin column (Qiagen) instead of a 20 gauge needle. Lysates were added to the Qiashredder columns and spun at 13,000 rpm for 2 minutes, and flow through was used for RNA purification. cDNA was then synthesized using the Superscript First Strand Synthesis System (Invitrogen). Briefly, 2µl of purified cell lysate RNA was mixed with 1µl of dNTP mix (10mM), either 1µl of WNV gene-specific reverse primer (Table 2.2) for each of the three WNV genes (2µM) or 2µl of random hexamers (50ng/µl) and brought up to 10µl with nH_2O. Reactions were incubated at 65°C for 5 minutes and placed on ice. The following components were then added to the reaction: 2µl of 10X RT buffer (200 mM Tris-HCl (pH 8.4), 500 mM KCl), 4µl of $MgCl_2$ (25mM), 2µl of dithiothreitol (0.1M) and 1µl of RNaseOUT™ recombinant RNase inhibitor (40 Units/µl). The entire reaction was then incubated at 42°C for 2 minutes (gene-specific primer reactions) or 25°C for 2 minutes (random hexamers). To all tubes, 1µl of Superscript™ II reverse transcripatase (50 units/µl) was added, and incubation continued at 42°C for 50 minutes to allow transcription. The cDNA synthesis was then incubated at 70°C for 15 minutes to denature the enzyme and was placed on ice. To remove any contaminating RNA, *E. coli* RNase H (2 units/µl) was added and incubated at 37°C for 20 minutes.

Using the NCBI database (http://www.ncbi.nlm.nih.gov), WNV gene-specific primers were designed based on the NY99 strain (GenBank accession number NC_009942) of the WNV genome (Table 2.2). Restriction enzyme "linkers" were added to the 3' ends of the primers to permit "in frame" ligation into the yeast two hybrid (Y2H) vector pGBKT7. Restriction sites NdeI and SmaI were added to the forward and reverse primers, respectively. WNV M and NS1 genes were amplified using Platinum® *pfx* DNA polymerase (Invitrogen). The following was added to 1µl of random hexamer derived WNV-infected Vero cell lysate cDNA: 2.5µl of 10x *pfx* amplification buffer, 0.75µl of dNTP mix (10mM), 0.5µl of $MgSO_4$ (50mM), 0.75µl M/NS1 forward primer (20µM), 0.75µl M/NS1 reverse primer (20µM), 0.4µl *pfx* DNA polymerase (2.5U/µl) and 18.35µl of nH_2O. PCR reactions were then performed using the following amplification conditions: denaturation at 95°C for 3 minutes; 30 cycles of 95°C for 30 seconds, 60°C for 30 seconds and 72°C for 1.5 minutes; a final elongation step at 72°C for 3 minutes.

Due to difficulty with WNV E gene amplification, HotStar Hifidelity Polymerase (Qiagen) was used in conjunction with differing amplification conditions. Briefly, 1µl of random hexamer derived WNV infected Vero cell lysate cDNA was added to 10µl of 5x Hifidelity PCR buffer (Tris Cl, KCl, $(NH_4)_2$ SO_4, 7.5 mM $MgSO_4$, bovine serum albumin, Triton® X-100, Factor SB; pH 8.7 (20°C), 1.5 mM dNTPs), 2µl of E forward primer (20µM), 2µl of E reverse primer (20µM), 1µl of HotStar Hifidelity DNA polymerase (2.5U/µl) and 34µl of nH_2O. One half of the PCR reactions performed contained an additional 1µl of $MgSO_4$ (25mM) to facilitate primer binding. PCR amplification conditions used were the same as those for the WNV M and NS1 amplifications; however, 4 different annealing temperatures were tested: 50°C, 56.3°C,

62.8°C and 66°C. PCR products were combined with 6x loading buffer and were resolved on a 1% agarose gel at 100 volts for 35 minutes. Gels were stained with SYBR gold nucleic acid stain (Molecular Probes) to enable visualization using an ultraviolet transilluminator.

Table 2.2. WNV restriction enzyme site-linked amplification primers used to amplify portions of the NY99 strain genome (NC_009942). Restriction enzyme recognition sequences are in italics.

Primer Name	Primer Sequence
REMemForward	5' *CATATG* TCACTGACAGTGCAGACACAC 3'
REMemReverse	5' *CCCGGG* GCTGTAAGCTGGGGCCACCA 3'
REEnvForward	5' *CATATG* TTCAACTGCCTTGGAATGAGCAACAGAGAC 3'
REEnvReverse	5' *CCCGGG* AGCGTCGACGTTCACGGAGAGGAAGA 3'
RENS1Forward	5' *CATATG* GACACTGGGTGTGCCATAGACATCAGC 3'
RENS1Reverse	5' *CCCGGG* AGCATTCACTTGTGACTGCACGAGGGTCT 3'

To isolate sufficient amounts of WNV gene products and to eliminate non-specific PCR products, bands of appropriate sizes were band-stabbed and re-amplified. Sterile 20 gauge syringe needles were used to stab resolved bands, and soaked in the PCR reaction mixture to be used as template for the PCR reaction. The PCR protocol was performed as described above.

2.2.d. WNV Gene Ligation and Cloning

PCR-amplified WNV genes were first cloned into the T-tailed pDrive (Qiagen) PCR cloning vector. Ligation into pDrive requires an adenine overhang on the PCR product, which is commonly added to PCR products when using standard Taq polymerase, but not when using the proofreading Taq (*pfx)* polymerase. To add the required adenine overhang to the WNV gene products, an A-Addition kit (Qiagen) was used. Briefly, 8µl of PCR product was incubated with 2µl of 5x A-addition master mix at

37°C for 30 minutes. PCR products were then ligated into pDrive according to the following protocol: 4µl of PCR product were combined with 1µl of pDrive cloning vector (50ng/µl) and 5µl of 2x ligation master mix and incubated at 4°C for 2 hours. Transformation into EZ competent cells (Qiagen) was then performed according to manufacturer's protocol. Transformed cells were then plated on LB plates containing 50µg/ml of ampicillin and were incubated upside down overnight at 37°C.

Resulting bacterial colonies were screened via PCR to identify which ones contained recombinant pDrive plasmids. Briefly, individual bacterial colonies were touched with a sterile loop and placed into single PCR tubes to be used as PCR template. To the tubes, the following mixture was added: 1µl of 10x PCR buffer (200mM Tris-HCl (pH 8.4), 500mM KCl), 0.4µl of $MgCl_2$ (50mM), 0.4µl of dNTP mix (10mM), 0.4µl each of 20 µM T7 and SP6 primers (Table 2.3), 0.08µl recombinant *Taq* polymerase (Invitrogen) and 7.32µl nH_2O. The following PCR program was then used to amplify the pDrive insert (if present): 95°C for 3 minutes to crack open the bacterial cells; 25 cycles of 95°C for 15 seconds, 55°C for 15 seconds and 72°C for 90 seconds; 3 minutes at 72°C. PCR products were combined with 6x loading buffer and resolved on 1% agarose gel at 100V for 30 minutes. Gels were stained with SYBR gold nucleic acid stain (Molecular Probes) to enable visualization using an ultraviolet transilluminator.

Table 2.3. pDrive colony screening and sequencing primers.

Primer Name	Primer Sequence
T7	5' TAATACGACTCACTATAGGG 3'
SP6	5' GATTTAGGTGACACTATAGAAG 3'

Colonies containing appropriately-sized inserts were grown overnight in 2ml of LB broth plus 50µg/ml ampicillin at 37°C and plasmid DNA was extracted using a Qiagen Spin Miniprep kit according to the manufacturer's specifications. Minipreps of pDrive containing WNV genes were then prepared for sequencing at the University of Calgary Core DNA Services. Miniprep plasmid DNA concentration was determined using the UltroSpec 3100 Pro spectrophotometer (Amersham Biosciences), and 5µg of plasmid template was precipitated using 2.5 volumes of 100% ethanol and 0.1 volumes of 3M sodium acetate. Tubes were left overnight at -20°C then spun at 13,000 rpm for 15 minutes to pellet the DNA. All liquid was removed, the pellet was washed with 70% ethanol to remove contaminating salts and was then dried in the DNA120 SpeedVac vacuum drier (Thermo Savant) for 15 minutes. To the dried pellet, 10.4µl of nH_2O and 1.6µl of 20µM sequencing primer T7 were added and the DNA samples were sent to the University of Calgary for sequencing.

pDrive with WNV inserts M, NS1 of E as well as yeast two hybrid vector pGBKT7 (500ng/µl) were then restriction enzyme digested in order to permit ligation of the inserts into the yeast two hybrid bait vector pGBKT7. An overview of the entire cloning procedure is shown in Figure 2.1. A precipitation step was required between individual digestion reactions as digestion buffers were not compatible. Although the Clontech protocol suggests using *Sma*I to ligate genes into the pGBKT7 vector, *Cfr*9I was used instead, as it recognizes the same sequence as *Sma*I, but produces an overhang that facilitates ligation. Eight microliters of pDrive miniprep, or 1µl of pGBKT7 were combined with 4µl of 10x *Cfr*9I buffer, 2µl of *Cfr*9I (Fermentas), filled to 40µl with nH_2O and incubated at 37°C for 90 minutes. Digested miniprep DNA was then

precipitated by adding 100µl of 95% ethanol and 4µl of 3M sodium acetate and incubating at -20°C for 2 hours. DNA was then pelleted and washed as described above. The pellet was resuspended in10µl of nH_2O and was used for the second restriction enzyme digest. 4µl of 10x FastDigest® buffer, 2µl of FastDigest *Nde*I (Fermentas) and 24µl of nH_2O was added to the resuspended pellet, and the mixture was allowed to incubate at 37°C for 20 minutes. The entire reaction was then combined with 6x loading buffer and resolved on a 1% agarose gel alongside a 1 kb plus ladder (Fermentas) at 100 volts for 30 minutes and gel fragments were visualized as described previously (section 2.2.c).Digested DNA fragments were excised from the agarose gel and gel-extracted using the Qiagen Gel Extraction kit according to the manufacturer's specifications.

Isolated WNV genes were ligated into pGBKT7 plasmids using Invitrogen T4 DNA ligase. As the yields of some of the DNA fragments were too low to quantify accurately using spectrophotometric techniques, several different vector: insert ratios were ligated in order to maximize the likelihood of obtaining recombinant pGBKT7 plasmids that contained WNV genes.

Ligated plasmids were transformed into EZ competent cells (Qiagen) as described above. Transformations were plated onto LB plus 30µg/ml kanamycin agar plates and incubated overnight at 37°C. Colonies were PCR-screened as described above, using the Matchmaker DNA-BD vector insert screening amplimer pair (Table 2.4). Colonies containing appropriately sized inserts were grown overnight in 2ml of LB broth plus 30µg/ml kanamycin at 37°C to enable plasmid purification using the Qiagen spin miniprep kit (as described above).

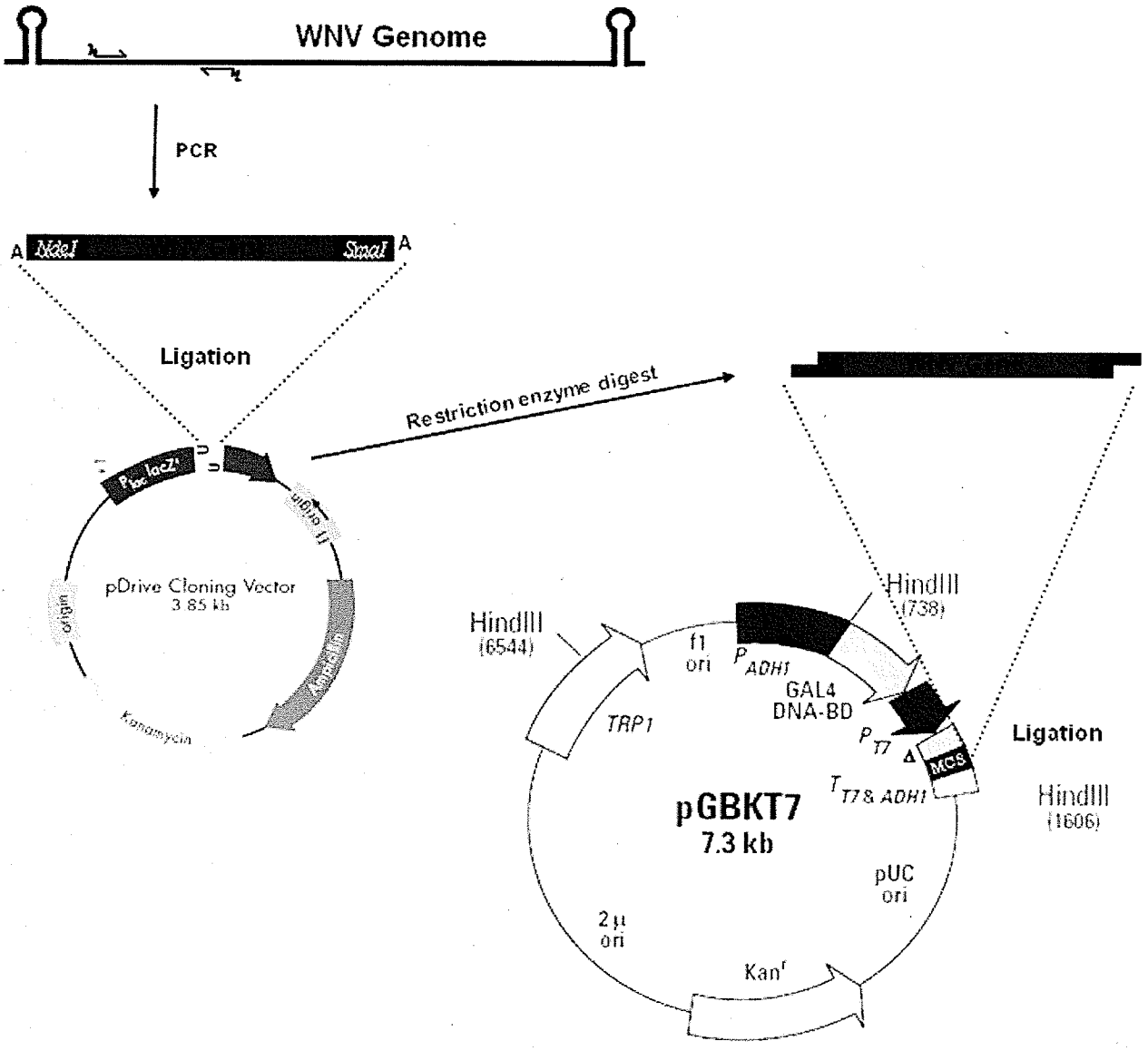

Figure 2.1. Cloning strategy used to insert WNV genes M and NS1 into pGBKT7 (vector images from Qiagen PCR Cloning Handbook 04/2001 and Clontech Protocol #PT3955-1.)

Table 2.4. pGADT7 insert screening and sequencing primers.

Primer Name	Primer Sequence
5' Sequencing Amplimer	5' CTATTCGATGATGAAGATACCCCACCAAACCC 3'
3' Sequencing Amplimer	5' GTGAACTTGCGGGGTTTTTCAGTATCTACGAT 3'

2.3. Yeast Culturing

Yeast strain AH109 was used for the yeast two hybrid assays. Yeast was grown on YPD agar plates supplemented with 30mg/L of adenine hemisulfate (YPDA) to prevent spontaneous ade1 or ade5 mutations (1). Colonies that had grown to 2-3mm diameter within 3-4 days, and were less than 30 days old, were chosen for the Y2H assay.

2.4. Yeast Two Hybrid Assay

2.4.a. Preparation of Competent Yeast

A small amount of frozen AH109 yeast stock was removed from its -80°C storage and streaked on a YPDA plate. Growth was allowed to occur for 4 days, and a single colony was used to inoculate 3ml of YPDA medium. The culture was incubated at 30°C for 8 hours, then 5µl was used to inoculate 50ml of YPDA medium. Yeast cultures were grown for up to 20 hours until the optical density (OD) reached a minimum of 0.15. Cells were then pelleted by centrifugation at 700 x g for 5 minutes, and resuspended in 100ml YPDA medium. The culture was further incubated for 4 hours until the OD reached a minimum of 0.4. Cells were then washed by once again pelleting and resuspending in 60ml of nH_2O. Finally, cells were pelleted again and resuspended in 3ml of 1.1x TE/LiAc solution. Cells were split into two 1.5 ml tubes, pelleted by centrifugation for 15 seconds and resuspended in 600µl of 1.1x TE/LiAc solution.

2.4.b. Transcriptional Activation/Toxicity Test of the DNA-BD WNV Fusion Protein

In a 15ml tube, the following solutions were added to 200µl of competent yeast cells in order to transform the bait plasmid: 6.66µl of denatured herring testes carrier DNA (10mg/ml) and 1.66µg of pGBKT7+M or NS1 insert. Following a brief vortex,

0.83ml of PEG/LiAc solution was added, the solution was vortexed again, and incubated at 30°C for 45 minutes. Following incubation, 53.3µl of DMSO added and the tube was placed in a 42°C water bath for 20 minutes. The cells were then pelleted by centrifugation at 700 x g for 5 minutes and resuspended in 1ml of YPD plus liquid medium. The culture was incubated at 30°C for 90 minutes, pelleted, and resuspended in 2ml of NaCl solution (0.9%). Six 100µl aliquots were then spread plated on three different selection plates: Minimal synthetic defined (SD) media lacking tryptophan (SD –Trp), lacking tryptophan and histidine (SD –Trp –His), or lacking tryptophan and adenine (SD –Trp –Ade).

Toxicity of the DNA-BD WNV fusion protein was assayed by inoculating 50ml of SD-Trp medium plus kanamycin with one large yeast colony containing pGBKT7 alone, or containing pGBKT7-M or NS1. The culture was incubated at 30°C for 24 hours with shaking at 250 rpm. The optical densities of the WNV bait plasmid cultures were compared to the empty plasmid to ensure no major inhibition of growth occurred. A total of 100µl of each of the 3 cultures was then measured using a spectrophotometer, with uninoculated media used as a blank.

2.4.c. Yeast Two Hybrid Screening by Cotransformation

The following components were added to 600µl of competent yeast cells (as described above), to cotransform the bait and target vectors: 20µl of mosquito gut cDNA, 6µl of *Sma*I linearized pGADT7 (0.5µg/µl), 5µg of pGBKT7 plasmid and 20µl of denatured herring testes carrier DNA. Following a gentle mix, 2.5 ml of PEG/LiAc solution was added and the cells were incubated at 30°C for 45 minutes, mixing every 15 minutes. DMSO (160µl) was then added and the cells were placed in a 42°C water bath for 20 minutes, mixing half way through. The cells were then pelleted by centrifugation

at 700 x g for 5 minutes, and resuspended in 3ml of YPD plus medium (Clontech). Cells were then incubated at 30°C with shaking for 90 minutes, pelleted, and resuspended in 6ml of 0.9% NaCl solution. To select for true protein interactions, cells were plated in 40µl aliquots on triple dropout plates (TDO) lacking histidine, leucine and tryptophan. To determine transformation efficiency, a 30µl aliquot of cells was diluted 25 fold in 0.9% NaCl solution and 150µl aliquots were spread on SD medium lacking either leucine or leucine and tryptophan.

Small scale transformations of Y2H controls were also performed to validate the yeast two hybrid assay. To 50µl of competent yeast cells the following components were added: 5µl of SV40 large T PCR fragment (25ng/µl), *Sma*I linearized pGADT7-Rec (500ng/µl), either 0.5µl of pGBKT7-53 (containing the murine p53 gene)(500ng/µl) as a positive control or pGBKT7-Lam (containing the human Laminin C gene)(500ng/µl) as a negative control, 5µl of denatured herring testes carrier DNA (10mg/ml) and 500µl of PEG/LiAc solution. The remaining protocol is identical to the one described above, except that the yeast was diluted 1:10, 1:100 and 1:1000 in 0.9% NaCl solution and plated on QDO plates as well as SD –Leu –Trp to check for transformation efficiency.

Yeast plates were allowed to incubate at 30°C for 3-4 days to allow yeast growth. To eliminate some of the yeast colonies that contained more than one type of recombinant pGADT7 plasmid, and to ensure that protein interactions were indeed authentic, individual yeast colonies were replated 2-3 times on quadruple dropout medium (QDO) lacking histidine, leucine, tryptophan and adenine. Yeast colonies that grew on QDO medium were then PCR screened for pGADT7 mosquito gut cDNA inserts using the Matchmaker AD LD-screening amplimer set (Clontech). Briefly, small amounts

of individual yeast colonies were placed in PCR tubes to be used as template, and the following components were added: 1µl of 10x Advantage 2 PCR buffer, 0.2µl of the 5' screening amplimer (20µM), 0.2µl of the 3' screening amplimer (20µM), 0.2µl of dNTP mix, 0.2µl of Advantage 2 polymerase and 8.2µl of nH_2O. The following PCR cycle was then performed to amplify the cDNAs contained within the pGADT7 vector: denaturation at 95°C for 30 seconds was followed by 25 cycles of 94°C for 30 seconds, and 68°C for 3 minutes. A final elongation step at 68°C for 3 minutes was performed to ensure all products were fully elongated. Following PCR amplification, all 10µl were combined with 6x loading buffer and resolved on a 1% agarose gel alongside a 1kb plus ladder (Fermentas). Individual bands were excised and the amplified DNA was extracted using the "freeze N squeeze" gel extraction protocol based on a procedure developed by Thuring et al. (119). Briefly, the excised bands were crushed using a sterile mortar and pestle and frozen at -80°C for 30 minutes. The frozen gel was then centrifuged at 13,000rpm for 15 minutes to pellet all of the solidified gel. The liquid supernatant was removed and to it, 2.5x 100% ethanol and 0.1x 3M sodium acetate was added to precipitate DNA as mentioned above. Washed DNA was then resuspended in 20µl of nH_2O.

2.4.d. pGADT7 Insert Sequencing

Mosquito gut cDNA inserts were prepared for sequencing using the Bigdye® terminator v3.1 cycle sequencing kit (Applied Biosystems). The cycle sequencing reaction was prepared by adding the following components to 2µl of gel extracted pGADT7 insert DNA: 3.5µl of 5x bigdye sequencing buffer, 1µl ready reaction mix, 1.6 µl T7 primer (2mM) and 11.9µl nH_2O. Sequencing products were then amplified as

follows: denaturation at 96°C for 1 minute, followed by 25 cycles of 96°C for 10 seconds, 50°C for 5 seconds and 60°C for 4 minutes. Amplified products were then precipitated by adding 5µl of 125mM EDTA and 60µl of 100% ethanol, and allowed to sit at room temperature for 15 minutes. Tubes were then centrifuged at 13,000 rpm for 15 minutes, and the pellet was washed with 70% ethanol. The pellets were then dried for 10 minutes in a vacuum drier and resuspended in 20µl of Hi-Di™ formamide (Applied Biosystems). DNA was denatured at 94°C for 5 minutes and immediately placed on ice to prevent re-annealing. Samples were then loaded onto a 48 well plate and sequenced using an Applied Biosystems 3130 Genetic Analyzer sequencer.

Aedes aegypti cDNA insert identity was determined using the genome and expression data available at the NCBI (http://www.ncbi.nlm.nih.gov/) and Vectorbase (http://aaegypti.vectorbase.org/index.php) databases.

2.5. Co-Immunoprecipitation

To validate the protein interactions between viral NS1 and selected mosquito gut proteins identified using the Y2H method, *in vitro* co-immunoprecipitation (Co-IP) using the Matchmaker™ Co-IP kit (Clontech) was performed. To obtain the cDNA plasmids required for *in vitro* transcription and translation, a yeast plasmid extraction was required. This was performed using lyticase, which degrades the yeast cell wall creating spheroplasts, followed by a modified miniprep using the Qiagen miniprep kit. Yeast lawns containing the plasmids of interest were first grown on QDO plates at 30°C for three to four days. Yeast were then scraped off the plates using a cover slip and placed in a microfuge tube. To the tubes, 100µl of lyticase solution (1.2M sorbitol, 0.1M $NaPO_4$,

pH 7.5, 5mg/ml lyticase [Sigma]) was added, and cells were incubated at 37°C for 30 minutes. To prevent nuclease degradation of the plasmids, 20µl of 50µg/µl proteinase K (Epicentre Biotechnologies) was added and the solution was incubated at 70°C for 10 minutes. To the reaction, 200µl of buffer P1 was then added, followed by 300µl of buffer P2, brief mixing, 470µl of N3 and a final mix. The entire mixture was then centrifuged at 13,000 rpm for 10 minutes and the supernatant was added to the miniprep spin column. The remaining protocol followed the manufacturer's specifications, and the plasmid was eluted into 50µl of EB buffer. This yeast plasmid extraction protocol invariably resulted in contamination with yeast genomic DNA, so plasmids were therefore retransformed into subcloning efficiency DH5α cells according to the manufacturer's specifications. Positive colonies were first screened with the plasmid sequencing amplimers (Table 2.4) using the protocol mentioned in section 2.2.d, and then purified using the Qiagen miniprep kit. To obtain the entire nucleotide sequences as well as their position within the Y2H vectors, chosen pGBKT7 and pGADT7 vectors were sequenced according to the protocol described in section 2.4.d.

Prior to Co-IP, radiolabeled proteins were produced using the TnT® T7 Coupled Reticulocyte Lysate System (Promega) and ^{35}S Methionine (Perkin Elmer). The reticulocyte lysate system is capable of transcribing and translating protein within a single reaction, using the Y2H plasmids as a template. The following reagents were combined and incubated at 30°C for 90 minutes: 12.5µl of TnT® rabbit reticulocyte lysate, 1µl of TnT® reaction buffer, 0.5µl of TnT® RNA polymerase, 0.5µl of amino acid mixture minus methionine (1mM), 1µl of ^{35}S methionine (>1000Ci/mmol at 10mCi/ml), 0.5µl of RNasin® ribonuclease inhibitor (40 units/µl), 2µg of either pGADT7-cDNA or

pGBKT7-NS1 plasmid, and nH_2O up to a final volume of 25µl. Control plasmids pGBKT7-53 and pGADT7-T containing murine p53 and SV-40 large T antigen respectively were translated alongside test samples to serve as a positive control (as was done in the Y2H assay). Denaturing polyacrylamide gel electrophoresis was used to analyse a small aliquot of the translation products. Briefly, 3µl of the reticulocyte lysate reaction was added to 5µl of 5x loading buffer and 17µl of nH_2O and the solution was heated at 95°C for 2 minutes to denature the proteins. Approximately 15µl was then resolved on a 10% polyacrylamide gel alongside 10µl of Precision Plus protein ladder (Bio-Rad) at 200V for 45 minutes. Following electrophoresis, the gel was wrapped in plastic wrap, and exposed to a phosphor screen for approximately 24 hours to ensure that sufficient radioactive emission struck the screen. The phosphor screen and the protein gel containing the prestained ladder were then scanned using the PharosFX Molecular Imaging System (Bio-Rad) and compared in order to estimate protein size.

Translated radiolabeled proteins containing their respective tags were then combined *in vitro* to confirm protein interactions via Co-IP according to the manufacturer's protocol (Figure 2.2). Briefly, 10µl of translated bait and library protein were combined and allowed to incubate at room temperature for 1 hour. 10µl of either c-Myc monoclonal antibody or HA-tag polyclonal antibody were then added and left to incubate at room temperature for 1 hour. Protein A beads were washed twice with PBS and 3µl of beads were added to each reaction. Tubes were then incubated at room temperature for 1 hour with rotation to ensure adequate mixing. Beads were then washed 5 times with wash buffer 1 and twice with wash buffer 2 to eliminate non-specific binding to the protein A beads. Beads were then resuspended in 20µl of denaturing gel

loading buffer, heated at 80°C for 5 minutes and quickly spun down. 15µl of supernatant was then resolved on a 10% polyacrylamide gel at 200V for 45 minutes, and visualized as described above.

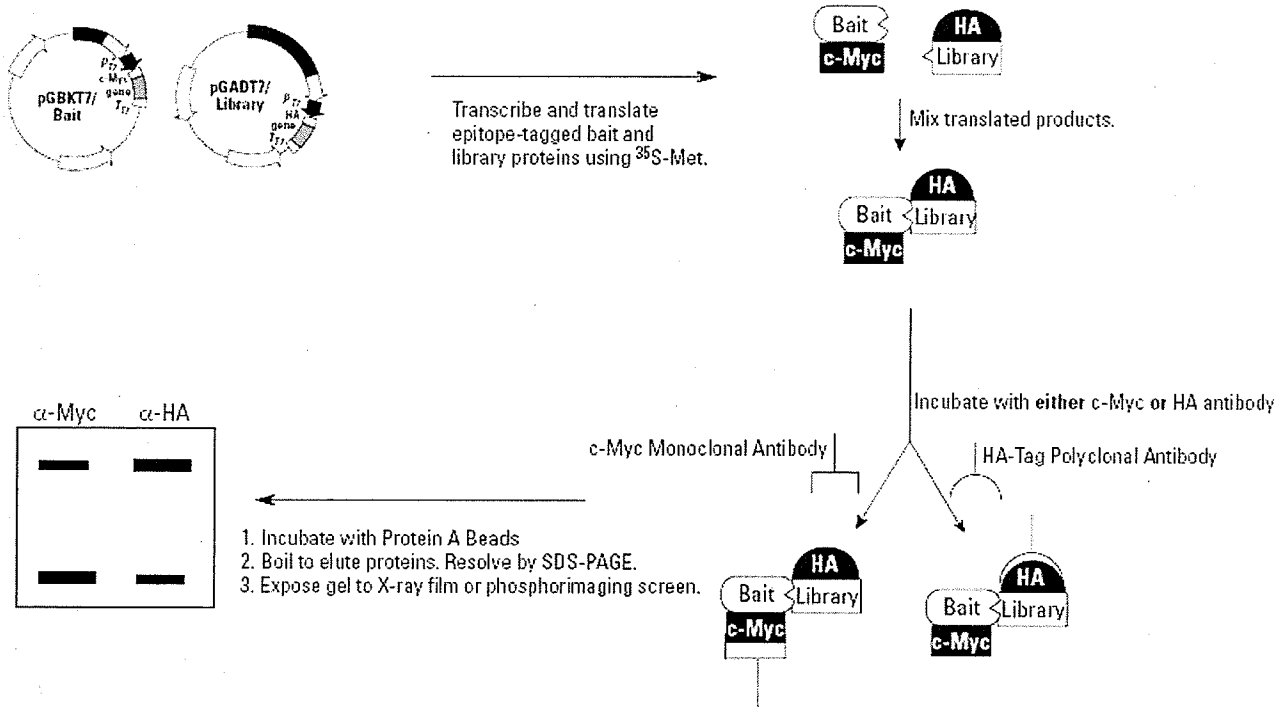

Figure 2.2. *In vitro* transcription and translation of Y2H genes followed by Co-IP and denaturing gel electrophoresis (from Clontech Protocol #PT3323-1).

2.6. Cloning of *Aedes albopictus* Homologues

2.6.a. Gene Fragment Amplification and Cloning

From the suite of protein interactions identified using the Y2H method, three interactions were chosen for further study. The mucin-like protein IMUC1, early trypsin and elongation factor 2 (EF2) identified using WNV NS1 as bait were chosen for follow-up work using cell culture infectivity assays. Unfortunately, there are no *Aedes aegypti*

cell lines available, and creating a primary cell line can be troublesome and time consuming. To bypass this problem, an already established embryonic cell line from *Aedes albopictus* (C6/36) was used.

Because homologues to the chosen genes have not been identified in *Aedes albopictus*, amplification was required using degenerate primers based on known sequences from mosquito and fly species. Gene homologues were identified using the BLAST feature of the NCBI database (http://blast.ncbi.nlm.nih.gov/Blast.cgi), and were then aligned using ClustalW multiple sequence alignment software. Primers were designed using conserved regions of the genes (Table 2.5), but amplifying the genes in their entirety was not possible due to lack of sequence data and conserved regions at the 5' and 3' termini.

Table 2.5. Degenerate primers used for the amplification of *Aedes albopictus genes.*

Primer Name	Primer Sequence*
MucinF1	5' CAGTTCYKSAGYYRTCMRCCA 3'
MucinF2	5' CGTYWCTKTTGGCKGTGACC 3'
MucinR	5' CKGCCARCKCTGGCCAATC 3'
TrypsinF	5' ATCGTHGGMMGGRTTCCAGATCG 3'
TrypsinR	5' TCTCCYTGGCARGMRTCCT 3'
EF2F	5' ATGGTYAACTTYACCGTYGAC 3'
EF2R	5' TTTACARYTTGTCCAAGTACTG 3'

* Single letter code used for degenerate primers: R (A/G), W (A/T), Y (C/T), K (G/T), S (C/G), M (A/C), H (A/C/T).

Aedes albopictus genomic DNA was kindly provided by Dr. Mahmood Iranpour (Department of Entomology, University of Manitoba), and was used for mucin and trypsin sequence PCR amplification. Genomic DNA was used because it was more readily available and the mucin and trypsin genes lacked introns within the amplified

regions. To facilitate amplification, multiple annealing temperatures and magnesium concentrations were used. Briefly, the following was added to 0.5µl of genomic DNA: 2µl of forward degenerate primer (20µM), 2µl of reverse degenerate primer (20µM), 1 or 2µl of $MgCl_2$ (50mM), 1µl of dNTP mix (10mM), 2.5µl of 10x PCR buffer (200mM Tris-HCl (pH 8.4), 500mM KCl), 0.2µl of recombinant *Taq* polymerase (Invitrogen), and topped up to 25µl with nH_2O. The following PCR program was used for sequence amplification: 95°C for 1 minute; 30 cycles of 95°C for 30 seconds, 53/55.5/60.4°C for 15 seconds and 72°C for 30 seconds; 3 minutes at 72°C. PCR products were combined with 6x loading buffer and resolved on 1% agarose gel at 120V for 40 minutes.

EF2 PCR required cDNA for sequence amplification due to large introns present within the amplified region. The *Aedes albopictus* embryonic cell line (C6/36) was kindly provided by Antonia Dibernardo at the National Microbiology Lab, and was used for an RNA extraction and cDNA synthesis. Briefly, cells were dislodged from the culture flask by forceful tapping, and the media was placed in a 25ml test tube. Cells were pelleted by centrifugation at 2500 rpm, and the supernatant was removed. Cells were placed in 600µl of buffer RLT and were homogenized using the Qiashredder column as mentioned in section 2.2.c. The Qiagen RNeasy kit was then used to extract total RNA from the cells according to the manufacturer's specifications. Extracted RNA was eluted into 50µl of nH_2O. Using 8µl of total RNA and oligo-dT primers, cDNA was produced using the Superscript First Strand Synthesis System (Invitrogen) as mentioned in section 2.2.c. To amplify the EF2 sequence, the following was added to 0.5µl of C6/36 cDNA: 0.4µl of EF2F primer (20µM), 0.4µl of EF2R primer (20µM), 0.4µl of $MgCl_2$ (50mM), 0.4µl of dNTP mix (10mM), 1µl of 10x PCR buffer (200mM Tris-HCl (pH 8.4), 500mM KCl),

0.08µl of recombinant *Taq* polymerase (Invitrogen), and 7.32µl of nH_2O. EF2 was then amplified according to the following PCR protocol: 95°C for 1 minute; 30 cycles of 95°C for 30 seconds, 50/55/59°C for 30 seconds and 72°C for 1 minute and 30 seconds; 3 minutes at 72°C. PCR products were combined with 6x loading buffer and resolved on 1% agarose gel at 100V for 30 minutes.

Gels were first stained with SYBR gold nucleic acid stain (Molecular Probes) to enable visualization using an ultraviolet transilluminator. Bands were then excised from gels and DNA was extracted using either the freeze N squeeze method (section 2.4.c) for mucin and trypsin gene fragments or the Qiagen gel extraction kit (section 2.2.d) for the EF2 fragment. To ligate the gene fragments into pDrive, 2µl of purified PCR product was added to 0.5µl of pDrive cloning vector (50ng/µl) and 2.5µl of 2x ligation buffer. Reactions were incubated at 12°C for 1 hour, and were then transformed into subcloning efficiency DH5α cells (Invitrogen) according to the manufacturer's specifications. Resulting colonies were screened using T7 and SP6 primers as mentioned in section 2.2.d. Positive colonies were used to inoculate 3ml of 2YT +Amp (50µg/ml) broth, and were grown overnight at 37°C. Plasmids were then extracted using the Qiagen Miniprep kit according to the manufacturer's specifications as in section 2.4.d.

To ensure that the amplified sequences were in fact *Aedes aegypti* homologues, the extracted plasmids were sequenced according to the protocol stated in section 2.4.d. using 2µl of plasmid. The Vectorbase database (http://aaegypti.vectorbase.org/index.php) was then queried to ensure that the sequenced inserts were in fact homologues to the identified *Aedes aegypti* sequences.

To enable the production of dsRNA, *Aedes albopictus* genes were ligated into the pL4440 plasmid, which contains T7 promoters flanking both the 5' and 3' ends (Figure 2.3). Briefly, 6µl of both pDrive containing *Aedes albopictus* genes and pL4440 were added to 2µl of 10x FastDigest buffer, 1µl of *Kpn*I (Fermentas), 1µl of *Sac*I (Fermentas) and 10µl of nH_2O. Reactions were incubated at 37°C for 20 minutes, combined with 6x loading buffer and resolved on a 1% agarose gel, run at 110V for 35 minutes. Digested inserts and pL4440 were then excised from the gel and DNA was extracted using the freeze N squeeze method (section 2.4.c). *Aedes albopictus* gene EF2 contains two *Kpn*I sites resulting in 3 products of approximately 250bp, 600bp and 1050bp. The 600bp fragment was chosen for ligation into pl4440. Gene fragments were ligated into pl4440 using T4 DNA ligase (Invitrogen) and a number of vector:insert ratios to maximize the likelihood of ligation. Ligated plasmids were then transformed into subcloning efficiency DH5α cells according to the manufacturer's description. To screen for vector inserts, pL4440 screening primers (Table 2.6) were used along with the protocol used in section 2.2.d. Positive colonies were then used to inoculate broth and extract plasmid using the Qiagen miniprep kit as stated above.

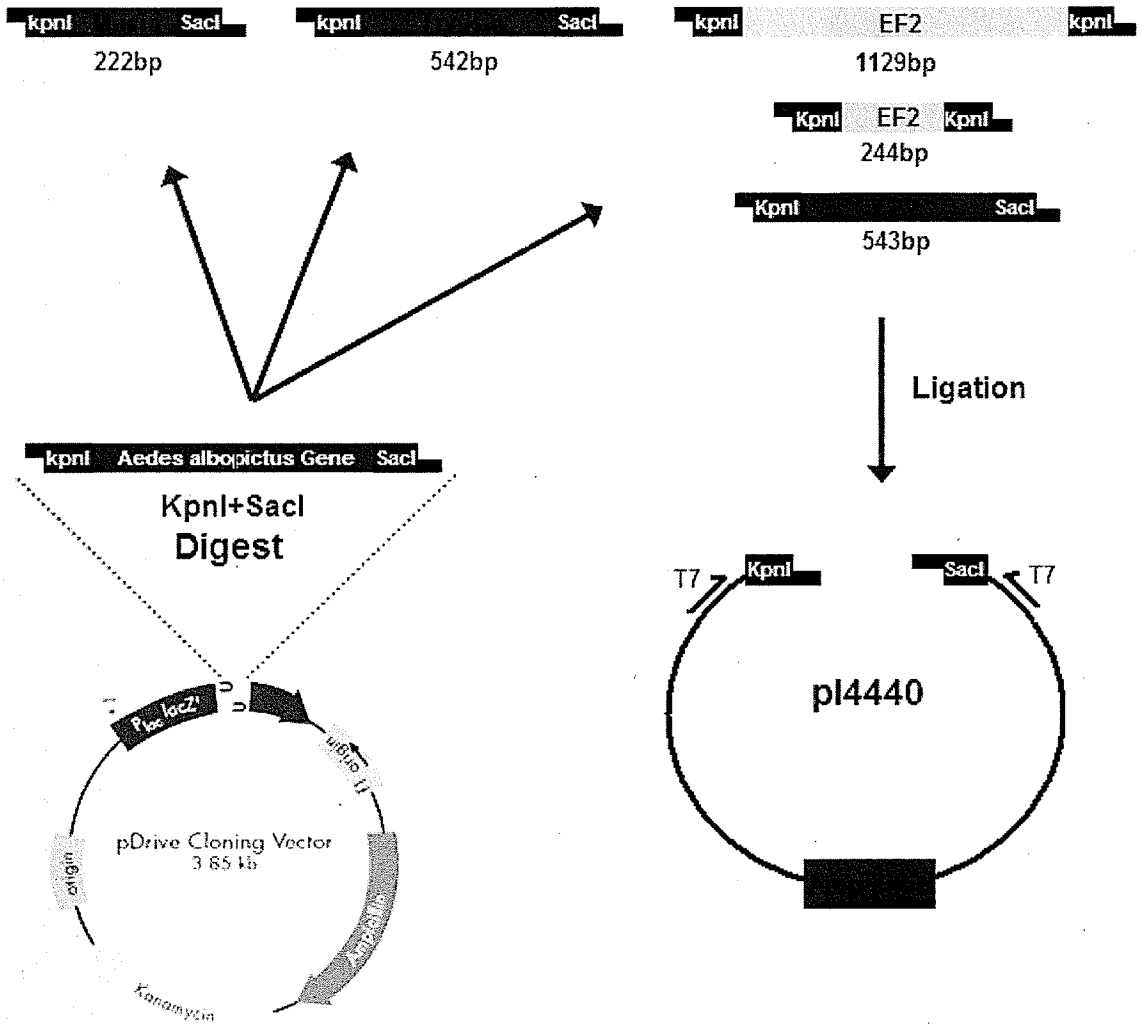

Figure 2.3. Cloning strategy for insertion of *Aedes albopictus* genes into pI4440. Grey gene segments were not chosen for ligation into pI4440 (pDrive vector from Qiagen PCR Cloning Handbook 04/2001).

Table 2.6. pL4440 screening primers

Primer Name	Primer Sequence
pI4440F	5' CCACCTGGCTTATCGAA 3'
pI4440R	5' TAAAACGACGGCCAGTGA 3'

2.6.b. Cloning of an *Aedes albopictus* Mucin Fragment for Real Time PCR

Time constraints prevented all three gene homologues from being followed up, and therefore the *Aedes albopictus* mucin gene (*AaImuc1*) was chosen for dsRNA synthesis and knockdown in WNV infectivity assays. In order to measure the expression of *AaImuc1* RNA in cell cultures effectively, a larger portion of the *AaImuc1* mRNA was required. If primers were designed that overlapped with the dsRNA being administered to C6/36 cells, they would amplify the cellular RNA as well as the added dsRNA, producing inflated measurements of mucin RNA levels.

Using the *AaImuc1* sequence data, as well as the sequence alignment explained in section 2.6.a., primers were designed to amplify a larger portion of the *AaImuc1* mRNA (Table 2.7). The resulting forward primer was *Aedes albopictus*-specific based on sequenced data and the reverse primers were *Aedes aegypti*-specific based on conserved regions within the mucin sequence. Briefly, the following was added to 0.5µl of *Aedes albopictus* genomic DNA: 1µl of forward primer (20µM), 1µl of reverse primer (either R1 or R2) (20µM), 1 of $MgCl_2$ (50mM), 1µl of dNTP mix (10mM), 2.5µl of 10x PCR buffer (200mM Tris-HCl (pH 8.4), 500mM KCl), 0.2µl of recombinant *Taq* polymerase (Invitrogen), and topped up to 25µl with nH_2O. The following PCR program was then used for sequence amplification: 95°C for 1 minute; 30 cycles of 95°C for 30 seconds, 53/56/59°C for 30 seconds and 72°C for 45 seconds; 3 minutes at 72°C. PCR products were combined with 6x loading buffer and resolved on 1% agarose gel at 100V for 30 minutes.

Resulting bands were then excised, and purified as described in section 2.6.a. Cloning and sequencing was then performed as described in section 2.6.a and the newly obtained mucin sequence was used for qRT-PCR primer design.

Table 2.7. *Aedes albopictus* mucin fragment amplification primers

Primer Name	Primer Sequence
AlbMucinF1	5' ACTTGGTCTTCCTGCCCCACG 3'
AlbMucinR1	5' ATGCCTCCCCATGTGCA 3'
AlbMucinR2	5' ACATCCGGCTTGGGCAGG 3'

2.7. Double Stranded RNA Synthesis

In order to understand whether *AaImuc1* plays a role in the infection and/or replication of WNV in cell culture, a dsRNA-mediated gene knockdown was performed. The Megascript™ RNAi kit from Ambion was used to create dsRNA necessary for *Aedes albopictus* gene knockdown using the T7 flanked pL4440 plasmids previously constructed. Prior to dsRNA synthesis, a large amount of linear DNA template containing flanking T7 promoters is required. This was achieved by PCR amplifying *AaImuc1* from the pL4440 plasmid, and precipitating it to concentrate the template. As a negative control, Dr. Steve Whyard kindly provided a pL4440 plasmid containing the *gus* gene. The *gus* gene, which codes for the *E. coli* protein beta-glucuronidase is a suitable dsRNA negative control as the gene is not found in other higher organisms.

To amplify template for the dsRNA construction kit, 2µl of pL4440 plasmid containing either *gus* or *AaImuc1* were combined with the following: 8µl of pL4440F primer (20µM), 8µl of pL4440R primer (20µM), 8µl of $MgCl_2$ (50mM), 8µl of dNTP mix (10mM), 20µl of 10x PCR buffer (200mM Tris-HCl (pH 8.4), 500mM KCl), 1.6µl

of recombinant *Taq* polymerase (Invitrogen), and 144.4µl of nH_2O. Mucin and gus gene fragments were then amplified according to the following PCR protocol: 95°C for 1 minute; 30 cycles of 95°C for 30 seconds, 55°C for 30 seconds and 72°C for 30 seconds (*AaImuc1*) or 1 minute and 30 seconds (*gus*); 3 minutes at 72°C. A small amount of PCR product was then combined with 6x loading buffer and separated on a 1% agarose gel followed by visualization using SYBR gold (Molecular Probes) to ensure that the specified genes were amplified. Template was finally ethanol precipitated overnight as mentioned in section 2.2.b, and resuspended in 30µl of nH_2O.

Synthesis of *gus* and *AaImuc1* dsRNA was performed according to the manufacturer's protocol. Briefly, 8µl of T7 flanked template (containing 1-2µg of DNA) was combined with 2µl each of 10x T7 reaction buffer, ATP (75mM), GTP (75mM), UTP (75mM), CTP (75mM) and T7 enzyme mix, followed by incubation at 37°C for 4 hours. Reactions were then heated to 75°C for 5 minutes and allowed to cool to room temperature to promote annealing of complementary RNA templates. Reactions were then nuclease digested and column purified as specified by the manufacturer. Finally, dsRNA was eluted into 150µl of nuclease free H_2O and a 1µl aliquot was combined with 6x loading buffer and visualized on a 1% agarose gel stained with SYBR gold (Molecular Probes) to ensure adequate transcription and purification took place.

2.8. Cell Culture Infectivity Assays

2.8.a. Cell Line Maintenance and Virus Propagation

An *Aedes albopictus* embryonic cell line (C6/36) kindly provided by Antonia Diberndardo of the National Microbiology Laboratory was cultured in Eagle's Minimal

Essential Media (MEM) with 10% fetal bovine serum (FBS). Cells were grown to near confluence at 30°C and 5% CO_2 and split 1:10 approximately every 7 days. Because C6/36 cells are semi-adherent, no trypsin was required to dislodge cells during passaging. Flasks were shaken vigorously to dislodge cells, and an aliquot was placed in new medium.

The Vero E6 cell line, isolated from kidney epithelial cells of the African green monkey, was used to culture WNV. Cells were cultured by Antonia Dibernardo at the National Microbiology Lab in BSL-3 containment using Dulbecco's Modified Eagle's Medium (DMEM) containing 10% FBS, at 37°C with 5% CO_2. Cells were grown to near confluence, and were passaged into fresh media at a ratio of 1:5 approximately every 7 days, using a 0.25% trypsin-EDTA solution to remove the cells from the substrate. Working stocks of WNV were produced by removing culture supernatants from infected Vero cell cultures exhibiting extensive cytopathic effects. Briefly, media was removed, and frozen to lyse any cells present. Once thawed, the lysate was centrifuged at 1500 rpm for 15 minutes and heat inactivated FBS was added to a final concentration of 20%. Virus was then aliquoted into 1.5ml tubes and frozen at -80°C until ready for use. Prior to performing infectivity assays, the number of plaque forming units was determined, as freeze thawing virus results in decreased infectivity.

2.8.b. Determination of WNV Infection Titer and Cell Plating Density

Prior to performing any assays measuring the effect of mucin expression on WNV infection and replication in mosquito cells, a suitable WNV titer had to be determined for infection. Too much virus was liable to overly inhibit cell growth and interfere with PCR

quantification (qRT-PCR), whereas too little virus may replicate too slowly in culture and/or prevent adequate measurement dsRNA-induced inhibition of viral replication.

Aedes albopictus C6/36 cells were first added to individual wells of a 12 well plate at a concentration of either 1 x 10^5 or 2.5 x 10^5 cells/ml. Cells were grown at 30°C for 42h to mimic conditions used in future infection assays (please see 2.8.c) followed by infection with WNV. Briefly, all but a small amount of media was removed from wells and 100µl of virus diluted in BA-1 medium was added. Vero cell cultured WNV was kindly provided by Antonia Dibernardo at a stock concentration of 6.5 x 10^7 pfu/ml. Three different dilutions of virus were added to both cell densities in duplicate: 6.5 x 10^7, 6.5 x 10^6 and 6.5 x 10^5 pfu/ml, resulting in final concentrations of 6.5 x 10^6, 6.5 x 10^5, 6.5 x 10^4 pfu/ml. WNV infection was then allowed to proceed at 30°C for 1 hour, with mild shaking every 15 minutes. After 1 hour, 900µl of Eagle's MEM was added to each well, for a final volume of 1ml. Cells were grown for 96h at 30°C, and were observed approximately every 24h for any visible cytopathic effects (CPE), as well as changes in cell densities over time resulting in growth, or viral inhibition thereof.

Because higher viral titers resulted in CPE, lower titers were assayed using quantitative real time PCR (qRT-PCR) to determine an appropriate virus:cell ratio that was adequate for future qRT-PCR measurement. Based on previous results, cells were plated at a density of 2.5 x 10^5 cells/ml and were infected with a titer of 6.5 x 10^6 and 6.5 x 10^4 pfu/ml. Post-infection, cells were either frozen immediately (0 h), or were incubated at 30°C in increments of 24h, up to 96h, and frozen. To determine the abundance of viral and host transcripts following dsRNA treatment as well as viral infection, RNA was extracted from cells, followed by cDNA synthesis and qRT-PCR.

Frozen cells were first thawed and 200µl of media was added to 400µl of buffer RLT (Qiagen). Freezing cells at -80°C results in a loss of adherence, and therefore no agitation was required to loosen cells from the substrate. The 200µl of media removed therefore included both intracellular and extracellular viral RNA as well as cellular RNA. Cells were first homogenized using the Qiashredder spin column (Qiagen) and RNA was extracted using the RNeasy kit (Qiagen) according to the manufacturer's specifications. RNA was eluted into a final volume of 40µl of nH_2O. To ensure that no contaminating DNA was present, an aliquot of extracted RNA was then DNase treated. Briefly, 8µl of RNA was added to 1µl of amplification grade DNase (Invitrogen) and 1µl of 10x DNase reaction buffer. The reaction was then incubated at room temperature for 15 minutes, followed by an addition of 1µl of EDTA (25mM) and incubation at 65°C for 10 minutes to denature the DNase. The High Capacity cDNA Reverse Transcription Kit with RNase Inhibitor (Applied Biosystems) was next used to produce cDNA from the DNase treated RNA. cDNA was synthesized by adding 6.6µl of RNA to 1µl of 10x RT buffer, 1µl of 10x random primers, 0.4µl of 25x dNTP mix (25mM), 1µl of RNase inhibitor and 1µl of MultiScribe™ reverse transcriptase. Reverse transcription was then performed according to the manufacturer's protocol.

qRT-PCR was performed next to determine the fold increase in WNV amplicons and cellular growth at specific time points post-infection. To measure WNV genome amplification, a segment of the 3' untranslated region (UTR) was used for amplification, whereas a segment of a ribosomal protein gene *RpL8* (GenBank accession number M99055) was used for quantification of cellular growth (Table 2.8). The following reagents were combined with 1µl of synthesized cDNA (in duplicate): 10µl IQ SYBR

Green Supermix (Biorad), 1µl of forward primer (10mM), 1µl of reverse primer (10mM) and 7µl of nH_2O. The Bio-Rad IQ5 RT-PCR detection system was used to amplify the cDNA using the following conditions: denaturation at 95°C for 3 minutes; 40 cycles of 95°C for 10 seconds and 55°C for 30 seconds. To ensure that non-specific primer annealing was not producing undesired PCR products, a melt curve analysis was performed post-PCR reaction. Tubes were heated for 80 cycles, beginning at 55°C with an increase of 0.5°C every cycle. Dissociation of double stranded DNA results in a decrease in SYBR Green fluorescence and therefore a melting temperature can be determined. Because each PCR product has a different melting point, multiple peaks in a melt curve indicate that multiple products are present.

Table 2.8. qRT-PCR primer list

Primer Name	Primer Sequence
RTrpl8F	5' TGGGGCGTGTTATTCGT 3'
RTrpl8R	5' TTTGGGCTCTCCCTTTC 3'
RTMucF	5' ACCCAAATCACACAGCCTTCTTGC 3'
RTMucR	5' GCAGATGCTGGCCTGTTGATTCC 3'
WNVUTRF*	5' AGAGTGCAGTCTGCGATAGTGC 3'
WNVUTRR*	5' CCTTTCGCCCTGGTTAACA 3'

*WNV UTR primers taken from (46).

The degree of WNV proliferation was determined using the ΔΔCt method (79, 109) to determine the fold increase in WNV. The *RpL8* standard was used to normalize the data relative to cell growth, and WNV growth at 48 h and 72 h was compared to time 0 h to determine the increase in viral genome copies.

To determine an adequate cell density for viral infection, three cell densities were plated in duplicate (from two separate cell populations) into 12 well plates. C6/36 cells

were plated at a density of 1 x 10^5, 2.5 x 10^5 and 5 x 10^5 cells/ml and cell density was counted at 48 h, 72 h and 96h using a hemocytometer. Cell density was also microscopically observed at all time points to ensure that high cell density would not interfere with cell growth.

2.8.c. Cell culture Infection and dsRNA Treatment

To determine whether the identified mucin plays a role in WNV infection in cell culture, C6/36 cells were infected with WNV following gene-specific dsRNA treatment. Cells were either treated with *gus* or *AaImuc1* dsRNA, followed by infection with WNV. To provide a basis for comparison, cells were also assayed with no dsRNA treatment as well as no WNV infection. Once treated and/or infected, cells were collected at three time points: 0 h (immediately after infection), 48 h and 72 h (Figure 2.4).

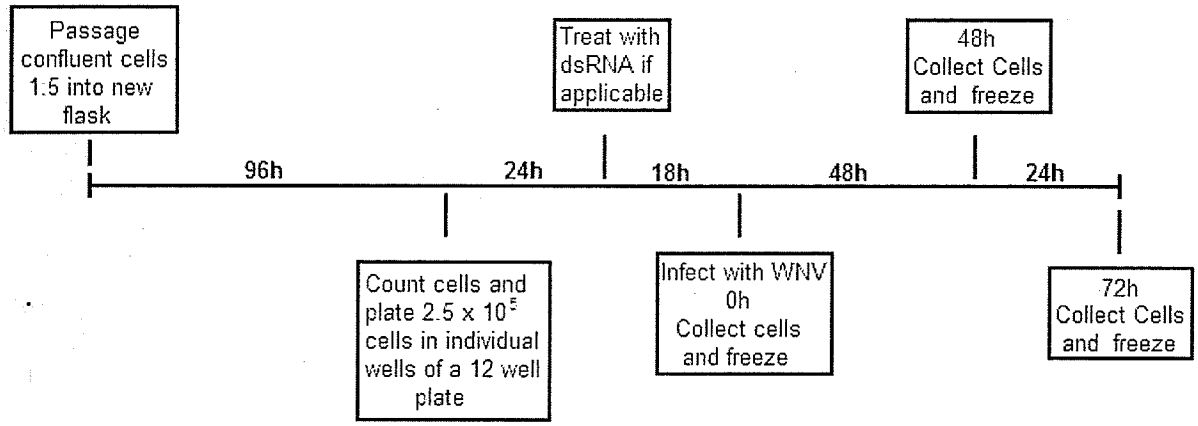

Figure 2.4. WNV Infectivity assay timeline

To facilitate infection assays performed in triplicate, three C6/36 cell populations were required. A confluent layer of cells was first split 1:5 into three separate flasks, each of which was maintained individually for the remainder of the infection trial. Once split,

cells were grown for 4 days at 30°C, and were then counted using a hemocytometer. Flasks were first shaken to dislodge the cells, and a 10µl aliquot was removed for counting. Cell numbers were counted twice using the hemocytometer and an average was taken. Once the number of cells per ml had been calculated, 2.5×10^5 cells were added to individual wells within a 12 well plate to ensure that all treatments used a similar starting number of cells. Eagle's MEM was then added for a total volume of 1 ml, and cells were grown for 24h at 30°C.

To transfect *AaImuc1* and *gus* dsRNA into C6/36 cells, Lipofectamine 2000 reagent (Invitrogen) was used. Briefly, 2µl of Lipofectamine reagent was combined with 98µl of Opti-MEM reduced serum medium (Invitrogen) and the resulting mixture was incubated at room temperature for 5 minutes. In a separate tube, either 5 or 10pmol of *AaImuc1*, or 10pmol of *gus* dsRNA was combined with Opti-MEM medium for a total volume of 100µl. Lipofectamine and dsRNA solutions were then combined and incubated at room temperature for 20 minutes to allow the formation of liposomes. 200µl of dsRNA Lipofectamine complexes were then added to individual wells seeded 24 h previously with 2.5×10^5 cells. Cells were incubated with dsRNA for 18h, washed with Eagle's MEM to ensure most of the Lipofectamine had been removed, and 1ml of new media was then added.

Immediately after removing the Lipofectamine from the treated wells, all but a small amount of media was removed from wells subjected to WNV infection. The stock solution of WNV was then diluted 1:1000 to 6.5×10^4 PFU and 100µl was added to each well, resulting in a final titer of 6.5×10^3 PFU per well. WNV infection then proceeded as explained in section 2.8.b. Post-infection, cells were either immediately frozen at -80°C

or incubated at 30°C for 48 h or 72 h followed by freezing, to prevent any nuclease digestion of host and viral RNA before qRT-PCR. To determine whether *AaImuc1* dsRNA treatment affected the release and/or re-infection of WNV, 200µl of media was removed from wells prior to freezing, on separate *gus* and *AaImuc1* dsRNA treated plates. Removed media only contained extracellular virus, and could be compared to total virus to determine whether *AaImuc1* knockdown alters viral release and/or re-infection.

Following infection, RNA was extracted from individual wells and cDNA was synthesized as explained in section 2.8.b. qRT-PCR was performed for each treatment in triplicate, as described in section 2.8.b, except that 2µl of cDNA was used in each reaction, as mucin expression is fairly low in cell culture. All cDNAs were assayed for mucin expression using primer sites not present in the mucin dsRNA (Table 2.8) to prevent the amplification of resulting cDNA from the dsRNA treatment. *RpL8* expression was measured as a standard and infected cells were assayed for WNV genome replication using WNV 3' UTR primers to determine if mucin knockdown affects viral replication.

To determine *AaImuc1* knockdown, the relative amount of *AaImuc1* gene transcripts was first normalized to the endogenous reference gene *RpL8*, and then normalized relative to the level of *AaImuc1* transcripts treated with *gus* dsRNA using the $\Delta\Delta C_t$ method. WNV replication in *AaImuc1* and *gus*-dsRNA treated cells was quantified as explained in section 2.8.b. The effect of mucin knockdown on cell proliferation was also measured using the *RpL8* standard as a measurement of cell growth.

2.8.d. Plaque Titration

To validate the results obtained using qRT-PCR and determine an approximate titer of virus at all time points post-dsRNA treatment, a plaque titration assay was

performed on all infected, dsRNA treated samples. Briefly, a 200µl aliquot was removed from all wells, and diluted 10^{-1} to 10^{-8} in BA-1. Because cells had already been frozen at -80°C, removed media contained both intact intracellular virus as well as virus from the media. Because C6/36 cells do not form monolayers, nor do they form plaques when infected with WNV, Vero cells were used to perform the plaque titration assay. Vero cells were previously grown at 37°C with 5% CO_2 in DMEM containing 10% FBS for approximately 3-4 days until a monolayer was formed. Cells were next infected in duplicate with dilutions 10^{-2}-10^{-8} of infected, dsRNA treated cell media from the infectivity assays. Infection was performed by removing all but a small amount of media from the Vero cells in 6 well plates, followed by the addition of 100µl of diluted, virus infected media. Cells were then incubated at 37°C for 1h with mild shaking every 15 minutes. Post-infection, cells were overlaid with 3ml of Medium 199 (Sigma) agarose overlay, and were incubated upside-down at 37°C for 72 h. At 72 h incubation time, 2ml of Medium 199 agarose overlay containing 0.01% neutral red was added to the first overlay, and cells were incubated again at 37°C upside down for 18h. After the second incubation time, plaques were visualized and a viral titer for each treatment was determined by taking the average of wells containing countable plaques. Due to the size of the wells and the viral plaques, no more than ~20 plaques could be counted per well.

Chapter 3. Results

3.1. Viral and Mosquito DNA Amplification and Cloning

RNA from adult female mosquito gut tissue was used to prepare a cDNA library using a Matchmaker Library Construction and Screening Kit (Clontech). For this kit, SMART primers are used, which add DNA sequences to the 5' and 3' ends of the cDNAs and allow for *in vivo* integration into the yeast plasmid pGADT7 via recombination. mRNA was first reverse-transcribed using MMLV reverse transcriptase (RT) and the CDS III primer. The CDS III primer binds to the poly-A tail of the RNA and adds a 27 nucleotide 5' sequence to the newly constructed cDNA (Figure 3.1). The use of MMLV RT results in the addition of a few deoxycytidines to the 3' end of the newly constructed cDNA. The SMART primer contains an oligo-G sequence that binds to the terminal C-sequence of the cDNA and is used by the MMLV RT to further extend the 3' end of the cDNA by 36 nucleotides. Long distance PCR (LD-PCR) is then performed to convert the single stranded DNA (ssDNA) into double stranded DNA (dsDNA) and amplify it to facilitate *in vivo* recombination.

To ensure that adequate amounts and sizes of cDNA were amplified, 7μl of PCR product were resolved on a 1% agarose gel (Figure 3.2). The Matchmaker library construction and screening kit manual indicates that a smear of cDNA from approximately 100bp to 4kb is expected. The resulting gel displays 2 cDNA reactions, each with a smear from approximately 100bp to 5kb.

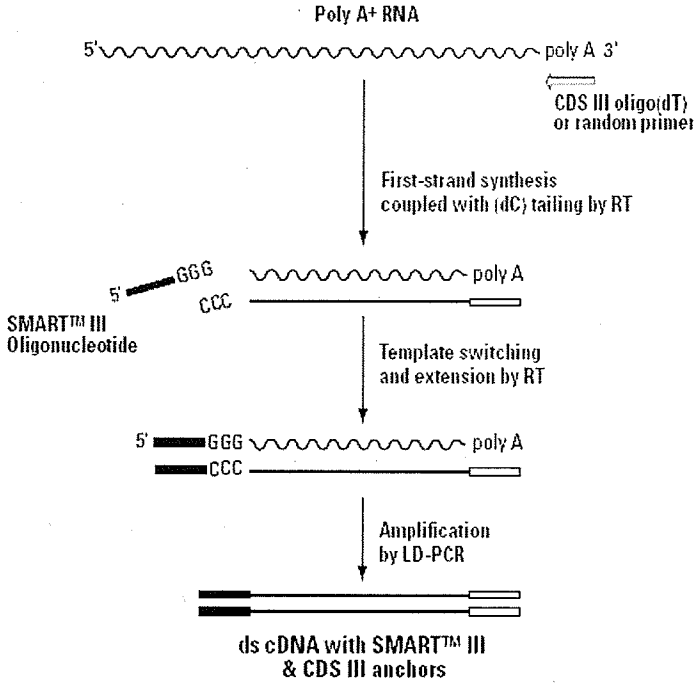

Figure 3.1. Synthesis of cDNA using SMART primers (Clontech Protocol #PT3955-1).

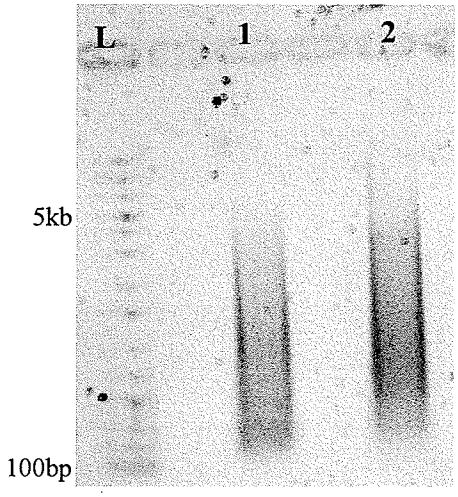

Figure 3.2. *Aedes aegypti* gut cDNA amplifications resolved on a 1% agarose gel. DNA ladder (L), followed by two cDNA reactions (Lanes 1 and 2)

WNV genes M, E and NS1 were all amplified from Vero cell lysates using proofreading Taq polymerase and WNV NY99 strain-specific primers that included

suitable restriction enzyme recognition sequences for subsequent cloning (see Table 2.2). The resulting amplified fragments, including the flanking restriction sites were 237bp, 1514bp and 1067bp respectively. The PCR products were first ligated into the PCR cloning vector pDrive and sequenced. Sequencing using the T7 primer followed by BLASTN search of Genbank confirmed the identity of all three amplified genes (results not shown). No point mutations were observed in the nucleotide sequences that would result in modified protein translations. All 3 viral genes were then excised from pDrive via restriction enzyme digestion, but only M and NS1 were successfully ligated into the yeast two-hybrid bait vector pGBKT7. In the case of the WNV E gene, *Nde*I and *Cfr*9I digestion of recombinant pDrive plasmid containing the WNV E gene was predicted to produce 3 bands: two of 2168 and 1683 bp would be derived from an internal *Cfr*91 restriction site within the pDrive vector, while the WNV E gene was 1514 bp (Figure 3.3). It proved difficult to resolve the 1514 bp WNV E fragment completely from the 1683 bp pDrive DNA fragment, despite trying several different concentrations of agarose gels. Several attempts at ligating the 1514 bp fragment into pGBKT7 proved unsuccessful, as each time only the 1683 bp pDrive fragment was subcloned. It was decided that further efforts to clone the WNV E gene into pGBKT7 would be abandoned, as research on the other viral genes became increasingly more productive.

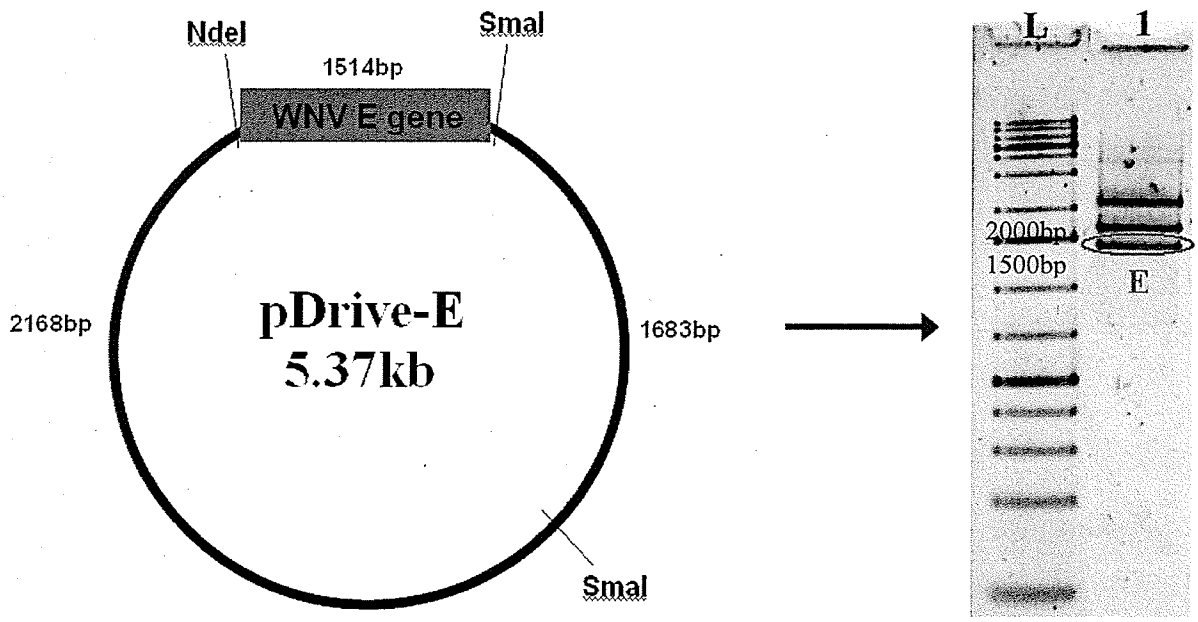

Figure 3.3. *Nde*I and *Sma*I digest of pDrive-E results in closely spaced bands that interfere with ligation into pGBKT7. DNA ladder (L), followed by pDrive-E restriction digest (Lane 1).

3.2. Yeast Two Hybrid Assay

The Y2H assay utilizes metabolically deficient yeast in combination with inducible metabolic genes to discover protein interactions. The yeast strain AH109 is a MATa strain that contains *trp1*, *his3* and *gal4* deletions as well as a *leu2-3,* 112 double mutation. AH109 also contains reporter genes, termed HIS3, ADE2, lacZ and MEL1 that contain upstream activating sequences (UASs) that are responsive to GAL4 transcriptional activation. To reduce the possibility of false positives, 3 different UASs were used to drive reporter gene transcription: GAL1, GAL2 and MEL1 (65). Interaction between bait and prey protein produces a working GAL4 transcriptional activator and results in the activation of these 4 reporter genes, and yeast growth on minimal media. While HIS3 and ADE2 activation are required for growth on dropout media, lacZ and

MEL1 produce coloured byproducts to enable visualization of true Y2H protein interactions.

Prior to performing the yeast two hybrid assay, the bait vectors containing the WNV genes M and NS1 were transformed individually into competent yeast cells to ensure that no toxicity or transcriptional activation of the reporter genes occurred. Transcriptional activation was tested by plating the transformed yeast on SD –Trp, SD –Trp –Ade and SD –Trp –His. Transformation of pGBKT7-M and NS1 resulted in growth on SD –Trp only, indicating that the plasmid was indeed conferring tryptophan production in the yeast. Lack of growth on the other selective media indicated that the reporter genes His and Ade were not transcribed and therefore no transcriptional activation was occurring without transformation of the cDNA vector pGADT7.

Toxicity was assessed by comparing yeast growth when transformed with the empty bait vector pGBKT7 and the bait vector containing M or NS1. Once incubated for 24 hours in SD –Trp medium, optical density was measured using uninoculated medium as a blank. According to the Clontech manual, transformed yeast should grow to an OD_{600} (optical density at 600nm) greater than 0.8 within 24 h if the recombinant protein is to be considered non-toxic. After 24 hours of growth, yeast transformed with an empty pGBKT7 vector (no viral gene present) had on OD_{600} of 1.15, yeast transformed with pGBKT7-M had an OD_{600} of 1.09 and yeast transformed with pGBKT7-NS1 had an OD_{600} of 0.822. Although the yeast transformed with pGBKT7-NS1 grew more slowly, the resulting optical density was above 0.8 and therefore expression of NS1 within the yeast was considered non-toxic.

Yeast two hybrid screens using WNV genes M and NS1 resulted in 5 and 66 yeast colonies respectively. Transformation efficiency was calculated using the number of yeast colonies that had grown on the SD – Leu (indicating that pGADT7 was transformed) and SD – Leu –Trp (indicating that both plasmids were transformed). Recommended transformation efficiencies using the Clontech vectors should be $\geq 1 \times 10^6$ transformants / 3μg pGADT7 and $\geq 5 \times 10^5$ clones / library (2). The transformation efficiencies for the cloning of the M and NS1 genes were calculated to be 3.02×10^6 and 3.66×10^5 transformants / 3μg pGADT7-M and pGADT7-NS1 respectively. When assayed for transformation of both pGBKT7 and pGADT7 plasmids, 4.24×10^5 and 5.89×10^5 clones/library were obtained for M and NS1 transformations respectively. Considering most tissues express approximately 30-40% of all genes (117), gut tissue should express between ~4,600 and 6,200 of the total 15,419 genes in the *Aedes aegypti* genome (100). By dividing the total number of clones/library that were transfected with both plasmids by the total number of genes expressed in gut tissues, the total "number of genomes" utilized by the M and NS1 Y2H assays can be calculated. Y2H assays utilized between ~68 and 92 genomes worth of transcripts for the M assay, and between ~95 and 128 genomes worth of transcripts for the NS1 assay. This indicates that the majority of genes should be represented in the library of clones, except for those minimally expressed (approximately $1/100^{th}$ the average).

Positive and negative controls were plated on QDO plates as well as SD –Leu – Trp and produced expected results. The positive control cotransformation, comprising of pGADT7-T (SV40 large T antigen) and pGBKT7-p53 (murine p53 protein) plasmids, resulted in 5.2×10^6 transformants / 3μg of pGADT7 while the negative control,

consisting of pGADT7-T and pGBKT7-Lam (human Laminin C protein), produced no colonies whatsoever.

All transformed yeast plates contained a number of bacterial colonies as a result of contamination, the source of which could not be determined. Individual components of the transformation assay were tested to identify any possible bacterial contamination but none could be found. Kanamycin was later added to the media in an effort to reduce bacterial growth but no reduction in bacterial colonies was observed. Luckily, yeast colonies were distinguishable due to their characteristic colony size, slight elevation and dull surface, whereas bacterial colonies were smaller, flatter and glistening. Individual yeast colonies that grew on TDO plates were replated twice on QDO plates to ensure no bacterial contamination remained and to eliminate the possibility of purifying yeast with multiple pGADT7 vectors. Once replated, individual colonies were used as template for PCR reactions in which sequencing amplimers (Clontech) were used to amplify cDNA inserts present in pGADT7. Amplified inserts were resolved on agarose gels to determine whether PCR products were pure enough to be used as sequencing template (Figure 3.4).

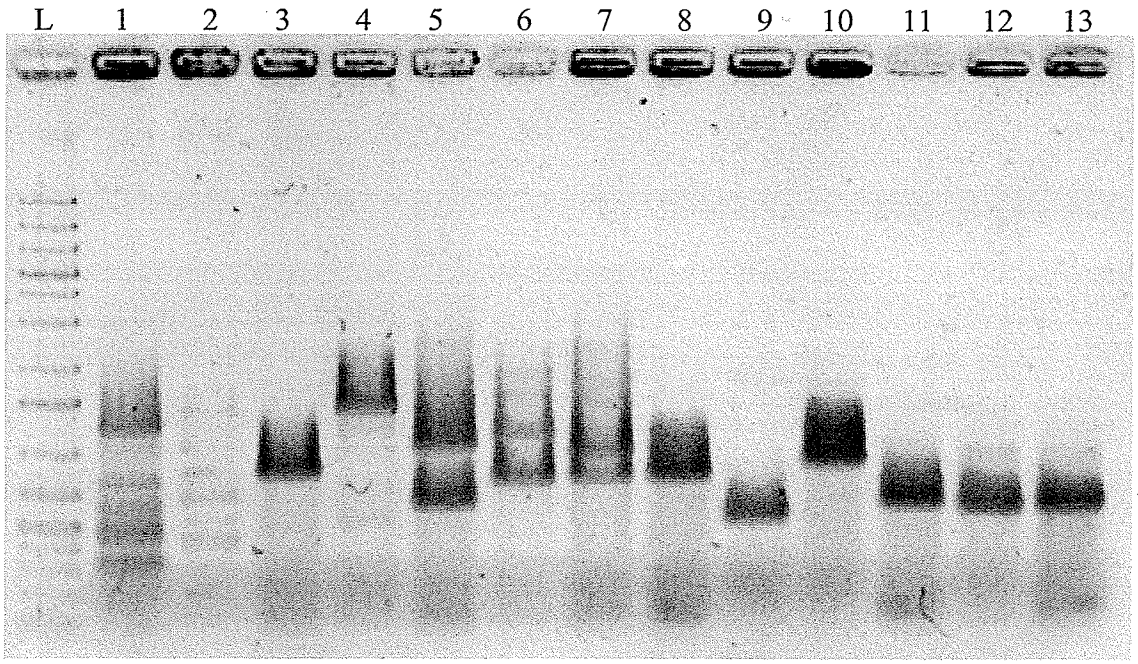

Figure 3.4. pGADT7 cDNA insert amplification products resolved on an agarose gel. Lane L contains a DNA ladder followed by 13 lanes of cDNA insert amplifications of various sizes.

As seen in Figure 3.4, many yeast colonies contained a single insert (lanes 3, 4, 8-13); however, a number contained multiple inserts (lanes 5-7) and others still produced multiple indistinguishable products (lanes 1 and 2) and their PCR products were not sequenced. Colonies were replated on QDO media up to four times, but there was usually no reduction in colonies containing multiple pGADT7 plasmids. Because pGADT7 + M screened colonies were so few in number, all resulting bands were excised and sequenced regardless of the number of cDNA plasmids per sample. Only one band from NS1-screened colonies containing multiple bands was chosen for sequencing due to the large number of samples. As Table 3.1 shows, the result is an increase in M-screened samples available for sequencing due to multiple screened bands, and a decrease in NS1 samples available for sequencing because some samples produced indistinguishable products. The vast majority of samples were successfully sequenced but two NS1 cDNA sequences

could not be resolved, presumably because multiple pGADT7 plasmids were present in those yeast colonies.

Table 3.1. Yeast two hybrid colonies, amplified cDNA inserts that were successfully purified and sequenced.

	Colonies	cDNAs Purified	Successfully Sequenced
M Screen	5	9	9
NS1Screen	66	54	52

Y2H sequencing results for M and NS1 protein interactions are displayed in Tables 3.2 and 3.3 respectively. M sample numbers followed by a letter indicate that multiple bands were sequenced from one colony whereas an asterisk following NS1 sample numbers indicates that two bands were present, but only one was sequenced. The proper functioning of the yeast two-hybrid system was confirmed using the provided positive control plasmids pGADT7 containing the large T antigen and the pGBKT7 plasmid containing the murine p53 fusion protein, which together interacted and promoted yeast growth on the dropout media.

Table 3.2. Identified *Aedes aegypti* gut mRNA sequences, whose translated products interact with WNV matrix (M) protein to produce functional transcription activators.

Sample Number	Accession Number	cDNA Identification	Band Size (bp)
9b	N/A	*Aedes aegypti* Supercontig 1.124, contig 7180	1100
30b	N/A	*Aedes aegypti* Supercontig 1.96, contig 5794	900
9d	AY432478	*Aedes aegypti* metalloendopeptidase mRNA	600
13	N/A	Vectorbase SUPP_AEDES009729 transcript	900
34	XM_001649415	*Aedes aegypti* hypothetical protein partial mRNA	2000
30a	XM_001654575	*Aedes aegypti* hypothetical protein partial mRNA	2500
7	XM_001654575	*Aedes aegypti* hypothetical protein partial mRNA	1500
9a	XM_001654575	*Aedes aegypti* hypothetical protein partial mRNA	2500
9c	XM_001656207	*Aedes aegypti* ATPase subunit partial mRNA	900

Table 3.3. Identified *Aedes aegypti* gut mRNA sequences, whose translated products interact with WNV non structural protein 1 (NS1) glycoprotein to produce functional transcription activators.

Sample Number	Accession Number	cDNA Identification	Band Size (bp)
2	AF308863	*Aedes aegypti* strain RED mucin-like protein (IMUCR1) mRNA	1400
17	AF308863	*Aedes aegypti* strain RED mucin-like protein (IMUCR1) mRNA	1500
19*	AF308863	*Aedes aegypti* strain RED mucin-like protein (IMUCR1) mRNA	1400
21	AF308863	*Aedes aegypti* strain RED mucin-like protein (IMUCR1) mRNA	1400
29*	AF308863	*Aedes aegypti* strain RED mucin-like protein (IMUCR1) mRNA	1400
44	AF308863	*Aedes aegypti* strain RED mucin-like protein (IMUCR1) mRNA	1400
45	AF308863	*Aedes aegypti* strain RED mucin-like protein (IMUCR1) mRNA	1500
51	AF308863	*Aedes aegypti* strain RED mucin-like protein (IMUCR1) mRNA	1400
67	AF308863	*Aedes aegypti* strain RED mucin-like protein (IMUCR1) mRNA	1400
N/A	AF324863	*Aedes aegypti* ribosomal protein L31 (RpL31) mRNA	750
6	AF487426	*Aedes aegypti* early trypsin-like protein precursor mRNA	750
9	AF487426	*Aedes aegypti* early trypsin-like protein precursor mRNA	700
10	AF487426	*Aedes aegypti* early trypsin-like protein precursor mRNA	1000
14	AF487426	*Aedes aegypti* early trypsin-like protein precursor mRNA	1200
26	AF487426	*Aedes aegypti* early trypsin-like protein precursor mRNA	700
30	AF487426	*Aedes aegypti* early trypsin-like protein precursor mRNA	600
34	AF487426	*Aedes aegypti* early trypsin-like protein precursor mRNA	900
36	AF487426	*Aedes aegypti* early trypsin-like protein precursor mRNA	800
37	AF487426	*Aedes aegypti* early trypsin-like protein precursor mRNA	700
38	AF487426	*Aedes aegypti* early trypsin-like protein precursor mRNA	1100
39*	AF487426	*Aedes aegypti* early trypsin-like protein precursor mRNA	1100
41	AF487426	*Aedes aegypti* early trypsin-like protein precursor mRNA	1100
56	AF487426	*Aedes aegypti* early trypsin-like protein precursor mRNA	900
58	AF487426	*Aedes aegypti* early trypsin-like protein precursor mRNA	1000
60	AF487426	*Aedes aegypti* early trypsin-like protein precursor mRNA	700
61	AF487426	*Aedes aegypti* early trypsin-like protein precursor mRNA	700
66	AF487426	*Aedes aegypti* early trypsin-like protein precursor mRNA	800
69*	AF487426	*Aedes aegypti* early trypsin-like protein precursor mRNA	1000
64	AY064082	*Aedes aegypti* clone chymotrypsin-like protein (CHYM) gene	900
1	AY064104	*Aedes aegypti* clone EF2Mc2 elongation factor 2 (Ef-2) mRNA	1400
43	AY064104	*Aedes aegypti* clone EF2Mc2 elongation factor 2 (Ef-2) mRNA	1000
32*	AY431885	*Aedes aegypti* chaperone mRNA sequence	1000
47	AY432458	*Aedes aegypti* cytosolic large ribosomal subunit L6 mRNA	800
5	AY432463	*Aedes aegypti* serine protease mRNA	500
8	AY432463	*Aedes aegypti* serine protease mRNA	900
15	AY432463	*Aedes aegypti* serine protease mRNA	1000
23	AY432463	*Aedes aegypti* serine protease mRNA	550
27*	AY432463	*Aedes aegypti* serine protease mRNA	900
35	AY432463	*Aedes aegypti* serine protease mRNA	500
46	AY432463	*Aedes aegypti* serine protease mRNA	600

50	AY432463	*Aedes aegypti* serine protease mRNA	500
57	AY432463	*Aedes aegypti* serine protease mRNA	700
68	AY432463	*Aedes aegypti* serine protease mRNA	900
18	AY432764	*Aedes aegypti* cytosolic small ribosomal subunit S24 mRNA	700
70*	AY432764	*Aedes aegypti* cytosolic small ribosomal subunit S24 mRNA	600
59	AY741683	*Aedes aegypti* 40S ribosomal protein S15 (40sRpS15) mRNA	800
20	BK006052	*Aedes aegypti* acetylcholinesterase (Ace1) gene	900
22*	DQ129690	*Aedes aegypti* chitinase mRNA	1000
25	DQ440015	*Aedes aegypti* 40S ribosomal protein S20 mRNA	600
7	DQ440059	*Aedes aegypti* clone AE-314 actin mRNA	900
12	DQ440059	*Aedes aegypti* clone AE-314 actin mRNA	900
42	X64362	*Aedes aegypti* mRNA 3A1 for putative trypsin	1000

Three of the identified proteins were chosen for further study. While the majority of the focus of the remaining study rests on the NS1 interaction with the intestinal mucin-like protein (AeIMUC1), the early trypsin and elongation factor (EF2) were also identified as candidates for further study. Homologues for all three genes were identified and cloned into pL4440, but IMUC1 alone was chosen for infectivity studies.

3.3 Co-Immunoprecipitation

Despite the abundance of putative protein-protein interactions identified in the Y2H screen, only two mosquito proteins that interacted with the NS1 WNV protein were selected for further analysis via Co-IP. To validate the apparent interaction of WNV NS1 and *Aedes aegypti* IMUC1 and early trypsin proteins, *in vitro* transcription and translation and Co-IP analyses were performed. Prior to performing the assays, the Y2H vector inserts were sequenced to estimate protein molecular weights (with tags), and to ensure that no premature stop codons were present and adequate methionine residues were included to allow incorporation of the radioactive label. Together with their respective protein tags, NS1 is ~42kDa and contains six methionines, mucin is ~36kDa and contains five methionines, and early trypsin is ~17kDa and contains seven methionines. Because

phosphor screen imaging is more sensitive than x-ray film exposure, it was anticipated that the expressed proteins would incorporate enough ^{35}S-methionine to be visualized.

Prior to performing the Co-IP, labeled protein products were visualized separately on polyacrylamide gels using a phosphorimager (Figure 3.5). Alongside viral and mosquito samples, the luciferase (~60kDa) positive control from the *in vitro* translation kit as well as the murine p53 (~35kDa) and SV-40 large T antigen (~65kDa) positive controls from the Co-IP kit were translated. The luciferase control from the translation kit produced an easily visualized band of approximately the correct molecular weight, indicating that the transcription and translation reactions were optimized for that template. Y2H vector-translated protein products were visible but protein production was clearly sub-optimal. *In vitro* transcription and translation of theY2H vector pGBKT7-NS1 produced the strongest band, while the pGADT7-IMUC1 vector produced a much fainter band and the pGADT7-early trypsin vector produced no visible protein, despite loading all of the 20ul of the *in vitro* translation reaction in each gel lane. As the interaction between NS1 and *Aedes aegypti* early trypsin could not be confirmed in the absence of early trypsin expression, the remaining focus was directed to the mucin-NS1 interaction. Signal intensity of translated Co-IP kit control proteins was similar to the other Y2H proteins assayed, indicating that the use of Clontech Y2H vectors with the Promega TnT® T7 Coupled Reticulocyte Lysate System clearly requires some optimization before significant amounts of protein can be produced *in vitro*.

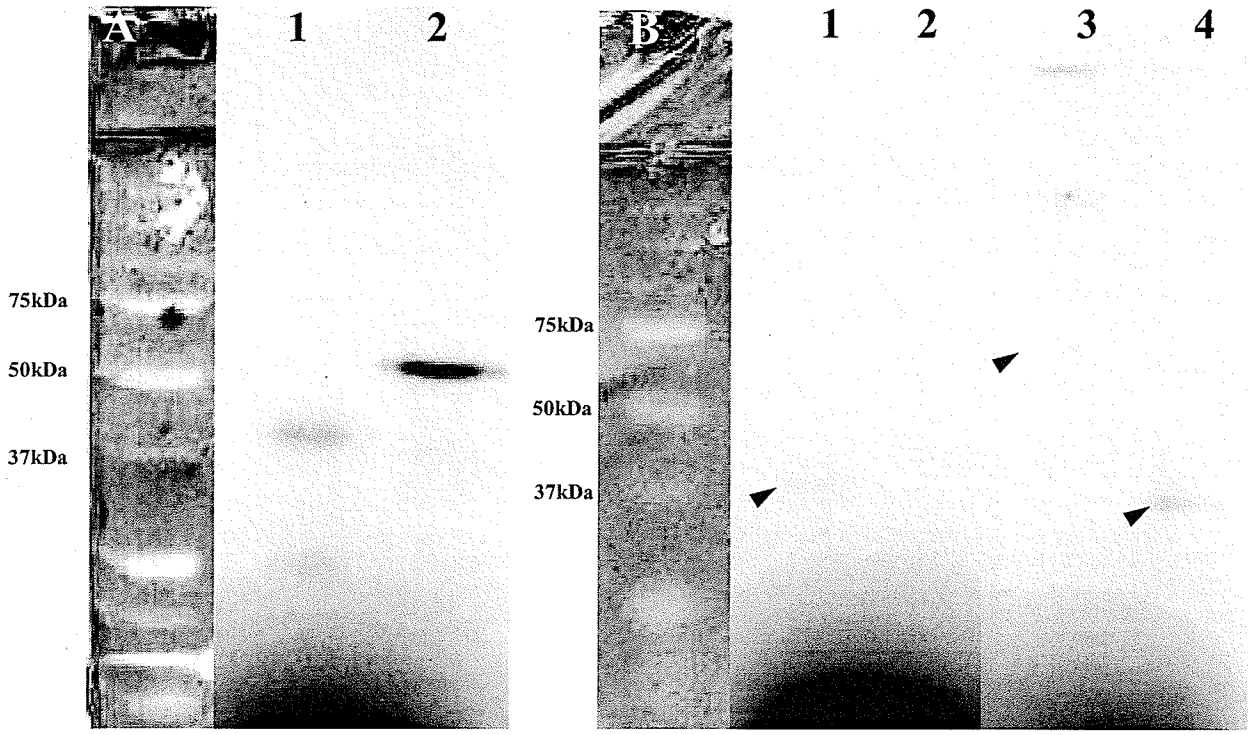

Figure 3.5. Phosphor images of *in vitro* transcription and translation protein products. (A) Prestained protein ladder, followed by WNV NS1 in lane 1 and luciferase positive control in lane 2. (B) Protein ladder, followed by *Aedes aegypti* mucin in lane 1 and early trypsin in lane 2. Co-IP positive control products for SV-40 large T antigen and murine p53 are in lanes 3 and 4 respectively. Fainter bands are identified by an arrow.

Labeled proteins were next combined *in vitro* and treated with either bait or prey protein tag-specific antibodies. Bait proteins NS1 and p53 were fused to the c-myc tag while prey proteins mucin and T antigen were fused to the HA tag, enabling antibody recognition. Proteins were purified using a spin column, and were visualized on a polyacrylamide gel. The presence of both bait and prey proteins on the gel would indicate that protein interaction occurred. Both IMUC1-NS1 and T antigen-p53 interactions were confirmed, as indicated by the presence of 2 bands in Figure 3.6, lanes 2, 3 and 4.

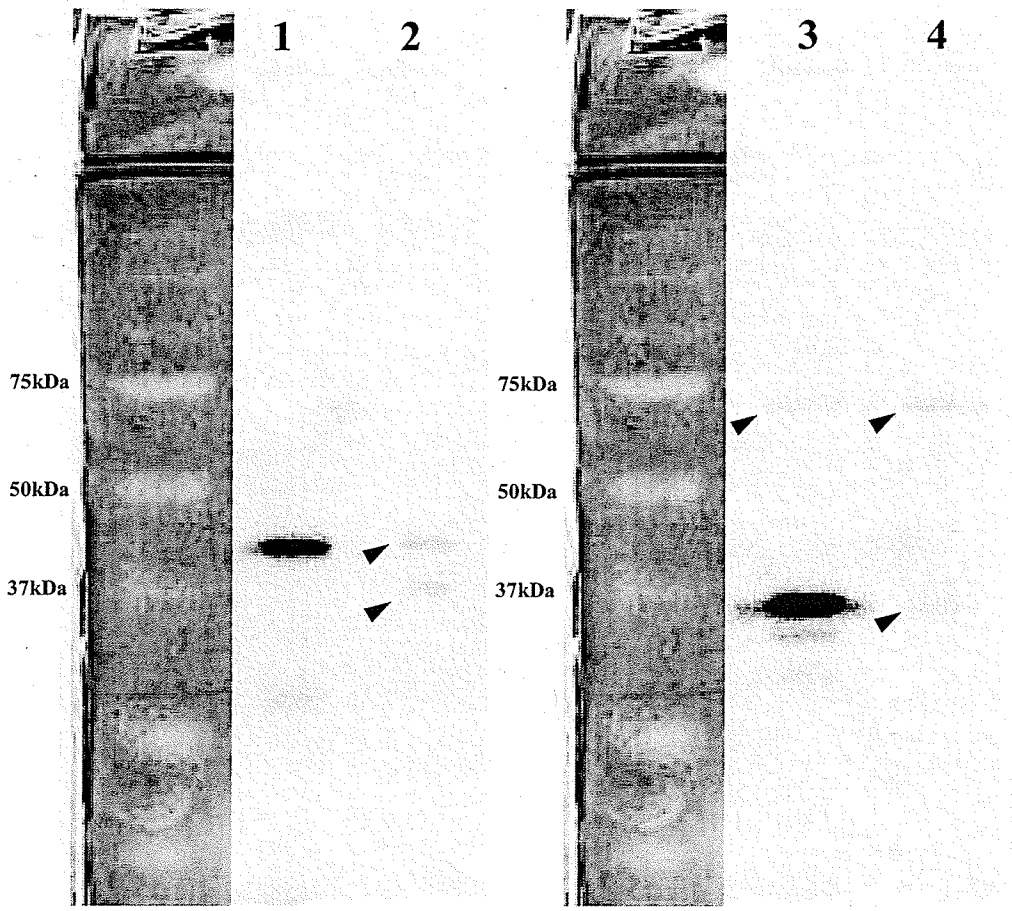

Figure 3.6. Phosphor image of Co-IP column eluates. NS1-IMUC1 interactions are displayed in lanes 1 and 2 and T antigen-p53 interaction are displayed in lanes 3 and 4. Lanes 1 and 3 used c-myc monoclonal antibodies whereas lanes 2 and 4 used HA polyclonal antibodies to detect the proteins. Fainter bands are identified by an arrowhead.

Negative controls were next performed by incubating IMUC1 or NS1 proteins alone with either the c-myc or HA antibodies (Figure 3.7). As expected, the bait proteins bound solely to the c-myc tag while the prey proteins bound to the HA tag.

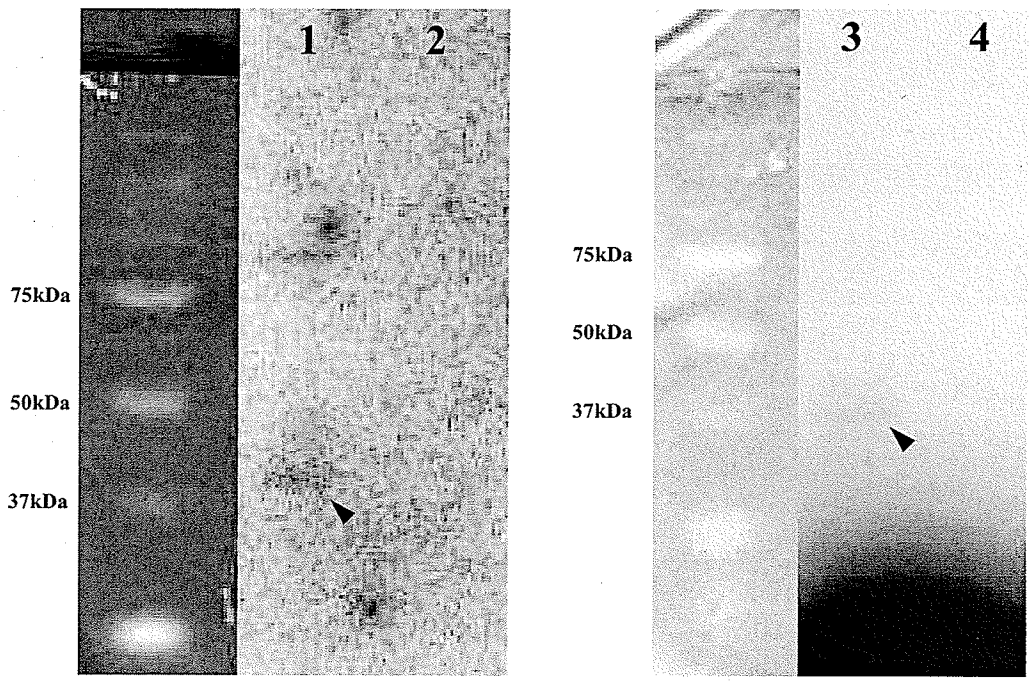

Figure 3.7. Phosphor image of negative control immunoprecipitation eluates. NS1 was incubated with either c-myc (lane 1) or HA (lane 2) antibodies. Mucin was also treated with HA (lane 3) or c-myc (lane 4) antibodies. Bands are identified by an arrow.

3.4. Y2H gene Homologue Identification

To help confirm the interactions between NS1 and the mosquito gut proteins, a mosquito cell-based interaction assay was subsequently developed. Unfortunately, no *Aedes aegypti* cell lines exist, so it was necessary to use a cell line developed from a related mosquito species, *Aedes albopictus*. *Aedes albopictus* is closely related to *Aedes aegypti* (Figure 3.8.) and it was anticipated that WNV proteins would interact with the same proteins identified from *Aedes aegypti*. Using degenerate primers based on mosquito and *Drosophila* sequence alignments, homologues of *Aedes aegypti* Y2H gut genes *AeImuc1*, early trypsin and EF2 were identified. Due to sequence divergence, primers could not be constructed that would amplify entire genes, and therefore only

segments of genes were isolated and cloned. Once genes were ligated into pDrive, sequencing was performed to confirm that amplified DNA was in fact the homologous sequence. Alignments of *Aedes aegypti* and *Aedes albopictus* sequences using the sequence alignment program ClustalW are shown in Figures 3.9-3.14. A fair degree of sequence conservation between both species is seen among all three genes, ranging from 71 to 97% identity, which is expected given that the two mosquito species belong to the same genus.

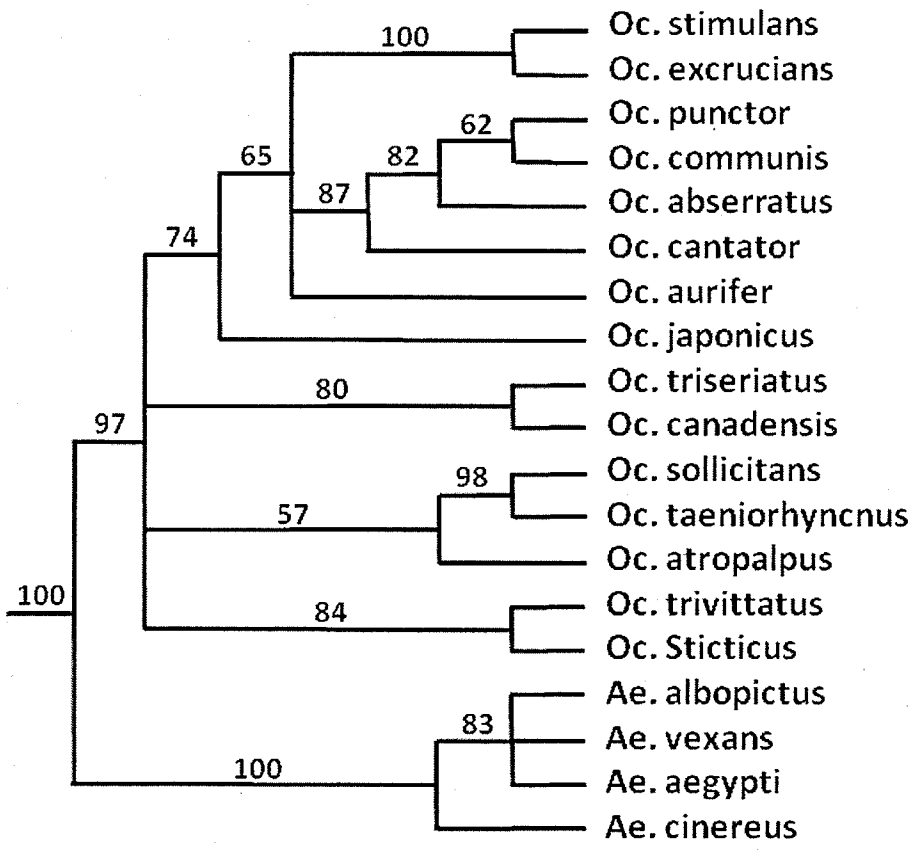

Figure 3.8. Bootstrap analysis demonstrating the phylogenetic relationship between *Aedes aegypti* and *Aedes albopictus* using alignment of 18s rRNA sequence corresponding to secondary structure (reproduced from (115)).

The 5' region of the *Aedes albopictus* homologue (*AaImuc1)* of the *Aedes aegypti* gene *AeImuc1* was amplified and sequenced (Figure 3.9). To ensure that the amplified sequence was orthologous to the *AeImuc1* gene, the nucleotide BLAST tool on the VectorBase website (http://www.vectorbase.org/Tools/BLAST/) was used to search the *Aedes aegypti* genome. With an E value of 4e-06, the best matched sequence identified was the homologue *AeImuc1* (VectorBase ID AAEL004798). This E value is indicative of only a modest degree of sequence identity, but it is worth noting that it is a result of short sequence length, and several short deletions within the interdomain region and mucin domain of the *A. albopictus* sequence. Paralogous mucins have been observed to have a variable number of tandem repeats (VNTRs) within their mucin domains (45). As there are differing numbers of repeats in the mucin domains of the two genes isolated from the two mosquito species, the question as to whether the genes are true orthologues arises. The *Aedes aegypti AeImuc1* gene does, however, have a high degree of sequence polymorphism within the mucin domain (93). Three alleles of the *AeImuc1* gene were found in *Aedes aegypti*, with the largest degree of sequence polymorphism found at the 3' end and within the mucin domain, where one allele contained an eight amino acid deletion (93).

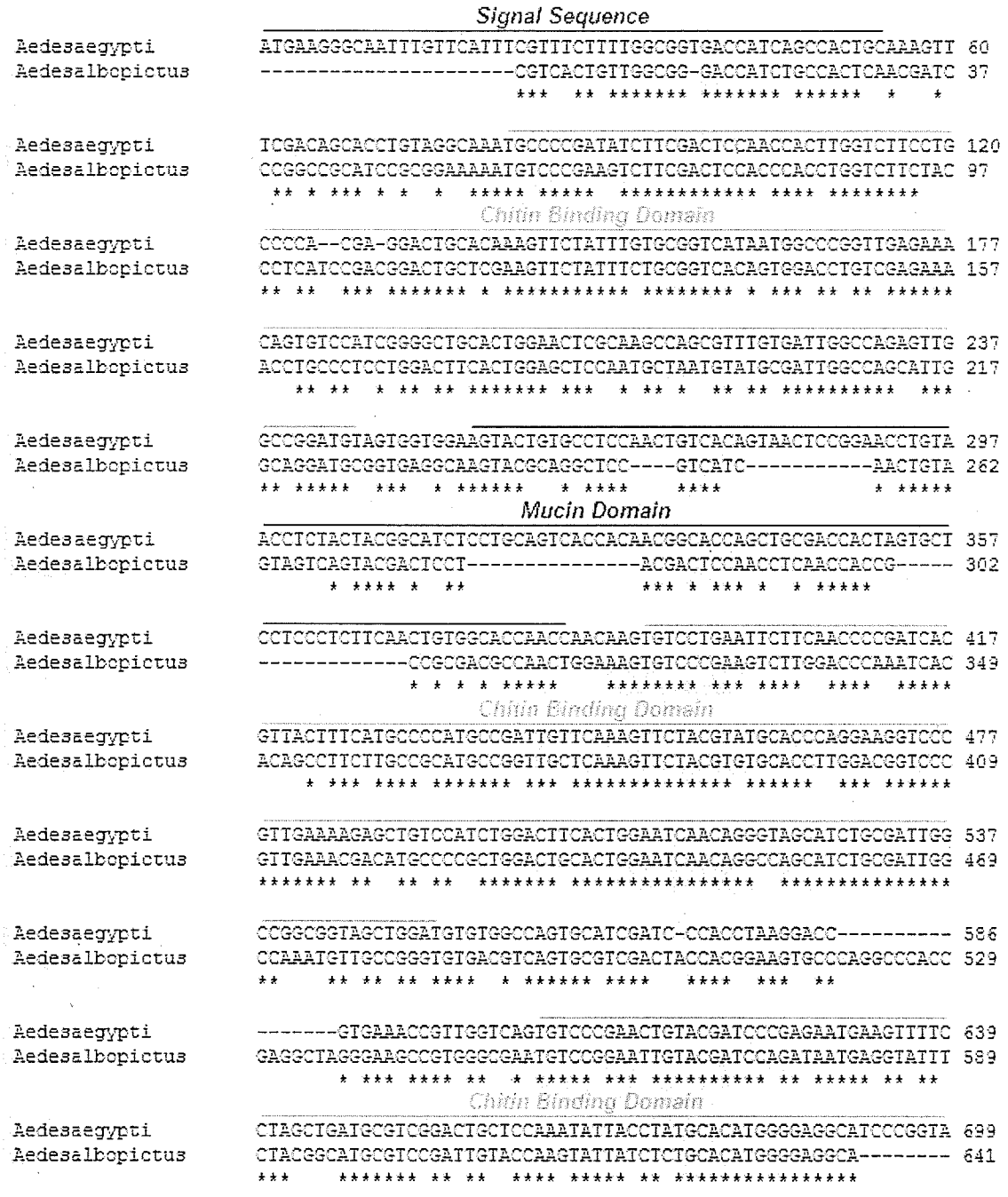

Figure 3.9. Alignment of *Aedes aegypti* and *Aedes albopictus* intestinal mucin sequences. Domains of the translated product are highlighted. * indicates identical residues.

```
Aedesaegypti        MKGNLFISFLLAVTISHCKVSTAPVGKCPDIFDSNHLVFLPH-EDCIKFYLCGHNGPVEK 59
Aedesalbopictus     --------VTVGGIICHSTIPAASAEKCPEVFDSTHLVFYPHPIDCSKFYFCGHSGPVEK 52
                           . :. **.*..:.:*.. ***;:***.**** **  **;***:***.*****
                                                          Mucin Domain
Aedesaegypti        QCPSGLHWNSQASVCDWPELAGCSGGSTVPPIVTVTPEPVTSTTASPAVTITAPAAITSA 119
Aedesalbopictus     TCPPGLHWSSNANVCDWPALAGCGEASTQAPSSTV----VVSTTP------ITPTSTTAA 102
                     **.****.*:*.***** ****. .** .*: **    *.***.      *:*::**:*

Aedesaegypti        PPSSTVAPTNKCPEFFNPDHVTFMPHADCSKFYVCTQEGPVEKSCPSGLHWNQQGSICDW 179
Aedesalbopictus     TP------TGKCPEVLDPNHTAFLPHAGCSKFYVCTLDGPVETTCPAGLHWNQQASICDW 156
                    .*      *.****.::*:*.:*:***.******** :****.:**:*******.*****

Aedesaegypti        PAVAGCVASAS------IPPKDRETVGQCPELYDPENEVFLADASDCSKYYLCTWGGIPV 233
Aedesalbopictus     PNVAGCDVSASTTTEVPRPTEAREAVGECPELYDPDNEVFLRHASDCTKYYLCTWGGX-- 214
                    * **** .***       *.: **:**:*******:***** .****:*********
```

Figure 3.10. Amino acid sequence alignment of *Aedes aegypti and Aedes albopictus* intestinal mucin-like proteins demonstrating the sequence divergence within the mucin domain.

The *Aedes albopictus* mucin-like protein contains a much smaller mucin domain than that of *Aedes aegypti* (Figure 3.10), but it is no doubt functionally important due to the conservation of proline, threonine and serine residues - a characteristic of mucin domains that gives them their stickiness (108).

A 542 bp fragment of the *Aedes albopictus* early trypsin homologue was amplified and sequenced (Figure 3.11). To ensure that the *A. albopictus* amplified fragment was a true orthologue of the *Aedes aegypti* early trypsin, the *A. aegypti* genome was searched for any sequence similarities. With an E value of 3e-80, the only match with a high degree of sequence identity was the Y2H identified early trypsin (VectorBase ID AAEL07818). Although more conserved than the mucin gene, some nucleotide polymorphism between the two species' early trypsin genes is apparent, even within the conserved nucleotide sequences encoding functional trypsin residues. Nonetheless, due to the degeneracy of the nucleotide code, functional residues remain the same in the translated product as seen in Figure 3.12.

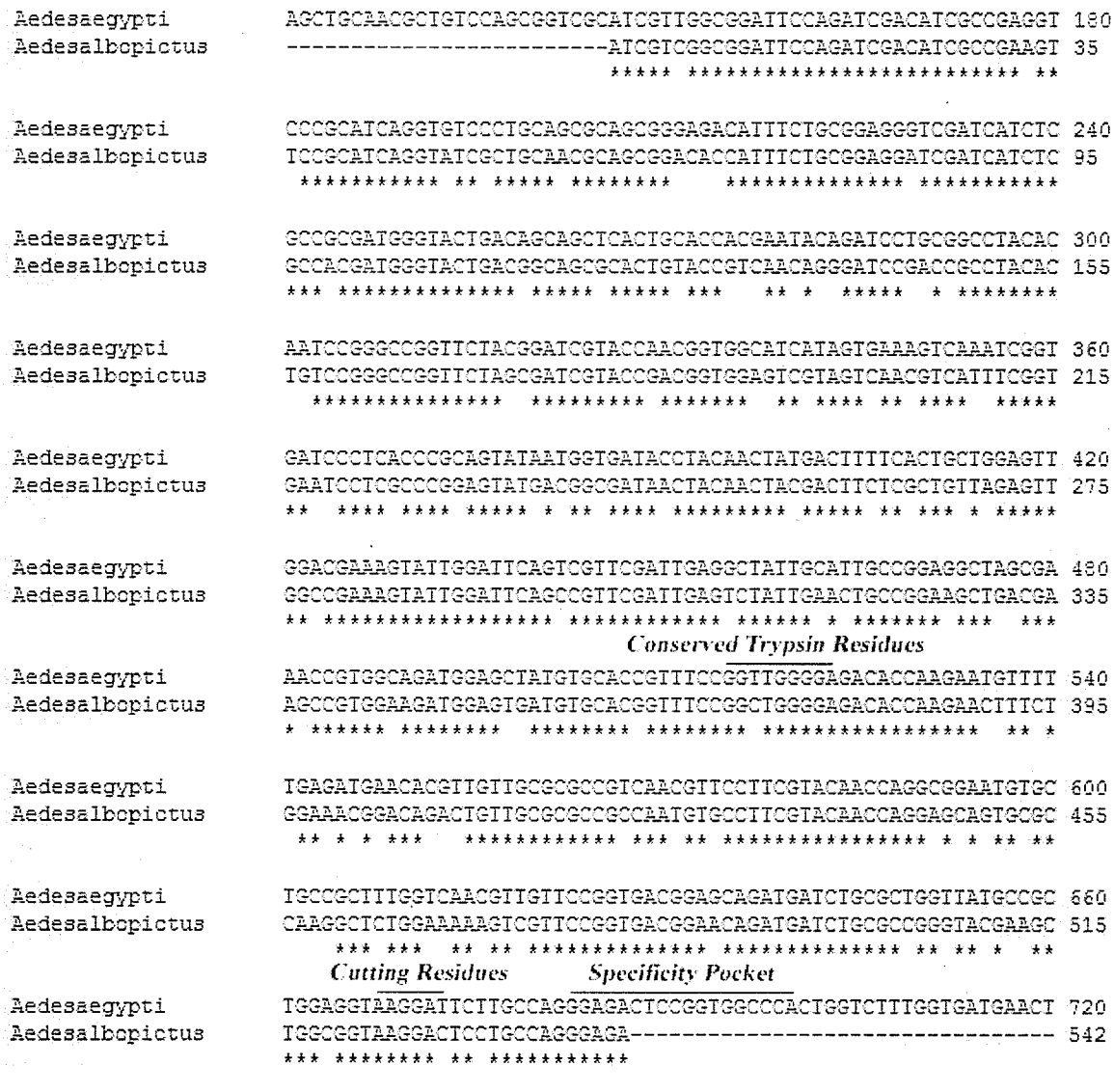

Figure 3.11. Alignment of *Aedes aegypti* and *Aedes albopictus* early trypsin sequences. Conserved trypsin residues of the translated product are highlighted (51). * indicates identical residues.

```
Aedesaegypti        MNQFLFVSFCALLGLSQVSAAILSSGRIVGGFQIDIAEVPHQVSLQRSGRHFCGGSIISP 60
Aedesalbopictus     ----------------------------IVGGFQIDIAEVPHQVSLQRSGHHFCGGSIISP 33
                                                ***********************:**********

Aedesaegypti        RWVLIAAHCTINIDPAAYTIRAGSIDRINGGIIVKVKSVIPHPQYNGDTYNYDFSLLELD 120
Aedesalbopictus     RWVLIAAHCTVNRDFTAYTVRAGSSDRIDGGVVVNVISVNPRPEYDGDNYNYDFSLLELA 93
                    **********.* **:***:****:***:**::*:* ** *:*:*:**.**********
                                          Conserved Trypsin Residues
Aedesaegypti        ESIGFSRSIEAIALPEASETVADGAMCTVSGWGDTKNVFEMNTLLRAVNVPSYNQAECAA 180
Aedesalbopictus     ESIGFSRSIESIELPEADEAVEDGVMCTVSGWGDIKNFLETDRLLRAANVPSYNQEQCAK 153
                    **********:* ****.*:* **.************.:* : ****.******* :**
                                Cutting Residues    Specificity Pocket
Aedesaegypti        ALVNVVPVIEQMICAGYAAGGKDSCQGDSGGPLVFGDELVGVVSWGKGCALPNLPGVYAR 240
Aedesalbopictus     ALEKVVPVIEQMICAGYEAGGKDSCQGX------------------------------- 181
                    ** :************* *********

Aedesaegypti        VSTVRQWIREVSEV 254
Aedesalbopictus     -------------- 
```

Figure 3.12. Amino acid sequence alignment of *Aedes aegypti* and *Aedes albopictus* early trypsin homologues.

Unlike the other two *Aedes albopictus* homologues, the EF2 gene is very highly conserved (Figure 3.13). When BLASTed against the *Aedes aegypti* genome, the Y2H identified EF2 (VectorBase ID AAEL004500) demonstrated an E value of 0.0, indicating that the two genes are orthologues. The pockets of divergent sequence at the 5' end of the sequence are the result of small dye blobs in the sequencing reaction and do not represent true sequence polymorphism. Translated EF2 products from both species are almost identical (Figure 3.14), indicating that the important function of EF2 in the translation machinery strongly selects against sequence mutation.

```
Aedesaegypti        ATGGTTAACTTTACCGTTGACGAAATCCGCTCCATGATGGACAGGAAGCGGAACATCCGT 60
Aedesalbopictus     ------------------------------------ATGGACAGGAAGCGGAAAAAAGG- 23
                                                         ****************** *   *

Aedesaegypti        AACATGTCCGTCATTGCCCACGTCGACCACGGCAAGTCC-ACGCTCACGGATTCGTTGGT 119
Aedesalbopictus     GACAGGTCCGTCATTGCCCACGTCGATCACGGCAAGAAAGAGGATGACCGATTCGTTGGT 83
                     *** ********************* *********    * * * ** ***********

Aedesaegypti        CTCGAAGGCCGGTATCATTGCCGGGGCCAAGGCCGGCGAAACCCGTTTCACCGACACCCG 179
Aedesalbopictus     CTCCAAGGCCGGTATCATCGCCGGTGCCAAGGCTGGAGAAACCCGTTTCACCGATACCCG 143
                    *** ************** ***** ******** ** ****************** *****

Aedesaegypti        CAAGGACGAGCAGGAACGGTGCATTACCATCAAGTCGACCGCCATCTCGATGTACTTCGA 239
Aedesalbopictus     CAAGGACGAACAGGAACGGTGCATTACCATCAAGTCGACTGCCATCTCGATGTACTTCGA 203
                    ********* ***************************** ********************

Aedesaegypti        GTTGGAAGACCAGGATCTGGTGTTCATCACCAACCCTGACCAGCGCGACAAGGACTGCAA 299
Aedesalbopictus     GTTGGAAGATCAGGATCTGGTGTTCATCACCAACCCTGACCAGCGCGACAAGGACTGCAA 263
                    ********* ************************************************

Aedesaegypti        GGGCTTCTTGATCAATCTGATCGATTCGCCCGGGCACGTTGATTTCTCCTCGGAAGTAAC 359
Aedesalbopictus     GGGCTTCTTGATCAATCTGATCGATTCGCCCGGGCACGTTGATTTCTCGTCGGAGGTAAC 323
                    ************************************************ ***** *****

Aedesaegypti        TGCCGCGCTGCGTGTCACTGACGGTGCCTTGGTCGTCGTCGATTGCGTTTCCGGTGTGTG 419
Aedesalbopictus     GGCCGCGCTGCGTGTCACTGACGGTGCCCTGGTCGTCGTCGATTGCGTTTCCGGTGTGTG 383
                     *************************** ********************************

Aedesaegypti        CGTACAGACCGAAACCGTGCTGCGTCAGGCCATCGCCGAACGTATCAAGCCGGTGCTGTT 479
Aedesalbopictus     CGTACAGACCGAAACCGTGCTGCGTCAGGCCATTGCCGAACGTATCAAGCCGGTACTGTT 443
                    ********************************** ******************** *****

Aedesaegypti        CATGAACAAGATGGACCGTGCTCTGCTGGAGCTGCAGCTGGATGCTGAAGATCTGTACCA 539
Aedesalbopictus     CATGAACAAGATGGACCGTGCCCTGCTGGAACTGCAGCTGGATGCGGAAGATCTGTACCA 503
                    ********************** ******** ************** **************

Aedesaegypti        GACCTTCCAGCGTATCGTTGAAAACGTCAACGTCATCATTGCCACCTACAACGACGATGG 599
Aedesalbopictus     GACCTTCCAGCGTATCGTTGAAAACGTCAACGTCATCATCGCCACCTACAACGACGATGG 563
                    ****************************************** ********************

Aedesaegypti        CGGCCCAATGGGAGAAGTCCGTGTCGATCCATCCAAGGGTTCCGTCGGTTTCGGTTCCGG 659
Aedesalbopictus     CGGCCCAATGGGAGAGGTCCGTGTCGATCCATCCAAGGGTTCCGTCGGTTTCGGTTCCGG 623
                    *************** ************************************************

Aedesaegypti        TCTGCACGGATGGGCCTTCACTCTCAAGCAGTTCGCTGAGATGTACGCCGCTATGTTCAA 719
Aedesalbopictus     TCTGCACGGATGGGCCTTCACCCTCAAGCAGTTCGCTGAGATGTACGCCGCTATGTTCAA 683
                    ********************** ****************************************

Aedesaegypti        GATCGATGTCGTCAAGCTCATGAACCGTCTGTGGGG-AGAGAACTTCTTCAACCCCAAGA 778
Aedesalbopictus     GATCGATGTCGTCAAGCTCATGAACCGTCTGTGGGGGAGAGAACTT-------------- 729
                    ************************************ *********
```

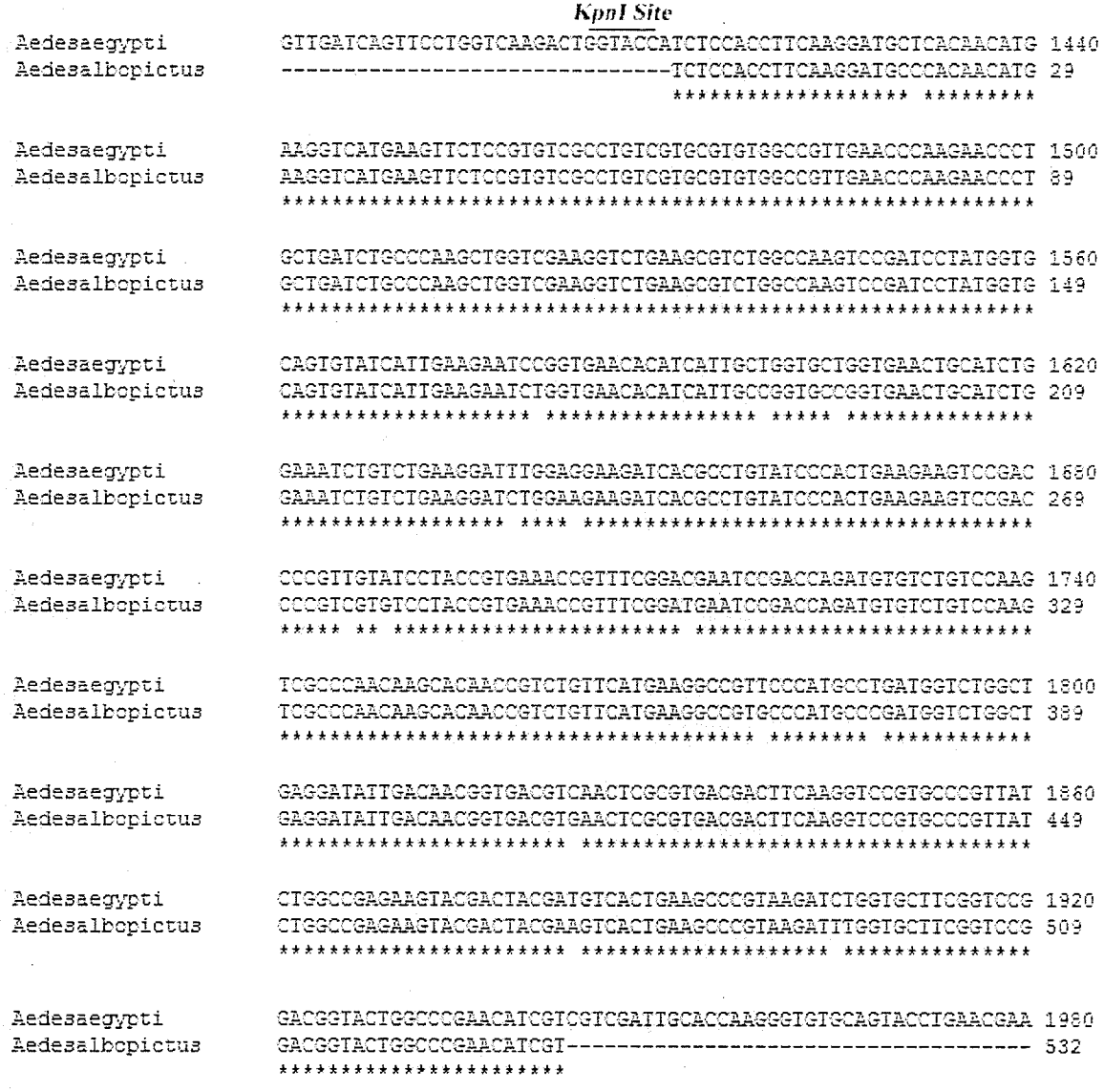

Figure 3.13. Alignment of *Aedes aegypti* and *Aedes albopictus* EF2 sequences. The fragment was sequenced from both 5' and 3' ends, but the size of the insert prevented the middle ~700bp from being obtained. The internal KpnI site used to ligate a 543bp portion of EF2 into pL4440 is highlighted. * indicates identical residues.

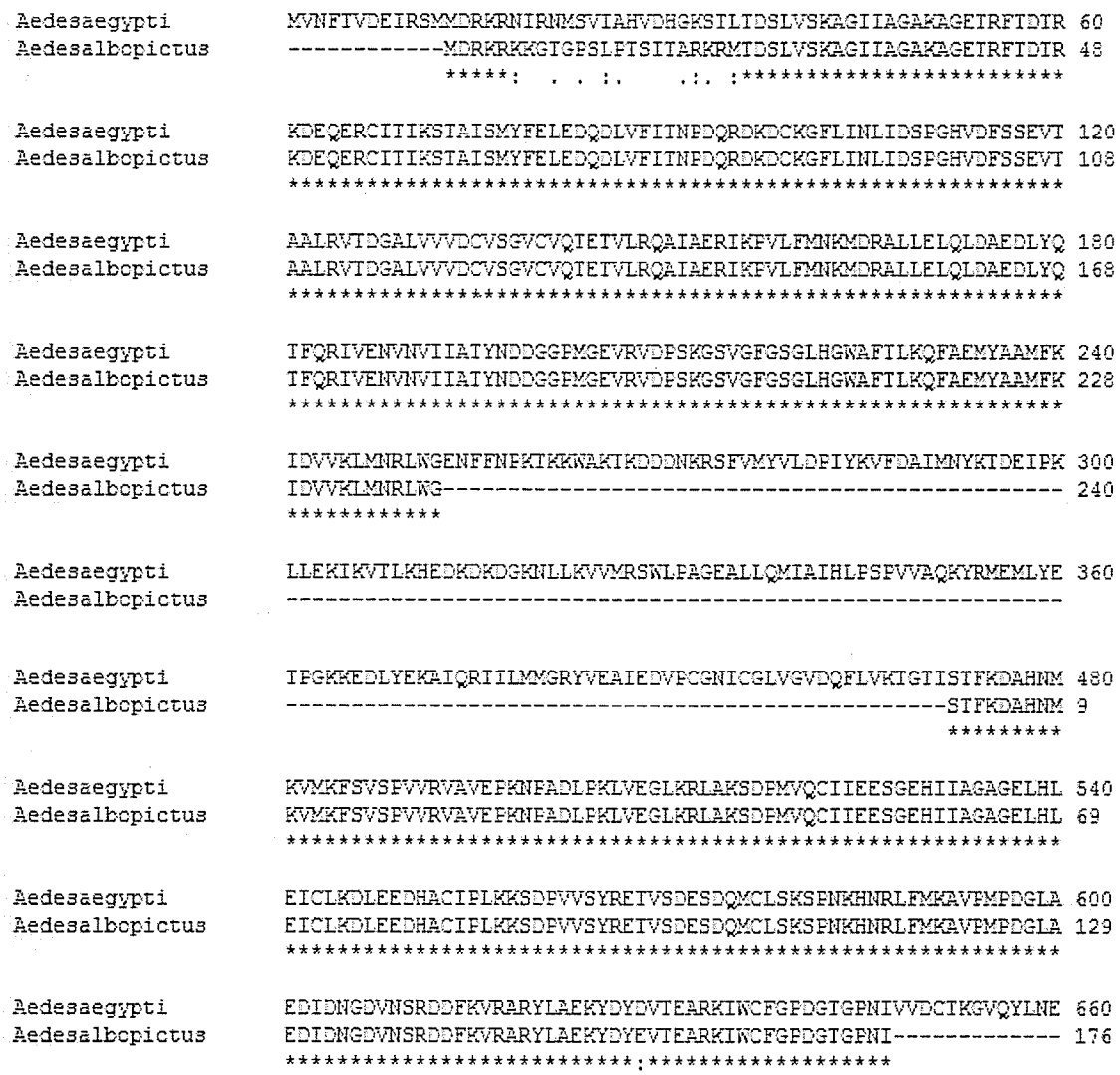

Figure 3.14. Amino acid alignment of *Aedes aegypti* and *Aedes albopictus* Elongation factor 2.

Although three *Aedes albopictus* genes were cloned and sequenced, only the *AaImuc1* gene was chosen for RNAi-induced gene knockdown and infection trials for the remainder of this study, due to its interesting function in mosquito innate immunity.

3.5. WNV Infectivity Trials

3.5.a. Establishment of an Optimal Cell:Virus Ratio

To determine an optimal C6/36 cell plating density and to ensure that plating cells in triplicate would result in similar cell growth numbers, three cell dilutions were plated in duplicate and cell numbers were counted after 48 h, 72 h and 96h. A paired t test was performed to determine whether differences between duplicate cell densities were statistically significant (GraphPad Instat), and no significant differences were found. A growth curve demonstrating the average of both duplicates for each time point and plated cell density is displayed in Figure 3.15. Based on cell growth and density in control and WNV infected assays, an optimal plating density of C6/36 cells was determined to be 2.5 x 10^5/ml. This density ensured that after 96h of growth at 30°C, cells would not be overcrowded, nor would growth be inhibited due to limited cell-cell interactions.

Prior to performing dsRNA-treated infections of C6/36 cells, an optimal amount of virus was required for infection. Two densities of C6/36 cells were first infected with 4 dilutions of WNV to observe any cytopathic effects that may prevent the analysis of future infections. After approximately 96 hours of growth, it was evident that infection using higher viral titers negatively affected the cells. There was a visible (~10%) loss of cell adherence to the plates when cells were infected with 6.5 x 10^6 pfu/well and a slightly lower loss of adherence (~5%) when cells were infected with 6.5 x 10^5 pfu/well. While the majority of cells remained bound to the plate, those that lost adherence formed grape-like clusters that were either bound to the plate by adherent cells, or were floating in the medium. It was therefore decided that a lower viral titer would be used for

subsequent experiments, to ensure that the combined stress of Lipofectamine-mediated RNAi and viral infection would not overly inhibit cell growth.

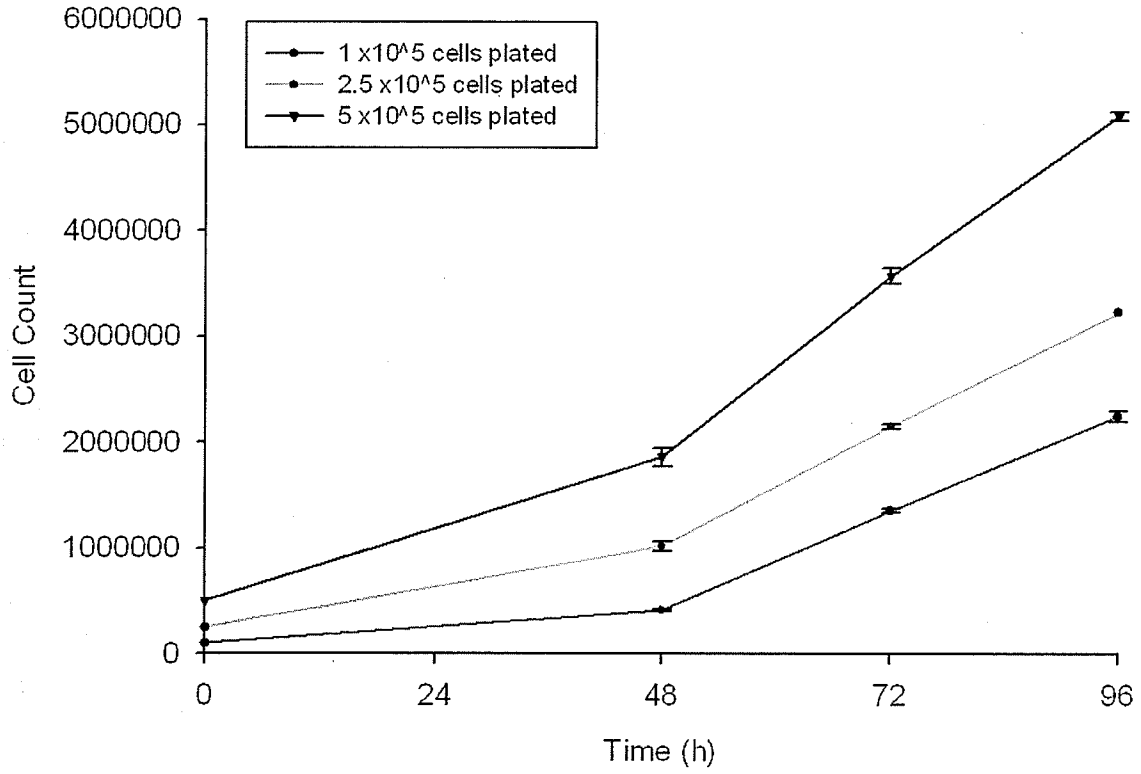

Figure 3.15. C6/36 mosquito cell growth curves using different cell plating densities. Each point represents the mean ± standard error of duplicate experiments.

Once it was determined that lower viral titers were required for C6/36 infection, qRT-PCR was performed to determine the optimal viral dilution and appropriate time point measurements for WNV quantification using qPCR. 2.5 x 10^5 cells were infected with either 6.5 x 10^5 pfu/well or 6.5 x 10^3 pfu/well, and viral replication was measured every 24h for 96h. Based on Ct values that best facilitated future analysis (data not shown), it was determined that 6.5 x 10^3 pfu/well would be used for infectivity assays.

Although initial cell density and viral titer are known, multiplicity of infection (MOI) remains still difficult to calculate because cells were grown 42 h prior to infection, and different treatments may result in different rates of growth.

To determine the optimal time points for the measurement of WNV genome copies, the fold increase in WNV replicons from time point 0 was calculated using the ΔCt method (Figure 3.16). The largest increase in WNV genome copies occurred between 48 h and 72 h, and best represents the "log" phase of viral growth. Based on Ct values measuring expression of the internal standard, *RpL8*, a modest degree of cell death was occurring by 96h post-infection. While cell growth increased rather steadily from 0 h to 72 h, approximately half of the cells died between 72 h and 96h. For these reasons, WNV genome copies were measured at 48 h and 72 h post-infection for future infectivity assays using dsRNA-mediated gene knockdown.

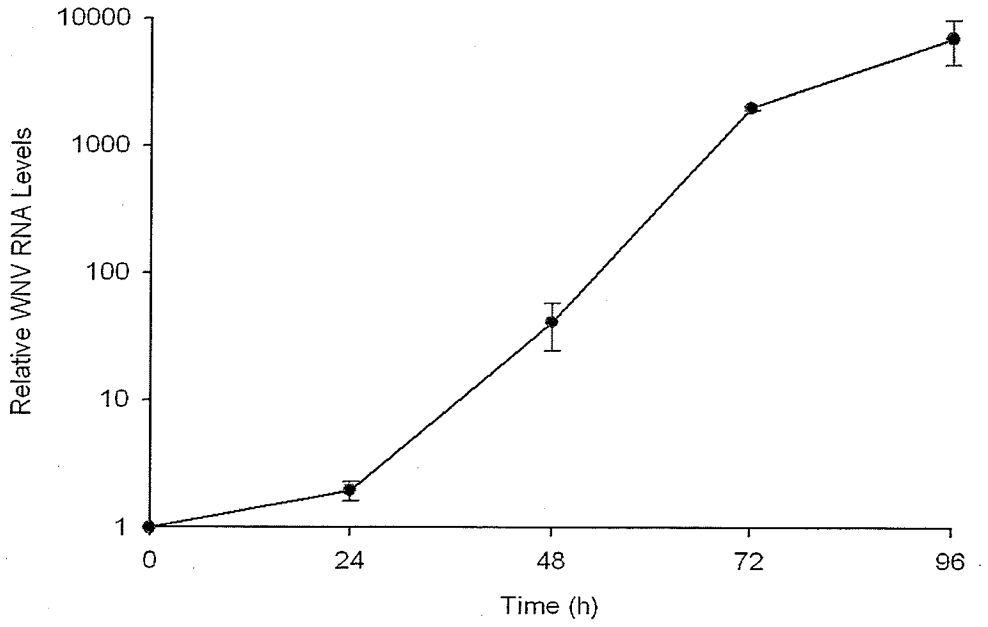

Figure 3.16. WNV growth curve demonstrating the fold increase in WNV genome copies from time 0 h. Values represent the means and standard errors of duplicate values at each time point.

3.5.b. WNV Infection Following dsRNA Mediated IMUC1 Knockdown

To understand whether AaIMUC1 plays a role in the infection and/or replication of WNV in *Aedes albopictus* cells, RNAi was used to knock down the expression of AaIMUC1 before infecting cells with WNV. To assess the efficiency of RNAi on the expression of the *Aedes albopictus* mucin gene (*AaImuc1*), C6/36 cells were first transfected with *AaImuc1* or *gus*-dsRNA and qRT-PCR was used to assess the extent of *AaImuc1* gene knockdown 48 and 72 h post-transfection. Although the *gus*-dsRNA was used as a negative control dsRNA, it curiously caused perturbations in *AaImuc1* transcript levels at each of the time points (Fig 3.17). At 0 h (18h post-transfection), the transfection of the cells with *gus*-dsRNA induced a small (~7%) initial increase in *AaImuc1* transcripts, but due to the fairly large standard error associated with this value, it is difficult to determine the exact change in expression. The gus-dsRNA-treated cells showed a 29% and 19% decrease in *AaImuc1* transcripts at 48 h and 72 h time points respectively when compared to untreated controls. Although unexpected, these results may be a stress response to lipofection or possibly a general protective response to the introduction of dsRNA. However, a sequence comparison of the *gus* and *AaImuc1* genes indicated that there were no 21 nt length regions of sequence identity that could induce off-target RNAi effects. For all subsequent analyses, the *AaImuc1*-dsRNA treatments were just compared to the *gus*-dsRNA-treated controls. At 48 h post-transfection, the lower dose (5 pmol) of *AaImuc1*-dsRNA showed no significant decrease in *AaImuc1* transcripts relative to the *gus*-dsRNA-treated cells (unpaired t test, $p>0.05$), but the higher dose (10 pmol) of *AaImuc1*-dsRNA induced a significant (~69%) decrease in *AaImuc1*

transcripts relative to the *gus*-dsRNA-treated controls (unpaired t test, $p<0.01$). By 72 h post-transfection, the 5 pmol of *AaImuc1*-dsRNA induced a slight, but not statistically significant (unpaired t test, $p= 0.093$) decrease in *AaImuc1* transcripts, while the 10 pmol *AaImuc1*-dsRNA still showed a significant (unpaired t test, $p<0.05$) ~80% reduction in *AaImuc1* transcripts.

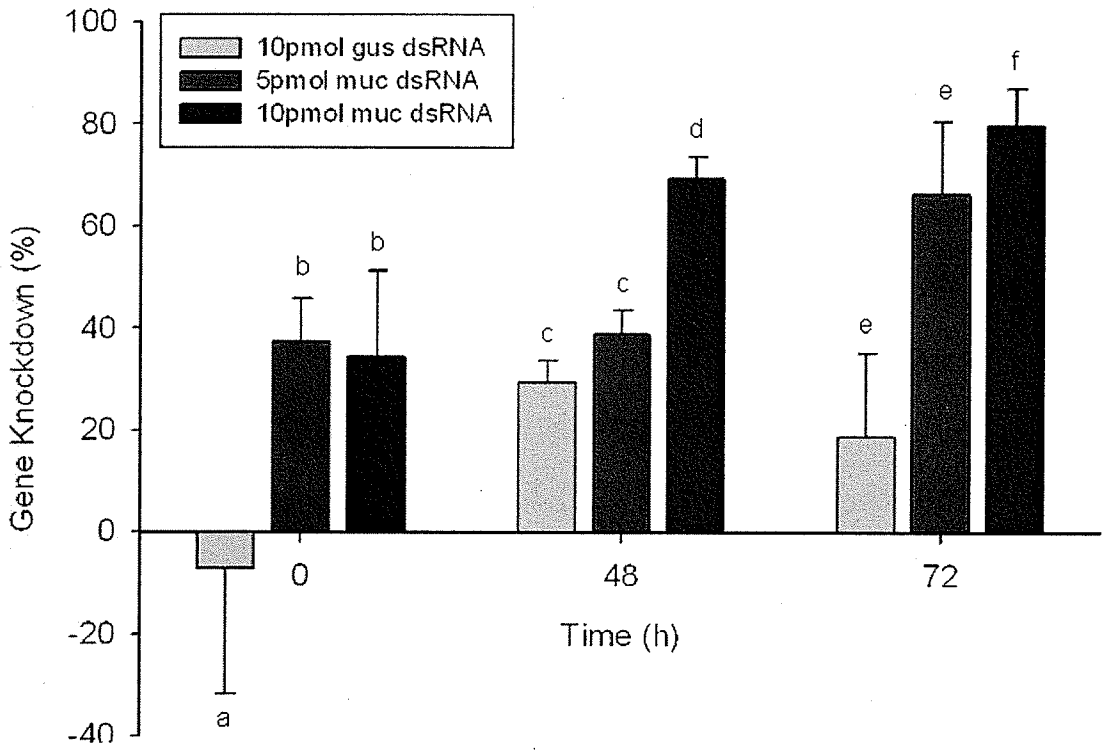

Figure 3.17. Mucin gene knockdown following *gus*- and *AaImuc1*- dsRNA lipofection. The percent gene knockdown values were normalized to the internal standard gene RpL8. Values represent the mean and standard error of three independent experiments. Different letters above the error bars denote values that are significantly different ($p < 0.05$, t-test) from one another for each individual time point.

Given that RNAi could reduce *AaImuc1* transcripts in the cultured cells, and presumably reduce mucin protein production, the dsRNA-transfected cells were

subsequently infected with virus 18 h post-transfection to determine whether changes in mucin expression affected virus replication. Replication of WNV was first assessed using qRT-PCR at 48 and 72 h post-infection to measure changes in WNV RNA levels relative to time zero, when the cells were first infected with virus (Figure 3.18). At 48 h post-infection, the higher dose (10 pmol) of *AaImuc1*-dsRNA produced a statistically significant 2.6-fold decrease in WNV genome replication (unpaired t test, $p<0.05$) when compared to *gus* dsRNA treatment results. The 5 pmol treatment produced 1.8-fold decrease in WNV, but this value is not statistically significant ($p = 0.11$) due to the large standard errors. By 72 h post-infection, the number of WNV genome copies was not significantly different (unpaired t test, $p>0.05$) among the different dsRNA treatments.

In this experiment and all subsequent measurements of either WNV transcripts or virus titration experiments, it was important to standardize the values relative to the number of cells within the treatment wells, as the different treatments affected the viability of the cells. As can be seen in Figure 3.17, the level of WNV transcripts in untreated cells (i.e. no liposomes or dsRNA) was lower than that of any of the dsRNA-transfected cells, including the negative controls treated with *gus*-dsRNA. This lower value is due to the fact that more cells survived the viral infection alone, compared to the virus + dsRNA treatments (based on *RpL8* Ct values), and hence, the virus/cell ratio in these wells was lower. The opposite was true for *AaImuc1* dsRNA treated wells, where increased cell death drove the virus/cell ratio higher.

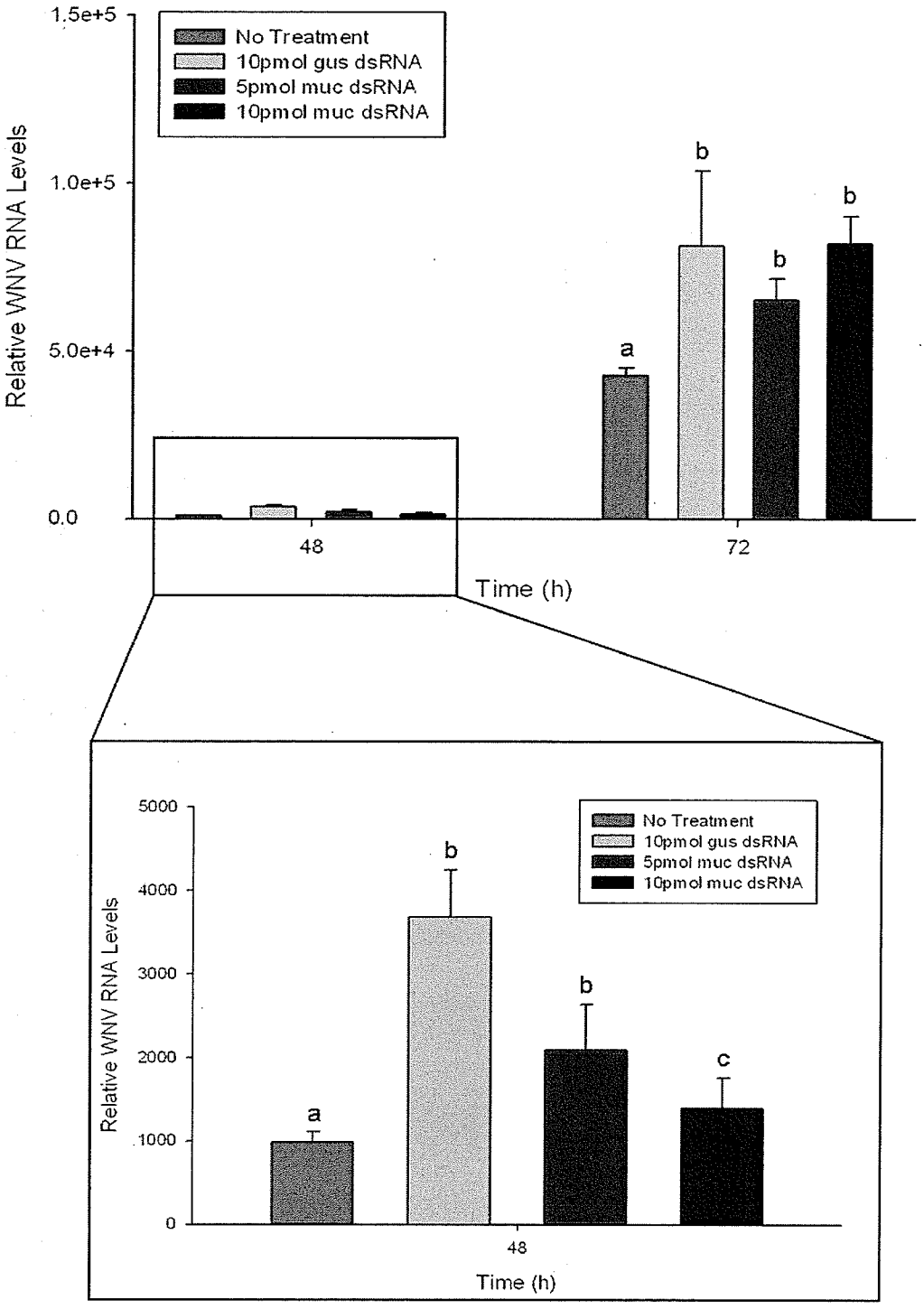

Figure 3.18. The level of WNV RNA recovered from combined cells and media at 48 and 72 h post infection, relative to time 0 h, following treatments with or without *AaImuc1* dsRNA. Values represent the mean and standard error for 3 replicates. Different letters above the error bars denote values that are significantly different from one another ($p < 0.05$, t-test).

To examine the negative impact of the viral infection and dsRNA treatments on cell numbers more closely, the cell numbers in all treatments were indirectly assessed by measuring the transcript levels of the cellular *RpL8* gene using qRT-PCR. At 48 h post infection (hpi), cell numbers (inferred from *RpL8* transcript levels) treated with virus alone had increased approximately 17-fold relative to time zero (Figure 3.19). Interestingly, cell growth in these virally infected cells appeared to stop, as the *RpL8* transcript levels remained virtually unchanged by 72 hpi. In contrast, all of the dsRNA + virus treated cells grew more slowly than cells infected with virus alone. *gus*-dsRNA + virus-treated cells showed a 5.2- and 9.5-fold increase in *RpL8* transcripts at 48 and 72 hpi. Cells treated with virus + 5 pmol *AaImuc1*-dsRNA showed no significant difference (unpaired t test, $p > 0.05$) in *RpL8* transcript levels compared to those of the *gus*-dsRNA-treated cells, but cells treated with 10 pmol *AaImuc1*-dsRNA had significantly lower *RpL8* transcript levels relative to the *gus*-dsRNA treated cells at 72 hpi, indicating there were fewer cells in these treatments by this time point. Due to these differential effects on cell viability and growth, all subsequent measures of viral transcripts and viral titers were normalized relative to the number of RpL8 transcripts present. By doing this, it would still be possible to assess the differential effects of the dsRNA treatments on virus replication.

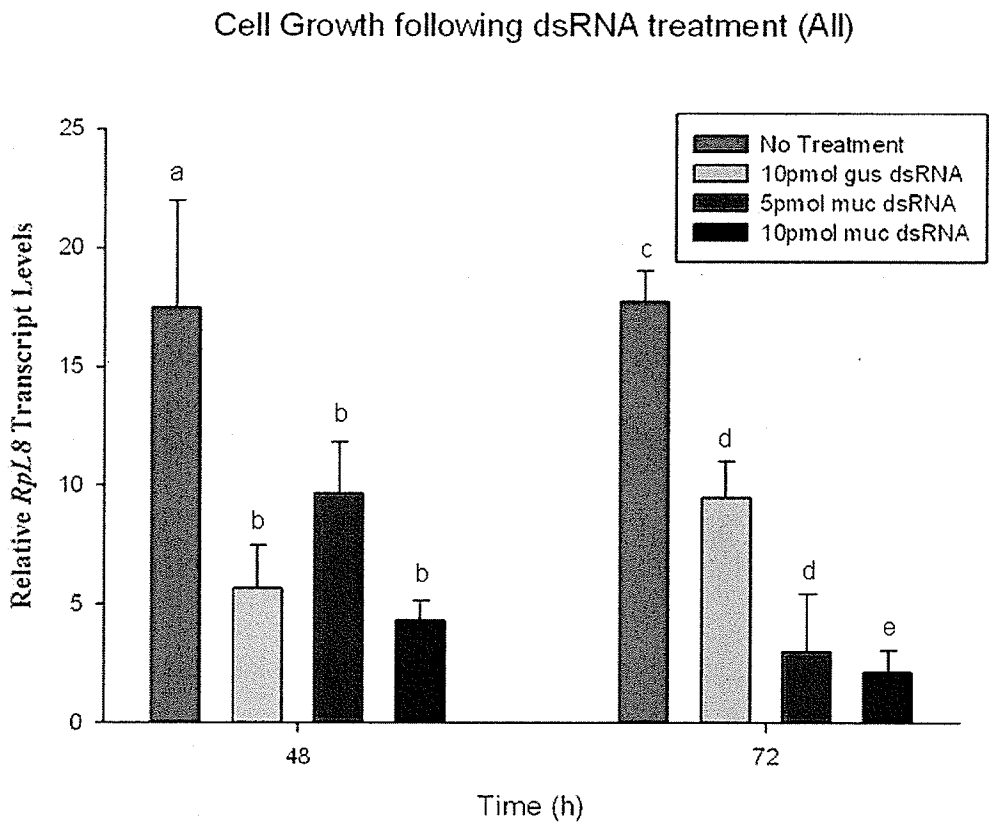

Figure 3.19. *RpL8* transcript levels at 48 and 72 h post infection following dsRNA treatments. The values represent the amount of *RpL8* transcripts relative to amounts detected at the time of infection (time zero), and therefore reflect relative cell numbers. Values represent the mean and standard error for 3 replicates. Different letters above the error bars denote values that are significantly different ($p < 0.05$, t-test) from one another for each individual time point.

To establish whether the reduction in WNV RNA correlated with reduced virus production, a plaque titration assay was performed to measure the amount of virus that could be extracted from dsRNA-treated cells and their media combined. The cell and media lysates were diluted between 10^{-1} to 10^{-8} before infecting confluent Vero cells to determine virus titers. Unfortunately by 72 h post-infection, virus levels were too high, such that even the greatest dilution (10^{-8}) of the lysates produced nearly confluent plaques and the virus titer could not be determined. In contrast, no visible plaques from all 0 h

dilutions were observed, which suggests that the vast majority of virus had already infected and uncoated within the C6/36 cells within the first hour of virus exposure, after which the cells and media were harvested for the first time point measurement. The virus titers at the 48 h post-infection time point, however, could be calculated, and the values support the results observed using the qRT-PCR method to quantify the virus. Figure 3.20 demonstrates that *AaImuc1* knockdown significantly affected the number of infectious virions (pfu) at 48 h post infection (unpaired t test, $p<<0.01$), reducing the amount of recoverable virus in the 5 pmol and 10 pmol *AaImuc1*-dsRNA-treated cells by ~108 and 740 fold, respectively, relative to the gus-dsRNA-treated controls.

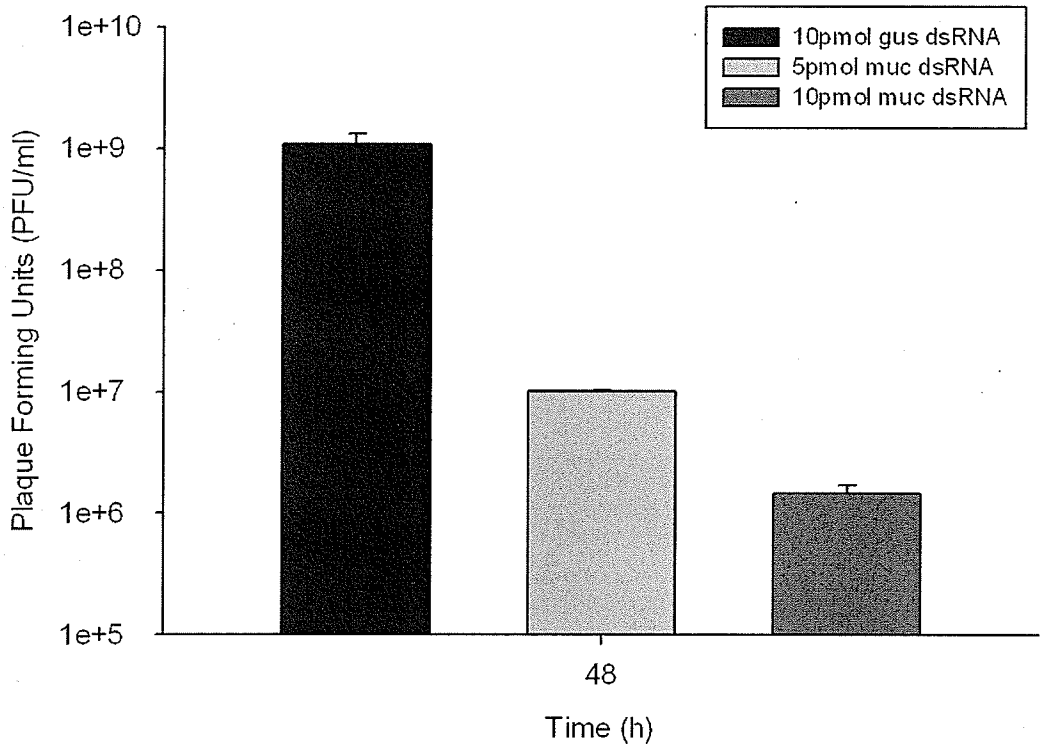

Figure 3.20. Number of infectious virions (pfu) at 48 h post-infection resulting from *gus* and *AaImuc1* dsRNA treatment. Values represent the mean and standard error for 3 replicates. Different letters above the error bars denote values that are significantly different ($p < 0.05$, t-test) from one another.

In the previous analyses, the RNA and the virus were recovered from the cells and their surrounding media combined, as the samples were frozen together with their media before extracting the RNA or virus. These values therefore reflect the combined intracellular and extracellular virus levels. To examine whether *AaImuc1* knockdown could affect viral release from the cells, the media was collected from infected cells at 48 and 72 h post infection, and extracellular viral RNA (derived from shed virus) was quantified using qRT-PCR (Figure 3.21). No evidence of C6/36 cellular RNA contamination was observed in the media, based on no detectable levels of *RpL8* RNA (data not shown). Because no *RpL8* Ct values were obtained from the supernatant, average *RpL8* Ct values from the previous total RNA extraction (cells and virus) were used to normalize the data. Figure 3.17 illustrates that the 10 pmol *AaImuc1*-dsRNA treatment resulted in a 7.8- and 2.9-fold reduction of extracellular virus compared to the *gus*-dsRNA treatment at 48 h and 72 h post-infection respectively (unpaired t test, $p<0.05$).

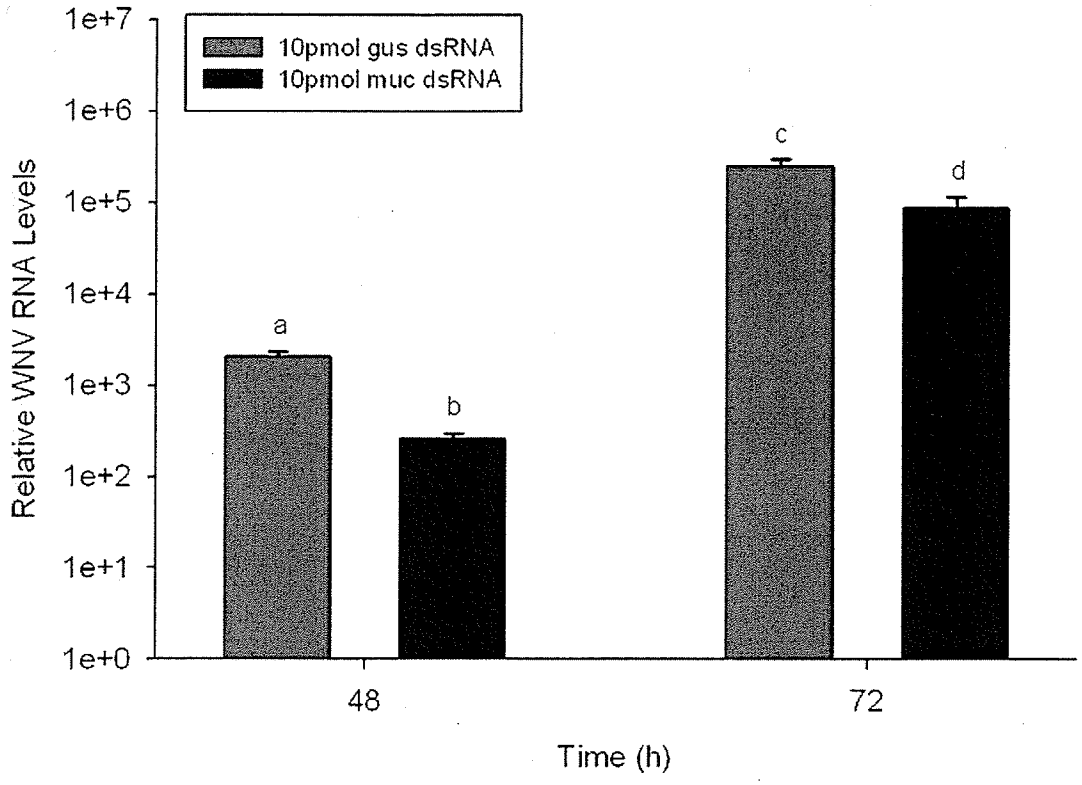

Figure 3.21. Relative levels of WNV RNA derived from extracellular virions at 48 h and 72 h post-infection for 10pmol *gus* and *AaImuc1* dsRNA treated cells. Values represent the mean and standard error for 3 replicates. Different letters above the error bars denote values that are significantly different from one another at each individual time point($p < 0.05$, t-tests).

In retrospect, it would have been useful to measure WNV transcripts and virus levels within infected cells alone, without the contaminating media, but unfortunately, due to time constraints and limited availability of the supporting staff at the National Microbiology Laboratory to help with the viral infections, these experiments are yet to be completed. Nevertheless, it is still possible to make some comparisons of the levels of WNV transcripts derived from combined cells and media with the levels of transcripts derived from extracellular virions alone. At 48 h post-infection, the level of extracellular viral transcripts had decreased ~8-fold relative to time zero, while the level of viral

transcripts derived from the cells and media combined was significantly less pronounced, showing slightly less than a 3-fold decrease (unpaired t test, $p<0.05$; Figure 3.22). Although a similar trend was observed at 72 h post-infection, the values are not significant for this time point (unpaired t test, $p>0.05$), due to some rather large standard errors in these measurements. These values suggest that knockdown of mucin expression results in a substantial reduction in the release of virus from infected cells, and that this reduced virus release may account for a significant portion of the measured reduction of WNV transcripts in the combined cell and media extracts.

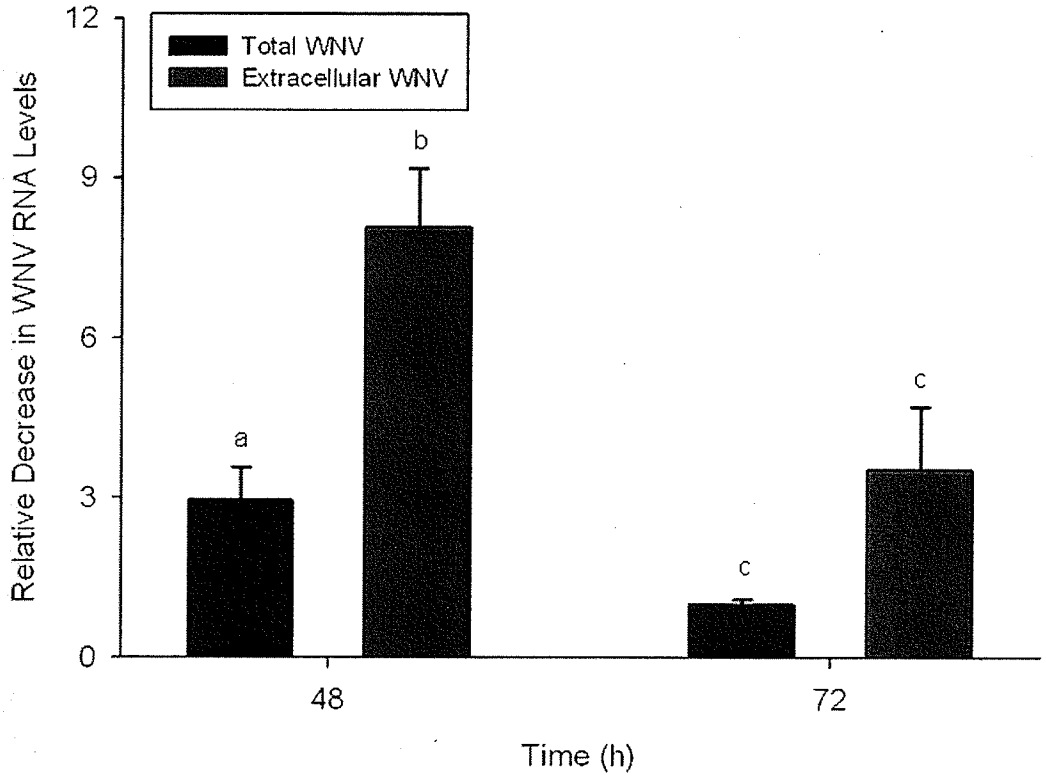

Figure 3.22. Comparison of the relative levels of WNV transcripts derived from cell + media extracts (black) with those derived from extracellular WNV transcripts (red) following *AaImuc1* knockdown. Values represent the mean and standard error for 3 replicates. Different letters above the error bars denote values that are significantly different from one another at each individual time point (using t tests).

CHAPTER 4. DISCUSSION

4.1. An Overview

To gain insight into the protein interactions that facilitate WNV infection and replication within the mosquito, a Y2H assay was performed using the viral NS1 and M proteins as bait. Twenty mosquito gut proteins were identified that appeared to interact with these viral proteins in the yeast cells, but due to constraints in time and funding, only a few were chosen to determine if they facilitate viral infection and replication. The candidate NS1-interacting proteins selected, namely mucin, EF2, and trypsin, were initially selected for further analysis for two principle reasons. Firstly, as will be discussed below, each of them have been associated with interactions with other pathogens in mosquitoes, and may similarly interact with WNV. Secondly, during the Y2H screening process, the frequency of occurrence of these three proteins was higher than that observed for many of the other proteins detected, which could reflect either a relatively strong interaction with NS1 or a high level of expression of the identified genes. One of these proteins, IMUC1, was chosen for a more thorough analysis of the interaction with the viral NS1 protein. The following discussion will leave the details of this particularly intriguing interaction until the end, and will therefore first provide an assessment of the utility of the Y2H approach in this study, followed by a brief description of the other proteins that were identified in the Y2H screen.

4.2 The Utility of the Y2H Assay and the Requirement for Controls

It is important to recognize that the protein interactions in this study were identified using recombinant proteins in a non-host species (yeast). Using yeast to assess heterologous protein-protein interactions has its advantages and disadvantages. Yeast are considered suitable recombinant protein expression hosts as they are simple eukaryotic organisms that are cheap to produce, can express high levels of recombinant protein, and for which the yeast two-hybrid system has been optimized over many years. Yeast are preferentially used to express eukaryotic proteins instead of the faster growing and more easily transformed bacteria because their post-translational protein modification processes are more similar to those of higher eukaryotes. However, all eukaryotic post-translational protein modifications are not the same, and the differences in these modifications can result in differences in protein properties in different hosts. For example, although N-linked glycosylation sites are the same for yeast and higher eukaryotes, yeast produce highly mannosylated glycans, whereas higher eukaryotes are capable of adding glycans containing fucose, galactose and sialic acid (38, 62). The differentially glycosylated proteins produced by yeast could result in differences in protein solubility, protease sensitivity, and in more drastic cases, alteration or inhibition of protein function (14).

Differential glycosylation in different host cells has been observed for a number of the WNV proteins, most notably the E and NS1 glycoproteins. Differential glycosylation patterns of the WNV E glycoprotein between species has prompted speculation as to whether these differences are related to the differential rates of infection and viral particle release from infected cells in different hosts (54). NS1 on the other hand

is present as a monomer, a dimer and a hexamer within infected cells; a feature that is speculated to be the result of differential glycosylation in dengue virus (44). While the dimeric form of NS1 contains high-mannose N-linked glycosylation, the hexameric secreted form of NS1 present only in mammalian cells contains complex, branched glycans on one of the two N-linked sites (44). High mannose glycosylation forms branches of mannose residues stemming from 2 *N*-acetylglucosamines, whereas complex glycosylation can contain any number of saccharides in a number of different branching patterns. Insect cells have been shown to produce high-mannose glycosylation (74), and not the more complex, branched glycans. The resulting lack of hexameric NS1 may explain why there is a lack of secretion of NS1 in the mosquito (84, 131). Interestingly, insects and yeast seem to possess a similar method of high-mannose glycosylation, which may have inadvertently made the yeast protein expression system the best option available.

Apart from the inherent protein modifications resulting from yeast protein expression, there are other factors that must be considered before concluding that any Y2H protein interactions are genuine. Firstly, in the Y2H system used in this study, translated proteins must be translocated to the nucleus, where they will potentially interact and act as transcriptional activators. Because the bait and prey protein are forced to interact within the nucleus, false positives or false negatives may occur as a result of the unnatural surrounding environment (nucleoplasm protein composition, osmolarity, pH, etc.). Also, proteins that may not normally interact because they are present in different cellular locations, are given an opportunity to do so in the nucleus (32). Although there may be a valid protein interaction, it may not be biologically relevant

because it would never naturally occur. Secondly, alternate tertiary structures may result from the fusion of DNA binding and transcriptional activating domains to the bait and prey proteins respectively (32). Unnatural protein interactions may therefore occur, providing false positives or negatives, and potentially wasting a great deal of time and effort attempting to validate them.

Lastly, even assuming that the Y2H proteins in question were translated and modified as they would be in insect cells, false protein interactions are commonplace and are nonetheless expected when performing two-hybrid techniques. It is estimated that high-throughput studies using two-hybrid techniques, affinity techniques and computational approaches produce 40-80% false negatives and 30-60% false positives (reviewed in (13)). While these numbers are seemingly quite high, and combined they produce over 100% error, they are merely estimations, and indicate that these techniques must be confirmed using different methods in order to be taken seriously. Even more surprising is the fact that only a small portion of identified protein interactions can be validated using a different technique (124). While false negatives could not be determined using the Y2H assay, a number of the results obtained were likely false positives. There is no definitive answer as to why certain proteins are so commonly identified using Y2H assays, but several theories have been proposed as to why they are repeatedly found. Some false positive proteins bind directly to the promoter sequence and are capable of activating reporter gene transcription without interaction with the bait protein (47). Others may be capable of binding to the DNA-binding domain of the bait, producing a functional transcriptional activator, but not as a result of interaction with the bait protein itself. They may also be merely "sticky" proteins that bind indiscriminately,

and are capable in one way or another of initiating transcription of the reporter genes. A survey conducted in 1996 of 223 investigators by Ilya Serebriiskii found the most common false positives to be heat shock proteins, ribosomal proteins, mitochondrial proteins, protease subunits and zinc-finger containing proteins among others (61). Representatives of most of these types of proteins were identified in the Y2H screen that I conducted, and some were suspected to be false-positive interactions, such as the ribosomal subunits L31, L6, S15, S20 and S24. In contrast, while the serine protease (AY432463) and early trypsin (AF508783) identified in the Y2H screen are typical of potential false-positive proteins, these two genes produced a multiplicity of Y2H positives. The frequency of their occurrences suggests that either they were genuine protein interactions, or they had a superior ability to activate the yeast selection promoter in one way or another.

Given that there are several potential sources of error when using the Y2H assay, it is important that the protein interactions identified were confirmed. To do this, ^{35}S-methionine labeled proteins were translated *in vitro* and co-immunoprecipitated using c-Myc or HA tag-specific antibodies. Using co-IP to confirm interactions has both its own advantages and disadvantages. A possible disadvantage of using an *in vitro* translation system to analyze the protein interactions is that the synthesized proteins are not necessarily post-translationally modified as they would be in a natural host cell. This may result in the production of incompletely processed proteins and which then fail to participate in genuine protein interactions. On the other hand, the co-IP approach reduces the risk of identifying false-positive interactions that are related to promoter activation in the Y2H system used in this study. To be more confident that the protein interactions are

genuine, the proteins could have been expressed in mosquito cells but there was insufficient time to clone the identified genes into insect expression vectors.

Like the Y2H assay, co-IP requires the translation of fusion proteins, except instead of being fused to a transcriptional activator or DNA binding domain, genes of interest are fused to protein tags. Although the production of tagged proteins may compromise the native tertiary structure of the translated proteins, the benefits outweigh the risk, because tag- specific antibodies are much less likely to bind non-specifically to various cellular proteins (13). Tagging proteins for use in co-IP also prevents the possibility of competition between the antibody and interacting protein for binding to the bait protein, ensuring that protein interactions can indeed occur (89).

The combination of both the Y2H and co-IP methods produces satisfactory evidence of the interaction between WNV NS1 and the mosquito gut mucin MUC1. Whether this interaction does in fact occur within the mosquito gut epithelium is yet to be determined; however, co-IP of mosquito translated proteins, or co-localization in mosquito cells may help provide the answer.

4.3. Y2H-Identified Proteins and Mosquito Innate Immunity

Although most of the Y2H identified protein interactions were not validated using co-IP in this study, it is worth considering their potential to interact with the WNV proteins, to help assess whether further studies of these proteins are warranted. By examining what is currently known of the different proteins' functions, their known or speculated interaction with other pathogens, and their expression profiles within mosquitoes, it is possible to offer some theories on how WNV NS1 interacts within host

cells to assist in viral infection, replication and dissemination within the mosquito gut. Knocking down the expression of these NS1-interacting proteins, or co-localizing viral and mosquito proteins within a cell would provide a clearer picture of the role NS1 plays in the viral replication cycle; however, time constraints limit the number of proteins that could be assayed in this manner, and consequently, I will use this section to propose which proteins are of greatest interest for future studies.

From the list of identified NS1 protein interactions, it becomes evident that a number of mosquito gut proteins play a role in the innate defenses within the gut. A common theme, and very possibly a requirement for most viral infections, is the modulation of the host's immune response to facilitate viral replication. As mentioned in Chapter 1, the mosquito has evolved many innate defenses within the gut to limit the infection of WNV as well as any pathogen that may be present in the blood meal. These include but are not limited to antihemostatic and digestive enzymes, peritrophic matrix (PM) formation, and altered pH in the midgut; all of which are a product of the cells lining the gut (12). It would therefore be beneficial for any pathogenic organism to evade or compromise the host defenses in order to reach and infect the midgut epithelium. Bosio *et al.* (20) identified several genes affecting vector competence for dengue virus in *Aedes aegypti*. They found that genes affecting virus titer within infected tissues had little effect on the capacity of a mosquito to transmit dengue virus. Instead, it was the genes associated with the midgut infection barrier (MIB) and midgut escape barrier (MEB) that most greatly affected vector competence. These would include genes whose altered expression or sequence polymorphism would prevent viral infection of the midgut epithelium (MIB) or dissemination from the gut into other tissues (MEB). Genes

encoding viral surface receptors of the midgut epithelium would be obvious candidates, as their proteins could facilitate flavivirus penetration into the midgut. Genes encoding gut proteases and pH regulating proteins, as well as peritrophic matrix proteins would also be in this group, as they regulate the conditions present in the mosquito gut where the virus first encounters the host.

The malaria parasite *Plasmodium* provides a stunning example of methods used by organisms to penetrate the mosquito's infection barriers. *Plasmodium* spp. secrete a chitinase that degrades the chitin component of the PM, enabling the parasite to free itself from the bolus and penetrate the epithelium prior to environmental changes within the midgut (proteolytic enzymes and changes in pH) (3, 63). Once released, the *Plasmodium* ookinete must pass through a highly glycosylated mucin and glycoprotein layer protecting the microvilli of the midgut epithelium. The method by which *Plasmodium* spp. penetrate the mucin layer is yet to be determined; however, many vertebrate parasites use mucins to bind and gain access to the intestinal epithelium. *Entamoeba histolytica*, a parasitic protozoan often found in feces-contaminated water sources, binds to galactose and N-acetyl-D-galactosamine residues of intestinal mucins and further degrades the mucin layer using proteases and glycosidases to gain access to the midgut epithelium (25, 33). Other parasitic organisms such as *Vibrio cholerae* up-regulate mucin secretion from the intestinal epithelium until the mucin reserves are depleted (76). The mucin secreted into the gut is soon sloughed away with peristaltic movement, resulting in an epithelium vulnerable to infection.

If able to overcome the aforementioned barriers, many outcomes are possible when the enteric pathogen reaches the intestinal epithelium. Parasites that require live

host cells to replicate, such as *Plasmodium* spp. as well as a variety of intestinal viruses use a cell surface receptor to bind and infect the intestinal epithelium of susceptible species. Once within the cell, the intracellular pathogen is able to use the host cell machinery to replicate itself and if possible, spread to other organs and systems resulting in disease pathogenesis.

4.4 The Identified Y2H Proteins and Their Possible Roles in WNV Interactions

Much research concerning the methods of viral and protozoal immune modulation and infection in the vertebrate model, as well as protozoal infection (*Plasmodium*) in the mosquito has been conducted, but contrastingly little is known about viral immune modulation in the mosquito. This allows for a great deal of interesting research to be conducted, facilitated by the large amount of information already known about these interactions in humans and other hosts. The mucin-NS1 protein interaction was confirmed using co-IP; however, many of the other interactions may potentially occur in the mosquito midgut. I will attempt to hypothesize functions for the remaining Y2H identified protein interactions, with an emphasis on innate immune system modulation.

4.4.a. Chitinase

NS1 demonstrated a protein interaction with an *Aedes aegypti* chitinase (accession number DQ129690) that like IMUC1, modulates the formation of the PM, but in the opposite direction, by breaking it down. Because the *Aedes aegypti* chitinase has not been well described, the Conserved Domain Architecture Retrieval Tool (CDART) (http://www.ncbi.nlm.nih.gov/Structure/lexington/lexington.cgi?cmd=rps) was used to identify domains within the protein sequence. An N-terminal chitinase/glycosyl hydrolase

domain was identified, followed by a chitin binding peritrophin-A domain. This supports its classification as a chitinase, as the domains are likely responsible for digesting and binding to PM chitin respectively. To further understand the expression of the *Aedes aegypti* chitinase, an *Anopheles gambiae* homologue termed AGAP006414 was identified using the NCBI protein BLAST tool. The *Anopheles gambiae* Gene Expression Database at UC Irvine was then queried, as it is the only mosquito expression database publicly available. The chitinase homologue was found to be expressed predominantly in the midgut and during all life stages (Figure 4.1). Interestingly, chitinase appears to be continually expressed in the adult female mosquito except immediately after consuming a blood meal. The expression of chitinase during the formation of the PM appears counter-intuitive, but may be necessary for the proper absorption of nutrients. While the addition of exogenous chitinase appears to inhibit the formation of the PM, the chemical inhibition of chitinase activity using allosamidin results in an irregular and excessively thick PM (42). The resulting thickened PM delayed blood meal digestion by 7-8 days. Chitinase expression is most probably reduced immediately post-blood meal to allow the early formation of the PM; however, expression climbs soon afterward to prevent the PM from becoming excessively thick. There is a clear trade-off between efficient blood meal digestion and protection of the midgut epithelium from ingested pathogens (123).

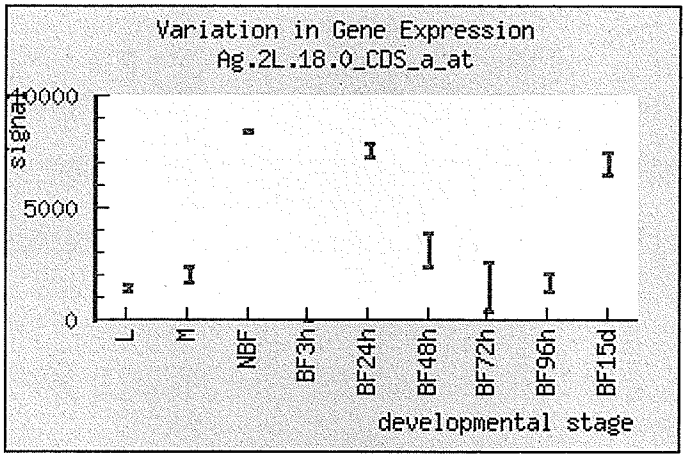

Figure 4.1. *Anopheles gambiae* transcript AGAP006414 expression profile (http://www.angaged.bio.uci.edu/). (L) larval stage, (M) male, (NBF) non blood fed, (BF) blood fed.

Interaction between WNV NS1 and *Aedes aegypti* chitinase may further inhibit the normal function of the PM. NS1 may induce the secretion of chitinase resulting in a weakened PM or prevent its secretion, thereby producing an irregular and inconsistent PM. It is also interesting to note that the *Aedes aegypti* chitinase as well as the IMUC1 protein identified using the Y2H both contain chitin binding domains, which suggests that NS1 may have an affinity for such domains. If this is the case, NS1 may limit the secretion of many PM components, drastically inhibiting its formation. This is somewhat unlikely though, as there were no other Y2H-identified proteins that contained chitin binding domains.

4.4.b. Early trypsin

Another protein with which NS1 was speculated to interact in theY2H screen was *Aedes aegypti* early trypsin (accession number AF508783). The early trypsin gene was first described by Kalhok *et al.* in 1993 (67) and has since been well characterized due to its important function in blood meal digestion. Classified as a serine protease, early

trypsin cleaves peptides at specific amino acid residues using a conserved serine within its active site. Each subclass of serine protease uses different recognition sequences, with trypsins cleaving on the carboxyl side of lysine and arginine residues (73). Early trypsin is a secreted serine protease that contains an N-terminal signal sequence that directs the trypsin into the gut lumen. Once there, the signal sequence is proteolytically removed to produce the active form of the trypsin.

Expression of the Y2H-identified early trypsin is adult female specific and is the most abundant early trypsin expressed in *Aedes aegypti* (105). Early trypsin is constitutively expressed in adult females and is translationally regulated to produce protein only when a blood meal has been taken (103). Once a meal has been ingested, early trypsin expression soon halts (Figure 4.2), and the resulting digested products (amino acids/peptides) activate the transcription of the late trypsin gene (8, 106). The result is a two stage trypsin release in which the first stage "gauges" the quality of the meal (based on the resulting pool of free amino acids), and the second stage functions in the majority of the digestion.

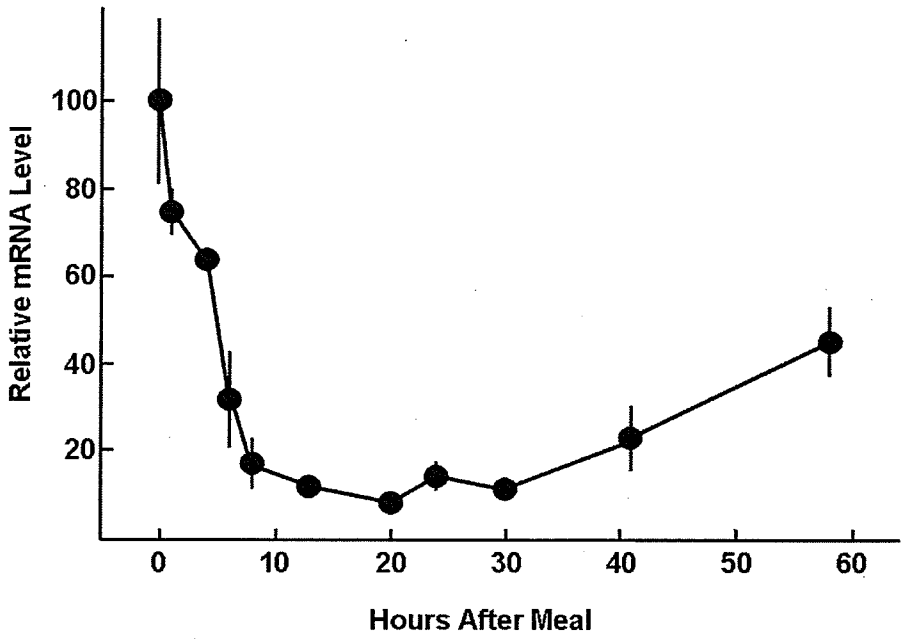

Figure 4.2. Early trypsin mRNA expression levels hours after feeding with a protein meal (150mg/ml γ-globulin) (reproduced from (103)).

The effect of trypsins on dengue virus infection has been previously examined. Using quantitative trait loci (QTL) analysis, polymorphisms of the early trypsin gene were found to affect not only the midgut infection barrier (MIB) but also the midgut escape barrier (MEB) and the disseminated infection within *Aedes aegypti* (21). Furthermore, trypsin digestion of mature dengue virus appears to increase short term infectivity and dissemination within the mosquito (92). These results indicate that trypsin affects dengue virus infectivity and replication within mosquito guts, and suggest that intact virus coat proteins may be affected. While it is understandable that WNV may also be affected by early trypsin due to its relation to dengue, the interaction with NS1 is not intuitively obvious. Because early trypsin is a zymogen, and is inactive within the epithelial cells, it is safe to assume that there is no processing of NS1 by trypsin. NS1

may, however, never come in contact with early trypsin *in vivo* due to differences in translation kinetics. Early trypsin transcripts are immediately translated after ingestion of the blood meal and their expression becomes drastically reduced soon thereafter. WNV infection, uncoating, genome translation and processing most likely takes longer than the hours required for early trypsin to perform its function. To determine whether NS1 has a direct interaction with early trypsin, more information on NS1 protein production and WNV replication kinetics within the first hours of mosquito infection is required.

It is perhaps more realistic to speculate that NS1 interacts with a related trypsin. In fact, nine trypsins were identified in the *Anopheles gambiae* peptide database, with E values above 1e-50 when aligned with the *Aedes aegypti* early trypsin (http://agambiae.vectorbase.org/Tools/BLAST/). The identified trypsins demonstrated a diverse range of expression profiles (Figure 4.3), indicating that it is very possible that NS1 interacts with a similar yet differentially expressed trypsin in *Aedes aegypti*. Alignment of the four trypsin amino acid sequences presented in Figure 4.3 using ClustalW (data not shown), calculated percent identity scores ranging between 65 and 79 with an average of 73.

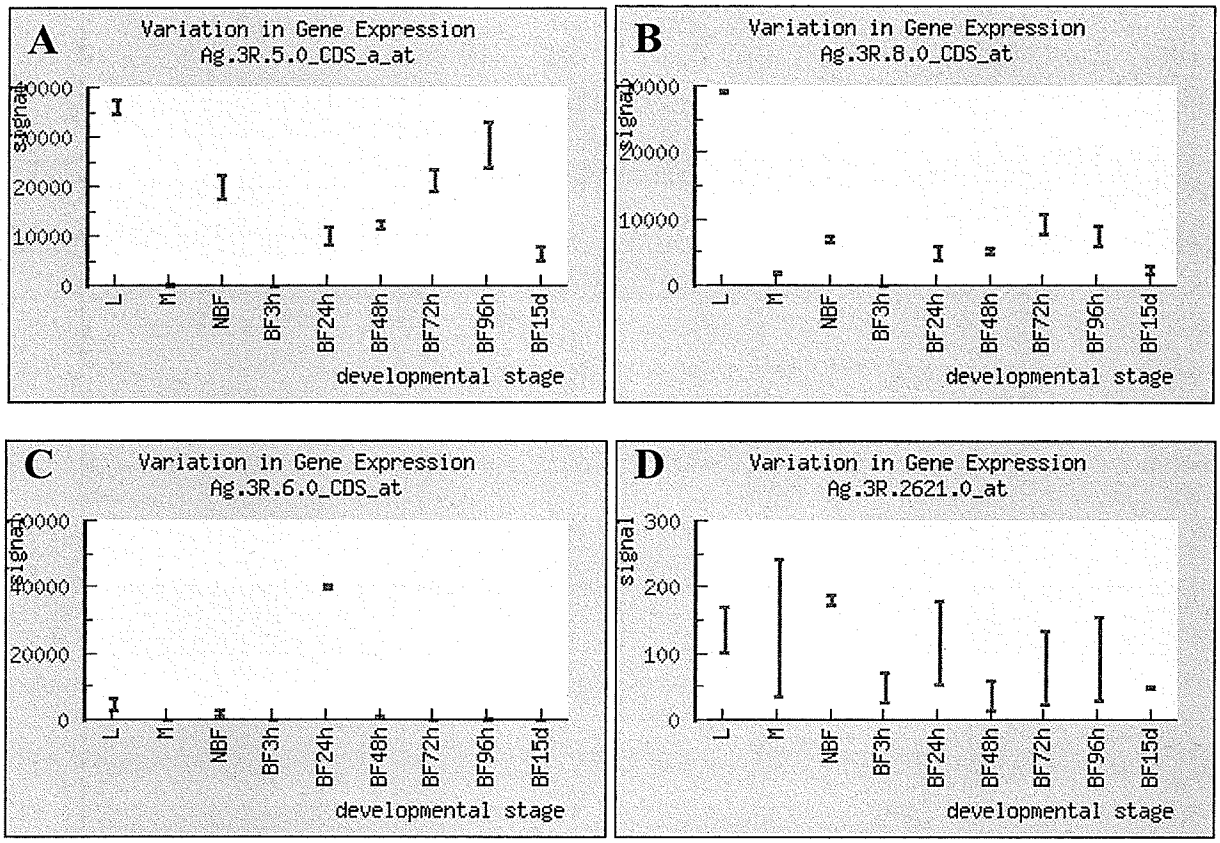

Figure 4.3. *Anopheles gambiae* expression profiles for transcripts (A) AGAP008292 (B) AGAP008294 (C) AGAP008295 and (D) AGAP008296 (http://www.angaged.bio.uci.edu/) demonstrating E values of 1e-79, 5e-74, 1e-71 and 1e-74 respectively when aligned with *Aedes aegypti* early trypsin. Expression profiles indicate a large degree of differential trypsin expression. (L) larval stage, (M) male, (NBF) non blood fed, (BF) blood fed.

4.4.c. Serine protease

Like the *Aedes aegypti* early trypsin, the serine protease (accession number AY432463) cleaves proteins in the lumen of the midgut, but does so using a different substrate site. The *Aedes aegypti* serine protease contains a hydrophobic substrate binding pocket indicative of a chymotrypsin, which cleaves proteins at bulky hydrophobic amino acid residues such as phenylalanine, tryptophan and tyrosine (15). Coincidentally, the expression of both transcripts appears to be regulated by juvenile hormone (JH), a

hormone responsible for a multitude of developmental processes in the mosquito (15, 104).

The expression of the chymotrypsin-like serine protease is similar to that of early trypsin at the mRNA level (Figure 4.6), which is not surprising due to their regulatory similarities. The major difference between the two lies in the level of protein production, where serine protease is present in the midguts of female mosquitoes before and after feeding (15). While serine protease is possibly a digestive endopeptidase similar to early trypsin, it may also fill one of the many immune related roles serine proteases carry out within the innate immune system of the mosquito. Serine proteases are directly and indirectly associated with pathogen recognition, melanizatation, antimicrobial peptide synthesis and hemolymph coagulation in the mosquito (50). The identified serine protease is also expressed in mosquito hemocytes following bacterial challenge (9), indicating that it is possibly immune-related and not specific to the mosquito gut. However, its specific role remains unknown.

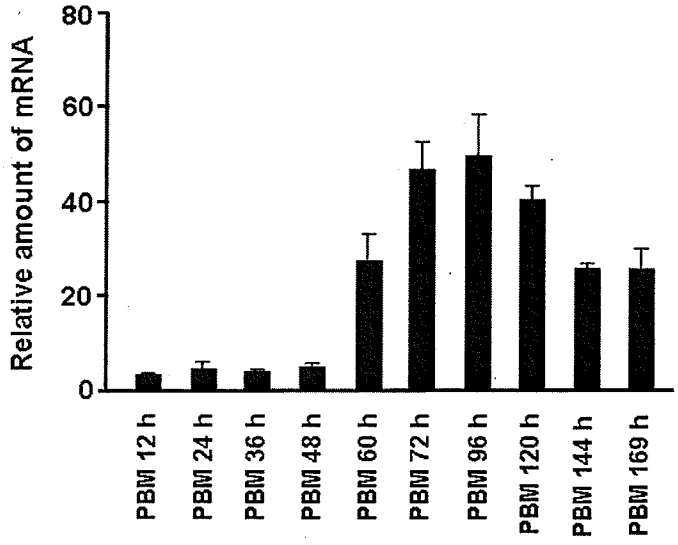

Figure 4.4. Expression profile of *Aedes aegypti* chymotrypsin-like serine protease relative mRNA levels post-emergence (PE) and post-blood meal (PBM) (reproduced from (15)).

Similar to the chitin binding domains in the mucin and chitinase proteins, it can be hypothesized that NS1 interacts with conserved serine protease residues within the two identified peptidases. This is however even more unlikely, as serine proteases retain important catalytic residues, but as a whole, can differ quite dramatically in amino acid sequence. This is also combined with the fact that only two serine protease transcripts were identified in high numbers, while no similar proteins demonstrated interaction with NS1. Considering the identified chymotrypsin-like serine protease is likely immune related, it would be advantageous for WNV to prevent its proper function. Interaction with NS1 may prevent the proper function of the serine protease by limiting its post-translational modifications or its secretion, but since the role of the identified serine protease is uncertain, no specific hypotheses can be made.

4.4.d. Prefoldin Chaperone

The *Aedes aegypti* chaperone sequence (accession number AY431885) identified using the Y2H assay is a prefoldin β protein responsible for binding unfolded and misfolded proteins within the cytosol. Prefoldin (PFD) is a hexameric protein composed of 2 prefoldin α and 4 prefoldin β subunits, resulting in a shape similar to that of an octopus (83). PFD has been shown to bind and escort unfolded/misfolded actin and tubulin molecules to the cytosolic chaperonin (c-cpn) molecule that folds them in their native conformation (122). Prefoldin likely binds other proteins, but none have been uncovered to date.

To determine the expression of PFD-β, a homologue was identified by querying the *Anopheles gambiae* transcript database

(http://agambiae.vectorbase.org/Tools/BLAST/). With an E value of 2e-51 the Anopheles peptide AGAP012235 was identified. The *Anopheles gambiae* Gene Expression Profile Database at UC Irvine indicates that expression is fairly constant throughout all developmental stages and post-blood feeding (http://www.angaged.bio.uci.edu/). Combined with its role as a chaperone, these data indicates that the PFD complex is likely important for cellular homeostasis in the mosquito.

Given that actin and tubulin are responsible for some of the most important cellular processes (cytoskeleton formation, motility, cell division and vesicular transport), interfering with their proper folding could be catastrophic to a cell. Combined mutation of PFD and ssb-class HSP70s in yeast results in a growth deficiency (57), indicating that PFD may be required for proper cell growth, but not survival. During WNV infection, PFD may simply play a role in the proper folding of NS1, but the interaction may be more complicated and interesting than that. The Y2H assay also demonstrated an interaction between NS1 and *Aedes aegypti* actin, which is required for viral endocytosis (37) and budding out (27). NS1 may bind to, and facilitate the interaction between actin and PFD to ensure adequate, properly folded actin is available for the egress of WNV from the cell. Actin clumping has in fact been demonstrated at the periphery of WNV infected Vero cells (Figure 4.7), indicating that the large numbers of virions exiting the cell may produce a great deal of stress on the secretory machinery, including the actin filaments.

Disruption of normal actin function within the *Aedes aegypti* midgut may also affect the midgut epithelial response to viral infection. Infection of *Aedes aegypti* with *Plasmodium gallinaceum* results in the expulsion of single infected cells into the midgut

lumen, via an actin mediated cone zipper mechanism (53). Disruption of this mechanism may leave epithelial cells vulnerable to viral infection and further viral proliferation. Susceptible mosquito vectors may also undergo limited midgut cell apoptosis when compared to resistant species. C6/36 cells (belonging to the susceptible species *Aedes albopictus*) have demonstrated similar levels of inhibitor of apoptosis protein in control and LaCrosse virus (Bunyaviridae, Orthobunyavirus) infected cells (18), indicating that apoptosis may not be the dominant factor in midgut infection inhibition. Non-transmitting species *Culex quinquefasciatus* have demonstrated a significant amount of apoptosis in midgut epithelial cells, indicating that apoptosis may play a large role in their resistance to WNV transmission. By limiting the dominant method of programmed cell "expulsion" within the midgut of species that rely less on apoptosis in the gut, NS1 may facilitate the dissemination of WNV in susceptible mosquitoes.

4.4.e. Elongation factor 2

Elongation factor 2 (EF2) performs an essential role in the translation of proteins by facilitating the translocation of aminoacyl-tRNA molecules in conjunction with the eukaryotic ribosome. Not surprisingly, due to its role in protein translation, the expression of mosquito EF2 is fairly constant. Expression decreases soon after a blood meal and increases a few days afterwards, most likely as a result of the large pool of newly available amino acids from the blood meal. (http://www.angaged.bio.uci.edu/lookup2.php?geneid=Ag.3R.160.0_CDS_a_at).

Aedes aegypti EF2 (accession number AY064104) is a good candidate for interaction with NS1 due to its close interaction with cellular RNA. NS1 interacts with the viral dsRNA replication complex to facilitate replication of the RNA genome, and

NS1 mutation has been shown to inhibit viral propagation (77, 129). Like all viruses, WNV requires host translation machinery to produce its viral proteins and replicate its positive sense RNA genome. Elongation factor 1α (EF1α) has been shown to interact with the 3' stem loop region of WNV UTR and facilitate WNV minus strand synthesis during viral RNA replication (17, 35). The fact that NS1 is also required for viral RNA replication is perhaps not a coincidence, indicating that NS1 may very well interact with a suite of proteins that are required to replicate its RNA genome. Because EF1α has a close association with EF2 during protein translation, it would not be a stretch to hypothesize that both are utilized in WNV genome replication.

4.5. NS1-IMUC1 Interaction

The *Aedes aegypti* mucin-like protein ($IMUC^{R1}$) (accession number AF308863) identified using the Y2H assay, is an allele of the protein IMUC1, first identified by Rayms-Keller *et al.* in 2000 (111). IMUC1 is a gut specific mucin that is secreted by the intestinal epithelium to help form the PM surrounding the blood meal (36). Sequence analysis of the $IMUC^{R1}$ confirms the presence of a signal peptide, several chitin binding domains and a mucin domain (Figure 4.5). The chitin binding domains are rich in cysteine residues, and facilitate interaction with the chitin component of the PM (111). This, in combination with a number of other PM glycoproteins, results in the production of a tangled web of chitin fibrils that produce a pore size large enough to allow digestive enzymes into the PM but small enough to reduce a number of pathogens from reaching the midgut epithelium. Chitin binding domains have also demonstrated heme binding properties *in vitro*, suggesting that IMUC1 also plays a role in heme detoxification of the

blood meal (36). The mucin domain is rich in proline, threonine and serine residues, which give the mucin its characteristic "stickiness" (111). The serine and threonine residues are highly O-glycosylated, and can account for up to 80% of the weight of the mucin glycoprotein (113).

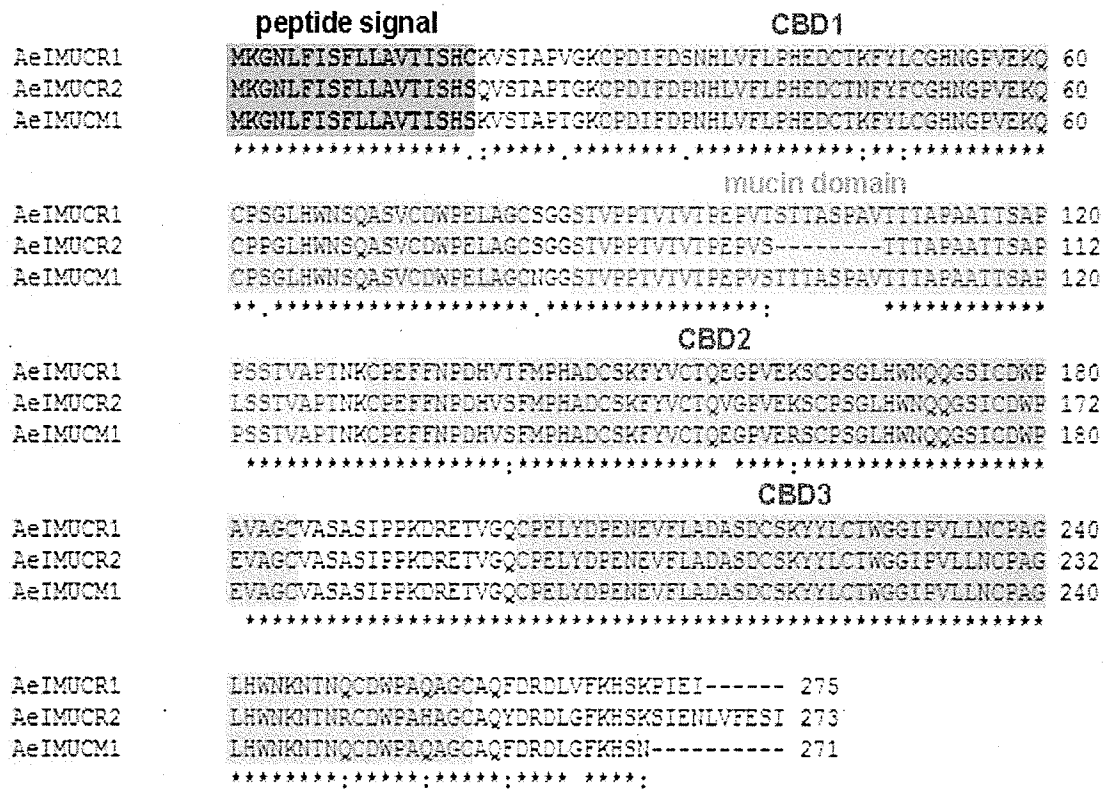

Figure 4.5. Amino acid sequence alignment of 3 IMUC1 alleles (sequenced in (93)) indicating sequence polymorphism and protein domains.

Mucin expression is specific to developmental status, sex, nutritional status and pathogenic challenge. IMUC1 is not expressed in the pupa or the male mosquito (11, 111), but is expressed in the female mosquito and is up-regulated post-blood meal ((11); Figure 4.6). In my study, however, the RNA used to prepare cDNA was obtained from

guts of non-blood fed female mosquitoes, when mucin expression should be low. The moderately high frequency of NS1-mucin interactions identified in the Y2H assay does not therefore likely reflect a large number of mucin RNA transcripts in the gut, but may instead indicate a biologically important interaction of these proteins in WNV-infected cells.

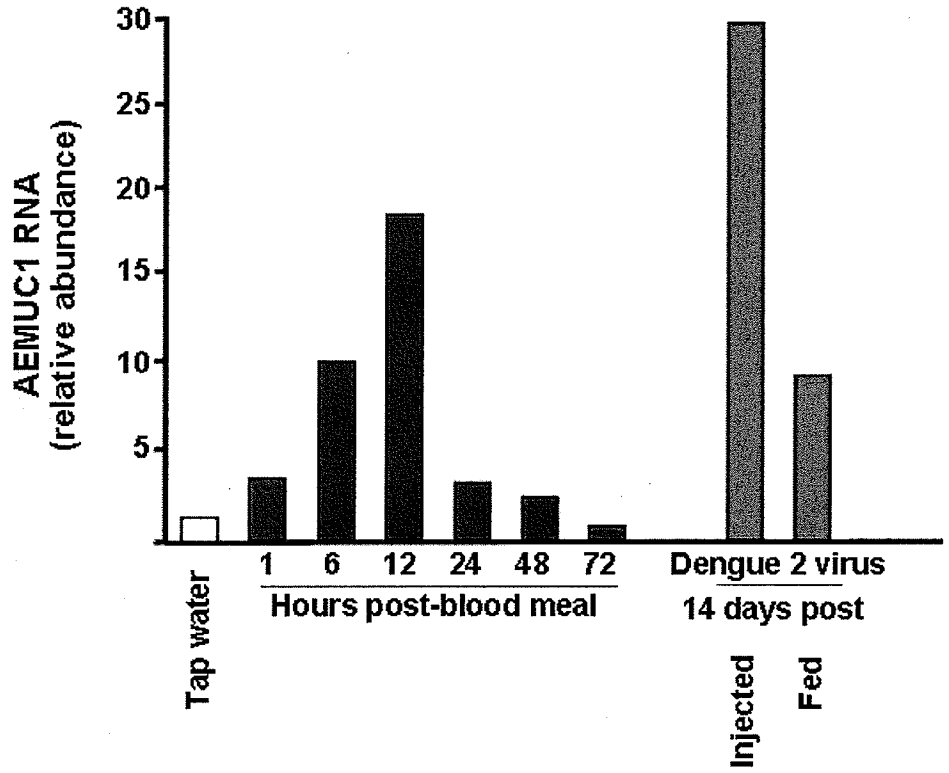

Figure 4.6. The relative abundance of *Aedes aegypti* mucin RNA in response to blood feeding, heavy metal exposure and dengue virus challenge (reproduced from (11)).

Interestingly, IMUC1 is also highly up-regulated when mosquitoes are injected or fed dengue virus (11). The role of mucin in innate immunity is further strengthened by the upregulation of the human mucin MUC2 following the expression of dsRNA in

airway epithelial cells (81). This increase in epithelial mucins likely plays a role in preventing pathogens from reaching the intestinal epithelium, and makes the observed interaction with WNV NS1 intriguing. In uninfected mosquitoes, IMUC1 expression peaks at approximately 12 h post-blood meal and slowly declines to basal levels by 3 days [52]. In contrast, IMUC1 expression persists at high levels for as long as 14 days post-dengue infection (see Fig 4.9; [53]). This relatively high expression of IMUC1 may reflect a prolonged host immune response that aims to reduce further virus infections of gut cells by preventing virions from penetrating the intestinal epithelium. Evidence of a protective role for the PM in limiting susceptibility to viral infections *in vivo* has been reported (125), where PM disruption using calcofluor resulted in an increased susceptibility to baculovirus infection in lepidopteran insects. Mucins have also been shown to mimic pathogen-binding sites on the intestinal epithelium, resulting in the competitive inhibition of infection (24).

The kinetics of viral infection as well as peritrophic matrix formation must be examined in order to fully understand the sequence of events leading to infection of the intestinal epithelium. The expression of IMUC1 appears up-regulated as early as 1 hour post-blood meal, but the complete formation of the peritrophic matrix takes approximately 18-24 hours after blood ingestion (94). The kinetics of flavivirus infection *in vivo* remains somewhat of a mystery; however, viral infection appears quite rapid in cell culture. Once bound to C6/36 cells, Japanese encephalitis virus and dengue-2 virus are both capable of infecting cells in minutes (58). Based on my measurements of extracellular WNV titers directly following infection of C6/36 cells, it appears that WNV also infects cells quickly (at least within the first hour of exposure). These rapid

infections within cell cultures do not, however, necessarily reflect the conditions within a mosquito's gut. Virus contained in the blood meal can become trapped by the forming PM as early as 3 hours after ingesting the blood meal (130). It is therefore likely that only a fraction of the virions reach the epithelial cells before the rest are trapped within the PM. One would predict that a blood meal containing a higher titer of virus would more often lead to a systemic infection of the mosquito. A study performed by Goddard *et al.* (48) demonstrated this fact using a variety of native Californian mosquito species. For example, only 11% of *Culex tarsalis* mosquitoes, a species native to Manitoba, became infected with WNV when fed with blood containing $10^{4.9}$ pfu/ml, compared to 81% with $10^{7.1}$ pfu/ml (48).

If we accept that mucin secretion by gut cells protects the insect from virus infection, it would be advantageous for a virus to reduce the secretion or proper function of mucins post-infection, as this would disrupt the PM integrity and possibly increase the rate of virus infection. While some virions have probably already infected some of the intestinal epithelial cells following ingestion of a viraemic blood meal, preventing the proper formation of the PM may facilitate subsequent infections of adjacent gut epithelial cells by virions produced in previously infected cells or virions still present in the gut lumen. The increase in viral infection within the gut lining may be what is required for WNV to disseminate throughout the entire mosquito.

Unfortunately, the experiments in this study cannot adequately assess the possible role of mucin in protecting the cells from viral infection, as the cultured cells would not likely produce sufficient mucin to create a PM. Similarly, it was not possible to determine from my experiments whether WNV could suppress mucin production in the infected

cells, although the results of the knockdown of *AaImuc1* expression by RNAi in the cultured cells surprisingly reduced viral replication. AaIMUC1 knockdown clearly adversely affected some part of the WNV replication cycle, whether it be infection, genome replication, particle assembly or particle release. Given the reduction in viral genome replication and the reduction of virus within the cells and media following the RNAi-induced knockdown of AaIMUC1, it is worthwhile to formulate some hypotheses on how mucin may interact with WNV proteins in the intact mosquito.

On one level, AaIMUC1 likely does plays a role in reducing virus infection of the gut cells of *Aedes albopictus* when the virus is first ingested. In the experiments knocking down AaIMUC1 in the C6/36 cells, extracellular virus levels were significantly reduced (Figure 3.18). Given that mucin may reduce virus entry into cells, it is possible, although not highly likely, that the reduction in mucin enabled any shed virus from infected cells to quickly re-infect cells, and thereby produce the low extracellular virus titers observed at 48 and 72 hpi. However, in light of the fact that AaIMUC1 knockdown also caused a reduction in viral replication, based on qRT-PCR measurements, there are other scenarios that might better explain the mucin-WNV interactions.

Because AaIMUC1 is a secreted protein, it is likely that an NS1-AaIMUC1 interaction would either assist virion assembly, exocytosis (via the secretory pathway), or (re)infection. Both NS1 and AaIMUC1 are transported through the endoplasmic reticulum and the Golgi apparatus where NS1's two N-linked glycosylation sites (97) and AaIMUC1's mucin domain becomes O-glycosylated (108). Once AaIMUC1 has been processed, it is likely secreted via the secretory pathway, where it would combine with chitin and other glycoproteins to form the PM *in vivo*. NS1 on the other hand, can remain

as a monomer or dimerize and localizes either in association with intracellular membranes or bound to the plasma membrane (129) in mosquito cells. The intracellular and extracellular route taken by both proteins permits interaction either within the ER and Golgi apparatus, during secretion (in secretory vesicles), and at the plasma membrane. Although it is possible that AaIMUC1 somehow facilitates WNV replication in conjunction with NS1, it is unlikely because flavivirus replication occurs predominantly in cytoplasmic vesicles and within the nucleus (121), both of which are subcellular locations where AaIMUC1 would not be normally located.

If NS1 and AaIMUC1 are co-localized in the same secretory vesicles as a consequence of their interaction, it is possible that when they reach the plasma membrane, NS1, which remains anchored in the membrane, could retain and trap AaIMUC1 on the outer membrane (Figure 4.7). Doing so could prevent the proper formation of the PM, but may also facilitate the infection process by acting as an attachment protein in the same manner that DC-SIGNR does in mammalian and mosquito cells (34). The pathogen-binding function of mucin could thereby be utilized to increase the chance of an interaction between WNV and the virus receptor. Interestingly, approximately 20% of plasma membrane-associated dengue virus NS1 may be GPI-linked (64), and therefore involved in signal transduction processes. These GPI-linked NS1 proteins may promote dengue viral release from infected cells [66], and it is possible that the interaction of NS1 with its associated AaIMUC1 may have a similar role in WNV infected cells. In agreement with this idea is the qRT-PCR results that show that the presence of AaIMUC1 results in more extracellular virus (Figure 3.18).

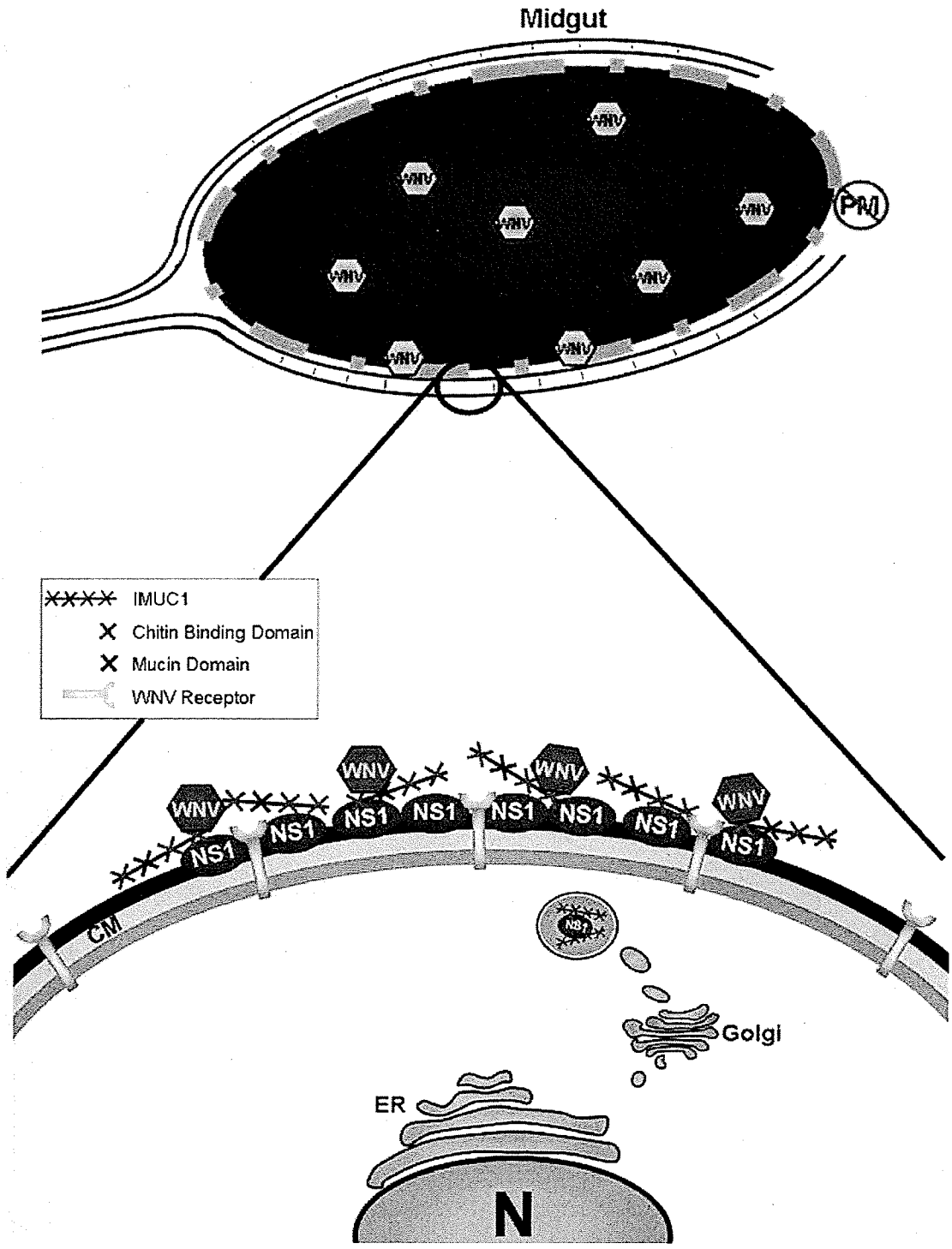

Figure 4.7. The hypothetical function of an NS1-AaIMUC1 interaction in *Aedes albopictus* cells. The interacting NS1-AaIMUC1 proteins are co-secreted and become membrane associated, thereby preventing the proper formation of the PM. AaIMUC1 is next used as an attachment protein to facilitate the interaction between WNV and virus receptors.

The NS1-AaIMUC1 interaction may also facilitate the secretion of virions from infected cells. In such a scenario, the interacting NS1-AaIMUC1 proteins within the trans-Golgi network may also complex with assembled virus. It is possible that NS1 acts as a link between AaIMUC1 and WNV to highjack secretory vesicles designed to secrete the mucin, although no protein interaction between NS1 and the viral E or M proteins have been demonstrated to date. An interaction between AaIMUC1 and the WNV coat proteins could possibly facilitate virion secretion, but this does not explain why an NS1-AaIMUC1 protein interaction is necessary. Nevertheless, given that knockdown of AaIMUC1 resulted in reduced virus exocytosis, it is conceivable that lack of mucin production resulted in a slowing or stoppage of the secretory pathways, and thereby inadvertently reduced virus release.

The secretion of the NS1-AaIMUC1 interacting proteins is also an interesting possibility, as it has generally been accepted that NS1 is not secreted from insect cells (84, 131). However, most reports of the absence of NS1 secretion have been observed in cell culture, most often using embryonic C6/36 cells, and not in an intact host organism. Flavivirus NS1 secretion may occur in mosquitoes and it would be even more interesting to see whether it occurs in the hemolymph, the midgut lumen, or both. There is one single report of NS1 secretion in C6/36 cells using a recombinant baculovirus expressed NS1 (43), which indicates that insect cells are capable of secreting a form of NS1. Perhaps, the NS1-AaIMUC1 interaction facilitates the secretion of NS1 into the gut lumen, where it becomes endocytosed by midgut epithelial cells, in a similar way that secreted NS1 is endocytosed by hepatocytes in cell culture (4). Dengue virus titers increased up to 6.7

fold in hepatocytes containing endocytosed NS1, indicating that secreted NS1 somehow facilitated the infection or replication of dengue virus in those cells (4). It is possible that a secreted form of NS1 *in vivo* could "prime" uninfected mosquito gut epithelial cells for infection, resulting in higher titer, and a greater likelihood of infecting its next host.

4.6. Conclusions and Future Directions

Several ideas have been presented to explain the Y2H-identified protein interactions, with emphasis on AeIMUC1. Although significant results were obtained pertaining to the NS1-IMUC1 interaction in C6/36 cells, time constraints and equipment limitations prevented a number of questions from being answered. In particular, cultured cells derived from *Aedes albopictus* mosquitoes were used to try to elucidate the nature of host-virus protein interactions in the related species *Aedes aegypti*, simply because these cells were the only mosquito cells available. The knockdown of the AeIMUC1 homologue AaIMUC1 did affect viral replication, and produced very interesting results, but the interaction of NS1 and IMUC1 should be assayed *in vivo* in order to understand fully the importance of the interaction. Although I will be unable to continue work on the IMUC1 and other protein interactions that were identified, a number of experiments should be performed in order to fully comprehend where and why they are occurring in live mosquitoes.

To determine the effects of WNV infection as well as IMUC1 knockdown on the formation of the PM, immunofluorescence could be used on cross sections of mosquitoes to determine the location of IMUC1 as well as NS1. This will also demonstrate where (and if) the protein interaction occurs *in vivo*, and may shed some light on the function of

the protein interaction that I identified using the Y2H method. The examination of IMUC1 knockdown in WNV infected *Aedes aegypti* mosquitoes would determine without a doubt that the protein interaction affects WNV replication *in vivo*, where the PM is produced, unlike cell culture. Assuming results similar to those that I observed are obtained, analysis of sequence polymorphism and expression of IMUC1 in different species with varying vectors competences could possibly shed some light on why certain mosquitoes are capable of transmitting the disease while others are not. Together, these assays will help determine the role of the identified protein interaction, and may lead to other experiments that may clarify the function of IMUC1 in the infection of mosquitoes with WNV.

Works Cited

1. 1991. Guide to yeast genetics and molecular biology. Methods Enzymol **194:**1-863.
2. 2007. Matchmaker Library Construction and Screening Kits User Manual, p. 59, PR742237 ed. Clontech Laboratories Inc.
3. **Abraham, E. G., and M. Jacobs-Lorena.** 2004. Mosquito midgut barriers to malaria parasite development. Insect Biochem Mol Biol **34:**667-71.
4. **Alcon-LePoder, S., M. T. Drouet, P. Roux, M. P. Frenkiel, M. Arborio, A. M. Durand-Schneider, M. Maurice, I. Le Blanc, J. Gruenberg, and M. Flamand.** 2005. The secreted form of dengue virus nonstructural protein NS1 is endocytosed by hepatocytes and accumulates in late endosomes: implications for viral infectivity. J Virol **79:**11403-11.
5. **Allison, S. L., J. Schalich, K. Stiasny, C. W. Mandl, C. Kunz, and F. X. Heinz.** 1995. Oligomeric rearrangement of tick-borne encephalitis virus envelope proteins induced by an acidic pH. J Virol **69:**695-700.
6. **Anderson, J. F., T. G. Andreadis, A. J. Main, F. J. Ferrandino, and C. R. Vossbrinck.** 2006. West Nile virus from female and male mosquitoes (Diptera: Culicidae) in subterranean, ground, and canopy habitats in Connecticut. J Med Entomol **43:**1010-9.
7. **Avirutnan, P., L. Zhang, N. Punyadee, A. Manuyakorn, C. Puttikhunt, W. Kasinrerk, P. Malasit, J. P. Atkinson, and M. S. Diamond.** 2007. Secreted NS1 of dengue virus attaches to the surface of cells via interactions with heparan sulfate and chondroitin sulfate E. PLoS Pathog **3:**e183.

8. **Barillas-Mury, C. V., F. G. Noriega, and M. A. Wells.** 1995. Early trypsin activity is part of the signal transduction system that activates transcription of the late trypsin gene in the midgut of the mosquito, Aedes aegypti. Insect Biochem Mol Biol **25:**241-6.

9. **Bartholomay, L. C., W. L. Cho, T. A. Rocheleau, J. P. Boyle, E. T. Beck, J. F. Fuchs, P. Liss, M. Rusch, K. M. Butler, R. C. Wu, S. P. Lin, H. Y. Kuo, I. Y. Tsao, C. Y. Huang, T. T. Liu, K. J. Hsiao, S. F. Tsai, U. C. Yang, A. J. Nappi, N. T. Perna, C. C. Chen, and B. M. Christensen.** 2004. Description of the transcriptomes of immune response-activated hemocytes from the mosquito vectors Aedes aegypti and Armigeres subalbatus. Infect Immun **72:**4114-26.

10. **Beasley, D. W.** 2005. Recent advances in the molecular biology of west nile virus. Curr Mol Med **5:**835-50.

11. **Beaty, B. J., R. S. Mackie, K. S. Mattingly, J. O. Carlson, and A. Rayms-Keller.** 2002. The midgut epithelium of aquatic arthropods: a critical target organ in environmental toxicology. Environ Health Perspect **110 Suppl 6:**911-4.

12. **Beerntsen, B. T., A. A. James, and B. M. Christensen.** 2000. Genetics of mosquito vector competence. Microbiol Mol Biol Rev **64:**115-37.

13. **Berggard, T., S. Linse, and P. James.** 2007. Methods for the detection and analysis of protein-protein interactions. Proteomics **7:**2833-42.

14. **Bhatia, P. K., and A. Mukhopadhyay.** 1999. Protein glycosylation: implications for in vivo functions and therapeutic applications. Adv Biochem Eng Biotechnol **64:**155-201.

15. **Bian, G., A. S. Raikhel, and J. Zhu.** 2008. Characterization of a juvenile hormone-regulated chymotrypsin-like serine protease gene in Aedes aegypti mosquito. Insect Biochem Mol Biol **38:**190-200.

16. **Black, W. C. t., K. E. Bennett, N. Gorrochotegui-Escalante, C. V. Barillas-Mury, I. Fernandez-Salas, M. de Lourdes Munoz, J. A. Farfan-Ale, K. E. Olson, and B. J. Beaty.** 2002. Flavivirus susceptibility in Aedes aegypti. Arch Med Res **33:**379-88.

17. **Blackwell, J. L., and M. A. Brinton.** 1997. Translation elongation factor-1 alpha interacts with the 3' stem-loop region of West Nile virus genomic RNA. J Virol **71:**6433-44.

18. **Blitvich, B. J., C. D. Blair, B. J. Kempf, M. T. Hughes, W. C. Black, R. S. Mackie, C. T. Meredith, B. J. Beaty, and A. Rayms-Keller.** 2002. Developmental- and tissue-specific expression of an inhibitor of apoptosis protein 1 homologue from Aedes triseriatus mosquitoes. Insect Mol Biol **11:**431-42.

19. **Bogachek, M. V., E. V. Protopopova, V. A. Ternovoi, A. V. Kachko, A. V. Ivanova, V. A. Ivanisenko, A. N. Shvalov, and V. B. Loktev.** 2007. [Immunochemical properties of West Nile virus protein prM and protein M C-end]. Mol Biol (Mosk) **41:**8-17.

20. **Bosio, C. F., B. J. Beaty, and W. C. t. Black.** 1998. Quantitative genetics of vector competence for dengue-2 virus in Aedes aegypti. Am J Trop Med Hyg **59:**965-70.

21. **Bosio, C. F., R. E. Fulton, M. L. Salasek, B. J. Beaty, and W. C. t. Black.** 2000. Quantitative trait loci that control vector competence for dengue-2 virus in the mosquito Aedes aegypti. Genetics **156:**687-98.

22. **Bressanelli, S., K. Stiasny, S. L. Allison, E. A. Stura, S. Duquerroy, J. Lescar, F. X. Heinz, and F. A. Rey.** 2004. Structure of a flavivirus envelope glycoprotein in its low-pH-induced membrane fusion conformation. EMBO J **23:**728-38.

23. **Brinton, M. A.** 2002. The molecular biology of West Nile Virus: a new invader of the western hemisphere. Annu Rev Microbiol **56:**371-402.

24. **Carlstedt-Duke, B.** 1989. The Normal Microflora and Mucin, p. 109-127. *In* R. Grubb (ed.), Regulatory and Protective Role of the Normal Microflora. Stockton Press.

25. **Chadee, K., W. A. Petri, Jr., D. J. Innes, and J. I. Ravdin.** 1987. Rat and human colonic mucins bind to and inhibit adherence lectin of Entamoeba histolytica. J Clin Invest **80:**1245-54.

26. **Chen, Y., T. Maguire, R. E. Hileman, J. R. Fromm, J. D. Esko, R. J. Linhardt, and R. M. Marks.** 1997. Dengue virus infectivity depends on envelope protein binding to target cell heparan sulfate. Nat Med **3:**866-71.

27. **Chu, J. J., B. G. Choo, J. W. Lee, and M. L. Ng.** 2003. Actin filaments participate in West Nile (Sarafend) virus maturation process. J Med Virol **71:**463-72.

28. **Chu, J. J., P. W. Leong, and M. L. Ng.** 2006. Analysis of the endocytic pathway mediating the infectious entry of mosquito-borne flavivirus West Nile into Aedes albopictus mosquito (C6/36) cells. Virology **349:**463-75.

29. **Chu, J. J., P. W. Leong, and M. L. Ng.** 2005. Characterization of plasma membrane-associated proteins from Aedes albopictus mosquito (C6/36) cells that mediate West Nile virus binding and infection. Virology **339:**249-60.

30. **Chu, J. J., and M. L. Ng.** 2004. Interaction of West Nile virus with alpha v beta 3 integrin mediates virus entry into cells. J Biol Chem **279:**54533-41.

31. **Chung, K. M., M. K. Liszewski, G. Nybakken, A. E. Davis, R. R. Townsend, D. H. Fremont, J. P. Atkinson, and M. S. Diamond.** 2006. West Nile virus nonstructural protein NS1 inhibits complement activation by binding the regulatory protein factor H. Proc Natl Acad Sci U S A **103:**19111-6.

32. **Coates, P. J., and P. A. Hall.** 2003. The yeast two-hybrid system for identifying protein-protein interactions. J Pathol **199:**4-7.

33. **Connaris, S., and P. Greenwell.** 1997. Glycosidases in mucin-dwelling protozoans. Glycoconj J **14:**879-82.

34. **Davis, C. W., H. Y. Nguyen, S. L. Hanna, M. D. Sanchez, R. W. Doms, and T. C. Pierson.** 2006. West Nile virus discriminates between DC-SIGN and DC-SIGNR for cellular attachment and infection. J Virol **80:**1290-301.

35. **Davis, W. G., J. L. Blackwell, P. Y. Shi, and M. A. Brinton.** 2007. Interaction between the cellular protein eEF1A and the 3'-terminal stem-loop of West Nile virus genomic RNA facilitates viral minus-strand RNA synthesis. J Virol **81:**10172-87.

36. **Devenport, M., P. H. Alvarenga, L. Shao, H. Fujioka, M. L. Bianconi, P. L. Oliveira, and M. Jacobs-Lorena.** 2006. Identification of the Aedes aegypti

peritrophic matrix protein AeIMUCI as a heme-binding protein. Biochemistry **45:**9540-9.

37. **Durrbach, A., D. Louvard, and E. Coudrier.** 1996. Actin filaments facilitate two steps of endocytosis. J Cell Sci **109 (Pt 2):**457-65.

38. **Eckart, M. R., and C. M. Bussineau.** 1996. Quality and authenticity of heterologous proteins synthesized in yeast. Curr Opin Biotechnol **7:**525-30.

39. **Edwards, M. J., and M. Jacobs-Lorena.** 2000. Permeability and disruption of the peritrophic matrix and caecal membrane from Aedes aegypti and Anopheles gambiae mosquito larvae. J Insect Physiol **46:**1313-1320.

40. **Fallon, A. M., and D. Sun.** 2001. Exploration of mosquito immunity using cells in culture. Insect Biochem Mol Biol **31:**263-78.

41. **Fields, S., and O. Song.** 1989. A novel genetic system to detect protein-protein interactions. Nature **340:**245-6.

42. **Filho, B. P., F. J. Lemos, N. F. Secundino, V. Pascoa, S. T. Pereira, and P. F. Pimenta.** 2002. Presence of chitinase and beta-N-acetylglucosaminidase in the Aedes aegypti. a chitinolytic system involving peritrophic matrix formation and degradation. Insect Biochem Mol Biol **32:**1723-9.

43. **Flamand, M., V. Deubel, and M. Girard.** 1992. Expression and secretion of Japanese encephalitis virus nonstructural protein NS1 by insect cells using a recombinant baculovirus. Virology **191:**826-36.

44. **Flamand, M., F. Megret, M. Mathieu, J. Lepault, F. A. Rey, and V. Deubel.** 1999. Dengue virus type 1 nonstructural glycoprotein NS1 is secreted from

mammalian cells as a soluble hexamer in a glycosylation-dependent fashion. J Virol **73:**6104-10.

45. **Fowler, J., L. Vinall, and D. Swallow.** 2001. Polymorphism of the human muc genes. Front Biosci **6:**D1207-15.

46. **Geiss, B. J., T. C. Pierson, and M. S. Diamond.** 2005. Actively replicating West Nile virus is resistant to cytoplasmic delivery of siRNA. Virol J **2:**53.

47. **Gietz, R. D., B. Triggs-Raine, A. Robbins, K. C. Graham, and R. A. Woods.** 1997. Identification of proteins that interact with a protein of interest: applications of the yeast two-hybrid system. Mol Cell Biochem **172:**67-79.

48. **Goddard, L. B., A. E. Roth, W. K. Reisen, and T. W. Scott.** 2002. Vector competence of California mosquitoes for West Nile virus. Emerg Infect Dis **8:**1385-91.

49. **Gorbalenya, A. E., E. V. Koonin, A. P. Donchenko, and V. M. Blinov.** 1989. Two related superfamilies of putative helicases involved in replication, recombination, repair and expression of DNA and RNA genomes. Nucleic Acids Res **17:**4713-30.

50. **Gorman, M. J., and S. M. Paskewitz.** 2001. Serine proteases as mediators of mosquito immune responses. Insect Biochem Mol Biol **31:**257-62.

51. **Gorrochotegui-Escalante, N., S. Lozano-Fuentes, K. E. Bennett, A. Molina-Cruz, B. J. Beaty, and W. C. t. Blackiv.** 2005. Association mapping of segregating sites in the early trypsin gene and susceptibility to dengue-2 virus in the mosquito Aedes aegypti. Insect Biochem Mol Biol **35:**771-88.

52. **Gould, L. H., and E. Fikrig.** 2004. West Nile virus: a growing concern? J Clin Invest **113:**1102-7.

53. **Gupta, L., S. Kumar, Y. S. Han, P. F. Pimenta, and C. Barillas-Mury.** 2005. Midgut epithelial responses of different mosquito-Plasmodium combinations: the actin cone zipper repair mechanism in Aedes aegypti. Proc Natl Acad Sci U S A **102:**4010-5.

54. **Hanna, S. L., T. C. Pierson, M. D. Sanchez, A. A. Ahmed, M. M. Murtadha, and R. W. Doms.** 2005. N-linked glycosylation of west nile virus envelope proteins influences particle assembly and infectivity. J Virol **79:**13262-74.

55. **Hannon, G. J.** 2002. RNA interference. Nature **418:**244-51.

56. **Hardy, J. L., E. J. Houk, L. D. Kramer, and W. C. Reeves.** 1983. Intrinsic factors affecting vector competence of mosquitoes for arboviruses. Annu Rev Entomol **28:**229-62.

57. **Hartl, F. U., and M. Hayer-Hartl.** 2002. Molecular chaperones in the cytosol: from nascent chain to folded protein. Science **295:**1852-8.

58. **Hase, T., P. L. Summers, and K. H. Eckels.** 1989. Flavivirus entry into cultured mosquito cells and human peripheral blood monocytes. Arch Virol **104:**129-43.

59. **Hayes, E. B., N. Komar, R. S. Nasci, S. P. Montgomery, D. R. O'Leary, and G. L. Campbell.** 2005. Epidemiology and transmission dynamics of West Nile virus disease. Emerg Infect Dis **11:**1167-73.

60. **Hayes, E. B., J. J. Sejvar, S. R. Zaki, R. S. Lanciotti, A. V. Bode, and G. L. Campbell.** 2005. Virology, pathology, and clinical manifestations of West Nile virus disease. Emerg Infect Dis **11:**1174-9.

61. **Hengen, P. N.** 1997. False positives from the yeast two-hybrid system. Trends Biochem Sci **22:**33-4.

62. **Herscovics, A., and P. Orlean.** 1993. Glycoprotein biosynthesis in yeast. FASEB J **7:**540-50.

63. **Huber, M., E. Cabib, and L. H. Miller.** 1991. Malaria parasite chitinase and penetration of the mosquito peritrophic membrane. Proc Natl Acad Sci U S A **88:**2807-10.

64. **Jacobs, M. G., P. J. Robinson, C. Bletchly, J. M. Mackenzie, and P. R. Young.** 2000. Dengue virus nonstructural protein 1 is expressed in a glycosyl-phosphatidylinositol-linked form that is capable of signal transduction. FASEB J **14:**1603-10.

65. **James, P., J. Halladay, and E. A. Craig.** 1996. Genomic libraries and a host strain designed for highly efficient two-hybrid selection in yeast. Genetics **144:**1425-36.

66. **Jindadamrongwech, S., C. Thepparit, and D. R. Smith.** 2004. Identification of GRP 78 (BiP) as a liver cell expressed receptor element for dengue virus serotype 2. Arch Virol **149:**915-27.

67. **Kalhok, S. E., L. M. Tabak, D. E. Prosser, W. Brook, A. E. Downe, and B. N. White.** 1993. Isolation, sequencing and characterization of two cDNA clones coding for trypsin-like enzymes from the midgut of Aedes aegypti. Insect Mol Biol **2:**71-9.

68. **Kanai, R., K. Kar, K. Anthony, L. H. Gould, M. Ledizet, E. Fikrig, W. A. Marasco, R. A. Koski, and Y. Modis.** 2006. Crystal structure of west nile virus envelope glycoprotein reveals viral surface epitopes. J Virol **80:**11000-8.

69. **Khromykh, A. A., P. L. Sedlak, and E. G. Westaway.** 1999. trans-Complementation analysis of the flavivirus Kunjin ns5 gene reveals an essential role for translation of its N-terminal half in RNA replication. J Virol **73:**9247-55.

70. **Khromykh, A. A., and E. G. Westaway.** 1996. RNA binding properties of core protein of the flavivirus Kunjin. Arch Virol **141:**685-99.

71. **Kimura, T., and A. Ohyama.** 1988. Association between the pH-dependent conformational change of West Nile flavivirus E protein and virus-mediated membrane fusion. J Gen Virol **69 (Pt 6):**1247-54.

72. **Koonin, E. V.** 1993. Computer-assisted identification of a putative methyltransferase domain in NS5 protein of flaviviruses and lambda 2 protein of reovirus. J Gen Virol **74 (Pt 4):**733-40.

73. **Kraut, J.** 1977. Serine proteases: structure and mechanism of catalysis. Annu Rev Biochem **46:**331-58.

74. **Kulakosky, P. C., M. L. Shuler, and H. A. Wood.** 1998. N-glycosylation of a baculovirus-expressed recombinant glycoprotein in three insect cell lines. In Vitro Cell Dev Biol Anim **34:**101-8.

75. **Lanciotti, R. S., J. T. Roehrig, V. Deubel, J. Smith, M. Parker, K. Steele, B. Crise, K. E. Volpe, M. B. Crabtree, J. H. Scherret, R. A. Hall, J. S. MacKenzie, C. B. Cropp, B. Panigrahy, E. Ostlund, B. Schmitt, M. Malkinson, C. Banet, J. Weissman, N. Komar, H. M. Savage, W. Stone, T.**

McNamara, and D. J. Gubler. 1999. Origin of the West Nile virus responsible for an outbreak of encephalitis in the northeastern United States. Science **286:**2333-7.

76. **Lencer, W. I., F. D. Reinhart, and M. R. Neutra.** 1990. Interaction of cholera toxin with cloned human goblet cells in monolayer culture. Am J Physiol **258:**G96-102.

77. **Lindenbach, B. D., and C. M. Rice.** 1997. trans-Complementation of yellow fever virus NS1 reveals a role in early RNA replication. J Virol **71:**9608-17.

78. **Liu, W. J., X. J. Wang, V. V. Mokhonov, P. Y. Shi, R. Randall, and A. A. Khromykh.** 2005. Inhibition of interferon signaling by the New York 99 strain and Kunjin subtype of West Nile virus involves blockage of STAT1 and STAT2 activation by nonstructural proteins. J Virol **79:**1934-42.

79. **Livak, K. J., and T. D. Schmittgen.** 2001. Analysis of relative gene expression data using real-time quantitative PCR and the 2(-Delta Delta C(T)) Method. Methods **25:**402-8.

80. **Lobigs, M., and E. Lee.** 2004. Inefficient signalase cleavage promotes efficient nucleocapsid incorporation into budding flavivirus membranes. J Virol **78:**178-86.

81. **Londhe, V., N. McNamara, H. Lemjabbar, and C. Basbaum.** 2003. Viral dsRNA activates mucin transcription in airway epithelial cells. FEBS Lett **553:**33-8.

82. **Lorenz, I. C., S. L. Allison, F. X. Heinz, and A. Helenius.** 2002. Folding and dimerization of tick-borne encephalitis virus envelope proteins prM and E in the endoplasmic reticulum. J Virol **76:**5480-91.

83. **Martin-Benito, J., J. Boskovic, P. Gomez-Puertas, J. L. Carrascosa, C. T. Simons, S. A. Lewis, F. Bartolini, N. J. Cowan, and J. M. Valpuesta.** 2002. Structure of eukaryotic prefoldin and of its complexes with unfolded actin and the cytosolic chaperonin CCT. EMBO J **21:**6377-86.

84. **Mason, P. W.** 1989. Maturation of Japanese encephalitis virus glycoproteins produced by infected mammalian and mosquito cells. Virology **169:**354-64.

85. **Mastrangelo, E., M. Milani, M. Bollati, B. Selisko, F. Peyrane, V. Pandini, G. Sorrentino, B. Canard, P. V. Konarev, D. I. Svergun, X. de Lamballerie, B. Coutard, A. A. Khromykh, and M. Bolognesi.** 2007. Crystal structure and activity of Kunjin virus NS3 helicase; protease and helicase domain assembly in the full length NS3 protein. J Mol Biol **372:**444-55.

86. **McLean, R. G., S. R. Ubico, D. E. Docherty, W. R. Hansen, L. Sileo, and T. S. McNamara.** 2001. West Nile virus transmission and ecology in birds. Ann N Y Acad Sci **951:**54-7.

87. **McMinn, P. C.** 1997. The molecular basis of virulence of the encephalitogenic flaviviruses. J Gen Virol **78 (Pt 11):**2711-22.

88. **Medigeshi, G. R., A. J. Hirsch, D. N. Streblow, J. Nikolich-Zugich, and J. A. Nelson.** 2008. West Nile virus entry requires cholesterol-rich membrane microdomains and is independent of alphavbeta3 integrin. J Virol **82:**5212-9.

89. **Miernyk, J. A., and J. J. Thelen.** 2008. Biochemical approaches for discovering protein-protein interactions. Plant J **53:**597-609.

90. **Mishra, A. C., R. S. Jadi, R. Paramasivan, and D. T. Mourya.** 2001. Antigen distribution pattern of West Nile virus in Culex tritaeniorhynchus, Culex vishnui and Culex pseudovishnui mosquitoes. J Commun Dis **33:**174-9.

91. **Mishra, A. C., and D. T. Mourya.** 2001. Transovarial transmission of West Nile virus in Culex vishnui mosquito. Indian J Med Res **114:**212-4.

92. **Molina-Cruz, A., L. Gupta, J. Richardson, K. Bennett, W. t. Black, and C. Barillas-Mury.** 2005. Effect of mosquito midgut trypsin activity on dengue-2 virus infection and dissemination in Aedes aegypti. Am J Trop Med Hyg **72:**631-7.

93. **Morlais, I., and D. W. Severson.** 2001. Identification of a polymorphic mucin-like gene expressed in the midgut of the mosquito, Aedes aegypti, using an integrated bulked segregant and differential display analysis. Genetics **158:**1125-36.

94. **Moskalyk, L. A., M. M. Oo, and M. Jacobs-Lorena.** 1996. Peritrophic matrix proteins of Anopheles gambiae and Aedes aegypti. Insect Mol Biol **5:**261-8.

95. **Mukhopadhyay, S., B. S. Kim, P. R. Chipman, M. G. Rossmann, and R. J. Kuhn.** 2003. Structure of West Nile virus. Science **302:**248.

96. **Mukhopadhyay, S., R. J. Kuhn, and M. G. Rossmann.** 2005. A structural perspective of the flavivirus life cycle. Nat Rev Microbiol **3:**13-22.

97. **Muylaert, I. R., T. J. Chambers, R. Galler, and C. M. Rice.** 1996. Mutagenesis of the N-linked glycosylation sites of the yellow fever virus NS1 protein: effects on virus replication and mouse neurovirulence. Virology **222:**159-68.

98. **Nall, T. A., K. J. Chappell, M. J. Stoermer, N. X. Fang, J. D. Tyndall, P. R. Young, and D. P. Fairlie.** 2004. Enzymatic characterization and homology model of a catalytically active recombinant West Nile virus NS3 protease. J Biol Chem **279:**48535-42.

99. **Navarro-Sanchez, E., R. Altmeyer, A. Amara, O. Schwartz, F. Fieschi, J. L. Virelizier, F. Arenzana-Seisdedos, and P. Despres.** 2003. Dendritic-cell-specific ICAM3-grabbing non-integrin is essential for the productive infection of human dendritic cells by mosquito-cell-derived dengue viruses. EMBO Rep **4:**723-8.

100. **Nene, V., J. R. Wortman, D. Lawson, B. Haas, C. Kodira, Z. J. Tu, B. Loftus, Z. Xi, K. Megy, M. Grabherr, Q. Ren, E. M. Zdobnov, N. F. Lobo, K. S. Campbell, S. E. Brown, M. F. Bonaldo, J. Zhu, S. P. Sinkins, D. G. Hogenkamp, P. Amedeo, P. Arensburger, P. W. Atkinson, S. Bidwell, J. Biedler, E. Birney, R. V. Bruggner, J. Costas, M. R. Coy, J. Crabtree, M. Crawford, B. Debruyn, D. Decaprio, K. Eiglmeier, E. Eisenstadt, H. El-Dorry, W. M. Gelbart, S. L. Gomes, M. Hammond, L. I. Hannick, J. R. Hogan, M. H. Holmes, D. Jaffe, J. S. Johnston, R. C. Kennedy, H. Koo, S. Kravitz, E. V. Kriventseva, D. Kulp, K. Labutti, E. Lee, S. Li, D. D. Lovin, C. Mao, E. Mauceli, C. F. Menck, J. R. Miller, P. Montgomery, A. Mori, A. L. Nascimento, H. F. Naveira, C. Nusbaum, S. O'Leary, J. Orvis, M. Pertea, H.**

Quesneville, K. R. Reidenbach, Y. H. Rogers, C. W. Roth, J. R. Schneider, M. Schatz, M. Shumway, M. Stanke, E. O. Stinson, J. M. Tubio, J. P. Vanzee, S. Verjovski-Almeida, D. Werner, O. White, S. Wyder, Q. Zeng, Q. Zhao, Y. Zhao, C. A. Hill, A. S. Raikhel, M. B. Soares, D. L. Knudson, N. H. Lee, J. Galagan, S. L. Salzberg, I. T. Paulsen, G. Dimopoulos, F. H. Collins, B. Birren, C. M. Fraser-Liggett, and D. W. Severson. 2007. Genome sequence of Aedes aegypti, a major arbovirus vector. Science **316:**1718-23.

101. **Ng, M. L.** 1987. Ultrastructural studies of Kunjin virus-infected Aedes albopictus cells. J Gen Virol **68 (Pt 2):**577-82.

102. **Noisakran, S., T. Dechtawewat, P. Rinkaewkan, C. Puttikhunt, A. Kanjanahaluethai, W. Kasinrerk, N. Sittisombut, and P. Malasit.** 2007. Characterization of dengue virus NS1 stably expressed in 293T cell lines. J Virol Methods **142:**67-80.

103. **Noriega, F. G., J. E. Pennington, C. Barillas-Mury, X. Y. Wang, and M. A. Wells.** 1996. Aedes aegypti midgut early trypsin is post-transcriptionally regulated by blood feeding. Insect Mol Biol **5:**25-9.

104. **Noriega, F. G., D. K. Shah, and M. A. Wells.** 1997. Juvenile hormone controls early trypsin gene transcription in the midgut of Aedes aegypti. Insect Mol Biol **6:**63-6.

105. **Noriega, F. G., X. Y. Wang, J. E. Pennington, C. V. Barillas-Mury, and M. A. Wells.** 1996. Early trypsin, a female-specific midgut protease in Aedes aegypti: isolation, aminoterminal sequence determination, and cloning and sequencing of the gene. Insect Biochem Mol Biol **26:**119-26.

106. **Noriega, F. G., and M. A. Wells.** 1999. A molecular view of trypsin synthesis in the midgut of Aedes aegypti. J Insect Physiol **45:**613-620.

107. **Nybakken, G. E., C. A. Nelson, B. R. Chen, M. S. Diamond, and D. H. Fremont.** 2006. Crystal structure of the West Nile virus envelope glycoprotein. J Virol **80:**11467-74.

108. **Perez-Vilar, J., and R. L. Hill.** 1999. The structure and assembly of secreted mucins. J Biol Chem **274:**31751-4.

109. **Pfaffl, M. W.** 2001. A new mathematical model for relative quantification in real-time RT-PCR. Nucleic Acids Res **29:**e45.

110. **Rappole, J. H., and Z. Hubalek.** 2003. Migratory birds and West Nile virus. J Appl Microbiol **94 Suppl:**47S-58S.

111. **Rayms-Keller, A., M. McGaw, C. Oray, J. O. Carlson, and B. J. Beaty.** 2000. Molecular cloning and characterization of a metal responsive Aedes aegypti intestinal mucin cDNA. Insect Mol Biol **9:**419-26.

112. **Reyes-Del Valle, J., S. Chavez-Salinas, F. Medina, and R. M. Del Angel.** 2005. Heat shock protein 90 and heat shock protein 70 are components of dengue virus receptor complex in human cells. J Virol **79:**4557-67.

113. **Seregni, E., C. Botti, S. Massaron, C. Lombardo, A. Capobianco, A. Bogni, and E. Bombardieri.** 1997. Structure, function and gene expression of epithelial mucins. Tumori **83:**625-32.

114. **Shao, L., M. Devenport, and M. Jacobs-Lorena.** 2001. The peritrophic matrix of hematophagous insects. Arch Insect Biochem Physiol **47:**119-25.

115. **Shepard, J. J., T. G. Andreadis, and C. R. Vossbrinck.** 2006. Molecular phylogeny and evolutionary relationships among mosquitoes (Diptera: Culicidae) from the northeastern United States based on small subunit ribosomal DNA (18S rDNA) sequences. J Med Entomol **43:**443-54.

116. **Stadler, K., S. L. Allison, J. Schalich, and F. X. Heinz.** 1997. Proteolytic activation of tick-borne encephalitis virus by furin. J Virol **71:**8475-81.

117. **Su, A. I., M. P. Cooke, K. A. Ching, Y. Hakak, J. R. Walker, T. Wiltshire, A. P. Orth, R. G. Vega, L. M. Sapinoso, A. Moqrich, A. Patapoutian, G. M. Hampton, P. G. Schultz, and J. B. Hogenesch.** 2002. Large-scale analysis of the human and mouse transcriptomes. Proc Natl Acad Sci U S A **99:**4465-70.

118. **Terra, W. R.** 2001. The origin and functions of the insect peritrophic membrane and peritrophic gel. Arch Insect Biochem Physiol **47:**47-61.

119. **Thuring, R. W., J. P. Sanders, and P. Borst.** 1975. A freeze-squeeze method for recovering long DNA from agarose gels. Anal Biochem **66:**213-20.

120. **Tio, P. H., W. W. Jong, and M. J. Cardosa.** 2005. Two dimensional VOPBA reveals laminin receptor (LAMR1) interaction with dengue virus serotypes 1, 2 and 3. Virol J **2:**25.

121. **Uchil, P. D., A. V. Kumar, and V. Satchidanandam.** 2006. Nuclear localization of flavivirus RNA synthesis in infected cells. J Virol **80:**5451-64.

122. **Vainberg, I. E., S. A. Lewis, H. Rommelaere, C. Ampe, J. Vandekerckhove, H. L. Klein, and N. J. Cowan.** 1998. Prefoldin, a chaperone that delivers unfolded proteins to cytosolic chaperonin. Cell **93:**863-73.

123. **Villalon, J. M., A. Ghosh, and M. Jacobs-Lorena.** 2003. The peritrophic matrix limits the rate of digestion in adult Anopheles stephensi and Aedes aegypti mosquitoes. J Insect Physiol **49:**891-5.

124. **von Mering, C., R. Krause, B. Snel, M. Cornell, S. G. Oliver, S. Fields, and P. Bork.** 2002. Comparative assessment of large-scale data sets of protein-protein interactions. Nature **417:**399-403.

125. **Wang, P., and R. R. Granados.** 2000. Calcofluor disrupts the midgut defense system in insects. Insect Biochem Mol Biol **30:**135-43.

126. **Weaver, S. C., and A. D. Barrett.** 2004. Transmission cycles, host range, evolution and emergence of arboviral disease. Nat Rev Microbiol **2:**789-801.

127. **Wengler, G.** 1991. The carboxy-terminal part of the NS 3 protein of the West Nile flavivirus can be isolated as a soluble protein after proteolytic cleavage and represents an RNA-stimulated NTPase. Virology **184:**707-15.

128. **Wengler, G.** 1993. The NS 3 nonstructural protein of flaviviruses contains an RNA triphosphatase activity. Virology **197:**265-73.

129. **Westaway, E. G., J. M. Mackenzie, M. T. Kenney, M. K. Jones, and A. A. Khromykh.** 1997. Ultrastructure of Kunjin virus-infected cells: colocalization of NS1 and NS3 with double-stranded RNA, and of NS2B with NS3, in virus-induced membrane structures. J Virol **71:**6650-61.

130. **Whitfield, S. G., F. A. Murphy, and W. D. Sudia.** 1973. St. Louis encephalitis virus: an ultrastructural study of infection in a mosquito vector. Virology **56:**70-87.

131. **Winkler, G., S. E. Maxwell, C. Ruemmler, and V. Stollar.** 1989. Newly synthesized dengue-2 virus nonstructural protein NS1 is a soluble protein but becomes partially hydrophobic and membrane-associated after dimerization. Virology **171:**302-5.

132. **Yu, L., M. Nomaguchi, R. Padmanabhan, and L. Markoff.** 2008. Specific requirements for elements of the 5' and 3' terminal regions in flavivirus RNA synthesis and viral replication. Virology **374:**170-85.

133. **Zhang, W., P. R. Chipman, J. Corver, P. R. Johnson, Y. Zhang, S. Mukhopadhyay, T. S. Baker, J. H. Strauss, M. G. Rossmann, and R. J. Kuhn.** 2003. Visualization of membrane protein domains by cryo-electron microscopy of dengue virus. Nat Struct Biol **10:**907-12.